Radiation Shielding calculations using MCNPX transport code for cost optimization of the shielding material to be used at iThemba LABS.

by

Phumlani Zipho Ngcobo

A Dissertation submitted for partial fulfilment of the requirements for the degree of Master of Science at the University of Zululand.

Department of Physics and Engineering
University of Zululand
Private Bag X1001, Kwa-Dlangezwa 3886
South Africa

Supervisors:

Prof. O. M. Ndwandwe
Department of Physics and Engineering

Dr R. A. Bark
Radioactive Ion Beam Project
iThemba LABS PO Box 722, Somerset West, 7129, Cape Town

April 2012

DECLARATION

I, the undersigned, hereby declare that the work contained in this thesis is my own original work and that I have not previously in its entirety or in part submitted it at any university for a degree.

…. 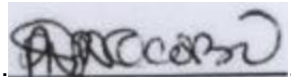 ….. ……16 April 2012……

Phumlani Zipho Ngcobo Date

ABSTRACT

At iThemba Laboratory for Accelerator Based Sciences (iThemba LABS), the shared use of the Separated Sector Cyclotron has reached the point where further advancement of the respective disciplines cannot be realised.

The new facility is proposed to respond to the demands of these, specifically a phased development of Radioactive Ion Beam (RIBs). This facility will include a 70 MeV negative-ion cyclotron with the development of 5 Radioisotope production stations and two production stations for RIBs for nuclear physics and materials science research.

The RIB Demonstrator project is suggested to test and demonstrate the advantages of the overall RIB project.

The new cyclotron accelerator, which will provide currents of up to 350 μA of 70 MeV protons, has a potential of producing strong sources of ionising radiation. The most challenging entities, which are part of the indirect ionising radiation, are neutral neutrons and photons.

There is a need to protect humans and materials from ionising radiation by providing adequate shielding to attenuate these particles, thus bringing their flux to acceptably low levels determined by the International Commission on Radiation Protection (ICRP) for designated personnel accessing this facility.

The Monte Carlo for Neutral Particles eXtended (MCNPX) code was used for the purpose of investigating the correct thickness of the shielding of the cyclotron vault and the RIB Demonstrator vault.

Results obtained confirmed that 4m and 3m thicknesses of concrete shielding will be adequate in the proposed cyclotron vault and RIB Demonstrator vault respectively.

ACKNOWLEDGEMENTS

This work reflects that TRUE NOBILITY is not being better than others but being better than you used to be. It has been always about finding my ‘true’ self and this work takes me closer to that.

I would like to thank Almighty God, the source of all life, for knowledge and inspiration.

To Dr Robert Bark, I thank you for everything that involves MSc student supervision, moreover, I will single out your tolerance in me, wanting only the best out of me. I am very grateful to have worked with you, and I hope this may continue

.

Dr John Cornell, thank you for all the interactions and guidance since the beginning of my MSc studies and for proofreading my dissertation countless times, this works is yours too.

I thank Professor Muzi Ndwandwe for opening the opportunity of Masters studies and providing necessary funding.

My gratitude goes to Johann van Rooyen and Zukile Zibi of NECSA for guidance with MCNPX calculations. You made this project your own.

Thanks to all Masters and PhD students that I have interacted with for giving me courage.

I would like to thank the ‘Masters in Nuclear Science’ lecturers, the Department of Physics Administration staff at the Universities of Zululand and of the Western Cape.
I would like to thank the National Research Foundation, iThemba LABS and the University of Zululand Research committee for providing funding.

I thank the Ngcobo family and siblings, particularly my uncle Fakazi Ngcobo, for funding my undergraduate studies and sister Samukelisiwe Ngcobo for all the social support, thank you.

To my dearest friend Sibongile Ngubane for compassion, words are not enough.

DEDICATION

- To John ‘Dube’ Ngcobo; Elias Ngcobo and Constance Ngcobo for their commitment in education.
- To my mother Delisiwe Ngcobo for unconditional love and wanting me to be myself.
- To my kids Mfundo and Zolunga,

CONTENTS

ABBREVIATIONS

ANS ..... American Nuclear Society

ANSI ..... American National Standards Institute

BTE ..... Boltzmann transport equation

BTO ..... Boltzmann transport operator

CN ..... Compound Nucleus

DAF ..... Dose Attenuation Factor

EURISOL ..... European Isotope Separation On-Line

FLUKA ..... FLUktuierende KAskade

FOM ..... Figure of Merit

IAEA ..... International Atomic Energy Agency

ICRP ..... International Commission on Radiation Protection

LANL ..... Los Alamos National Laboratory

MCNPX ..... Monte Carlo N-Particle eXtended transport code

NDR ..... Neutron dose rate

ORNL ..... Oak Ridge National Laboratories

PDR ..... Photon dose rate

PFN ..... Prompt fission neutron

RIB ..... Radioactive Ion Beams

RNG ..... Random Number Generator

RSICC ..... Radiation Safety Information Computational Center (at ORNL, USA)

SPES ..... Selective Production of Exotic Species

SRIM ..... The Stopping and Range of Ions on Matter

SS ..... Stainless steel

SS-304 ..... Stainless steel, type 304

SSC ..... Separated Sector Cyclotron

STP ..... Standard temperature and pressure

TDR ..... Total dose rate; usually TDR=NDR+PDR

TEM ..... Tissue Equivalent Material

VRT ..... Variance Reduction Technique

γ ..... Photon (usually energetic & ionising)

LIST OF TABLES

LIST OF FIGURES

CHAPTER 1: INTRODUCTION

1.1 Background

Overview

iThemba LABS is a South African national multidisciplinary research facility with laboratories situated in the Western Cape and Gauteng provinces. It is primarily a nuclear accelerator-based facility which supports research in nuclear and material sciences, provides cancer therapy based on neutron and proton beams, and provides hospitals in South Africa and abroad with radioisotopes for medical diagnostics. Clearly these activities position iThemba LABS as a significant player not only in Africa but globally. However this position is under threat.

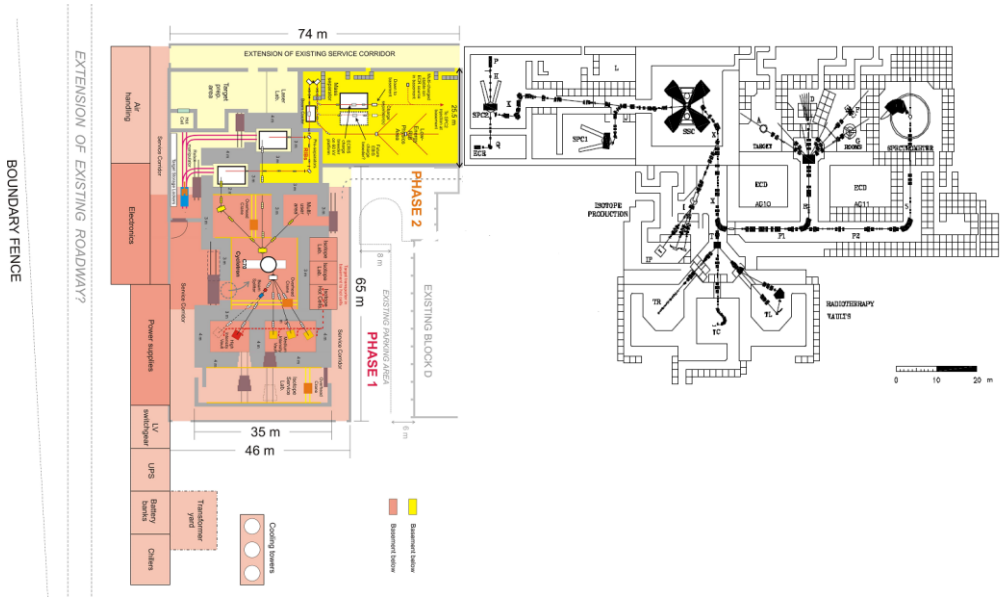

Figure 1: Top view plan of the existing structure (right - black & white) and the envisaged extension plan of the phase-based iThemba LABS Radioactive Ion Beam Project development (left - coloured) [1].

The Separated Sector Cyclotron (SSC) accelerator is central in the running of this multidisciplinary facility. Figure 1 shows the SSC feeding proton beams to different divisions. However, the shared use of the SSC has reached the point where further advancement of the respective disciplines cannot be realised [1].

- There is a growing demand for production of radioisotopes internationally, thus additional capacity is required.
- The current Nuclear Physics research and cancer treatments suggest a growing demand.

- There is a growing appetite in Nuclear Physics research for studying neutron-rich nuclides, which will further the understanding of nuclear forces and other aspects of nuclear physics. These nuclides cannot be produced by stable beams.
- Materials Research at iThemba LABS can benefit from the implantations of RIBs into industrial materials like semi-conductors, and for further understanding of the atomic structure of other materials.

It is suggested that the SSC must be relieved from other activities and be dedicated to proton therapy and nuclear physics research. The new facility must then respond to the demands of radioisotope production; neutron therapy treatments and neutron-rich nuclides & materials research. A commercial 70 MeV negative-ion cyclotron allows simultaneous extraction of two beams. This affords the possibilities for these activities to run concurrently.

A phased development of the Radioactive Ion Beam (RIB) is proposed, which will see two phases implemented progressively [1].
Phase 1 will realise a development of a 70 MeV negative-ion cyclotron with two Radioisotope production stations.
Phase 2 will add two RIB production stations for nuclear and materials research. (See Figure 2).

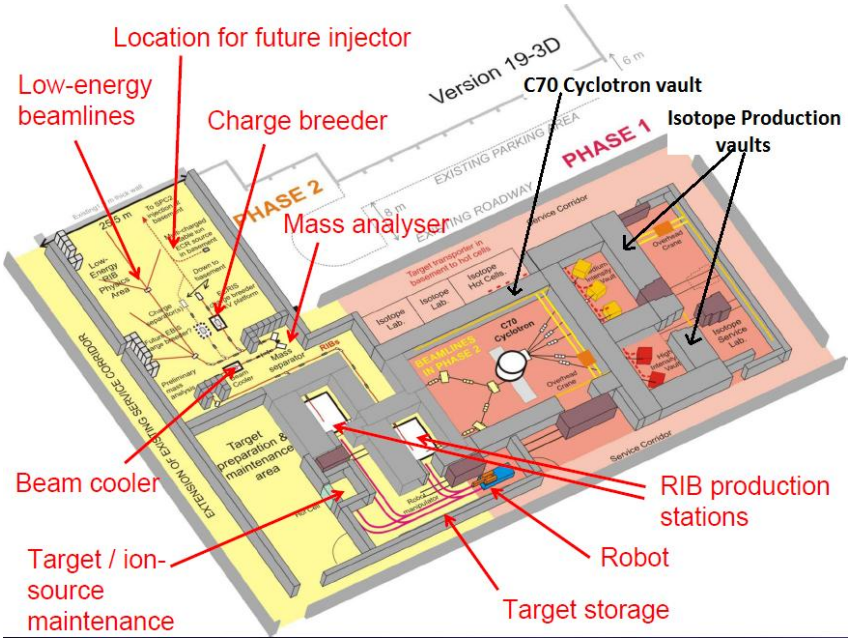

Figure 2: The 3D view of the phase-based iThemba LABS Radioactive Ion Beam (RIB) Project development [1].

The success of this RIB project is in line with the National Research Foundation (NRF) vision, strategic goals and values. This project will achieve a specialised world-class research facility, enhance international competitiveness and be people-centred [2].

One of the prime achievements of this facility has been to develop human capital in the areas of research that are directly involved with the research activities mentioned above. These are achieved through postgraduate programmes: one of them is a Masters in Nuclear & Materials Sciences (MaNuS/MatSci), which is a collaboration between iThemba LABS, University of Zululand and University of the Western Cape.

Current Research

Because large currents of up to 350 µA of 70 MeV protons will be provided by the new cyclotron accelerator, potentially strong sources of ionising radiation will be produced. This could result from many sources and is not restricted to the proton beam itself as it accelerates towards the target. It could also result from the fission products of the target irradiated by the beam. As can be seen in the figures showing the floor plan, areas around the cyclotron vault will need to be accessed, some normally and some only as the need arise.

The most challenging entities, which are part of the indirect ionising radiation, are neutral neutrons and photons. When these interact with matter, they transfer their energies to charged particles which then further directly ionise matter [6]. The challenge is that neutrons travel over a long range before they can be attenuated compared to charged particles, as with neutral particles there is no electromagnetic interaction at the atomic level. So to protect humans and materials from ionising radiation will mean providing enough shielding to attenuate these particles, thus bringing their fluence-rate to acceptably low levels according to International Commission on Radiation Protection (ICRP).

Shielding walls of ordinary concrete are shown in grey colour in the previous figures. For the purpose of investigating the correct thickness of this shield, we will consider the shielding of the cyclotron vault which is rectangular in shape, as shown in Figure 3. The aim is to simulate a worst-case scenario so that the recommended design of the thickness of the concrete shield is thick enough for the worst conceivable incidents. In Figure 3, we show an envisaged incident in which the proton beams of 350 µA at 70 MeV hits the beamline close to the wall.

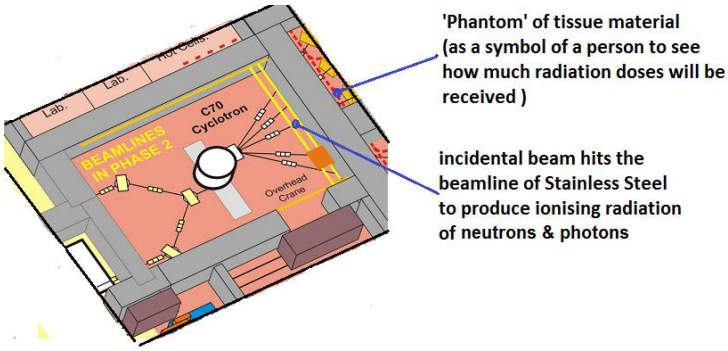

Figure 3: The 3D view of the Cyclotron vault with its ordinary concrete shield.

We then emulate a person standing on the other side so we can measure the fluence-rate of ionising radiation at that point. This fluence-rate must be converted into better understood quantities like effective dose rates and absorbed dose rate, because these quantities are used to determine the maximum annual occupancy times in the radiation area for radiation workers, general workers and the public. This correct thickness of the shielding wall, once determined, will form the basis for guidance in the broader shielding of the whole facility.

The iThemba LABS RIB project will require a huge financial commitment and thus building towards the final stage will involve steps that will confirm its feasibility. For that reason, the RIB Demonstrator project is proposed to test and demonstrate the advantages of the overall RIB project [1]. Figure 4 shows the area considered for this purpose. Because some structures like the proton beamline and the vault already exist, it can be considered a relatively low budget stage

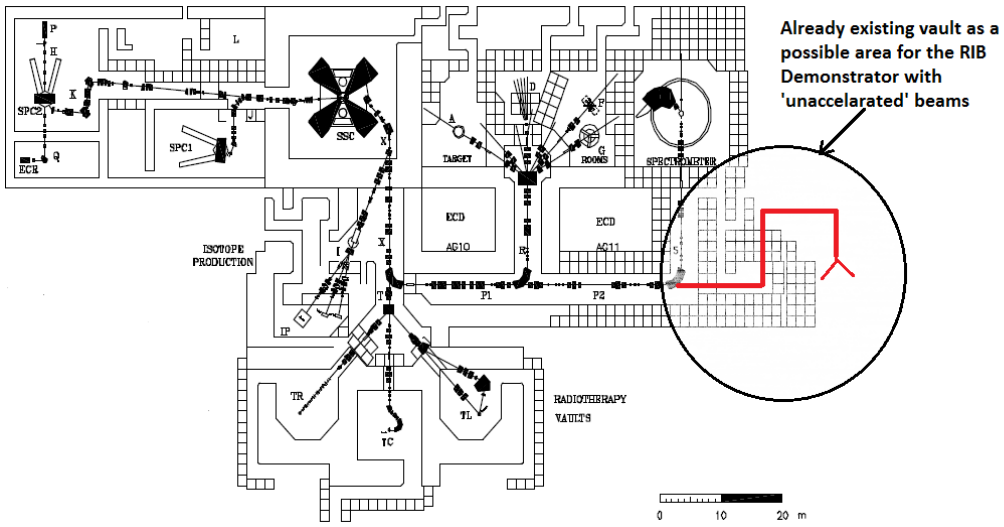

Figure 4: The floor plan of the existing structure of iThemba LABS. It also shows the possible location of the RIB Demonstrator facility. The red line shows the anticipated beamlines from the SSC to the shielded vault and then to the experimental room for RIB purposes.

However, RIBs produced with this demonstrator will not be accelerated, thus posing some limitations, but good enough to simulate the broader RIB project. Figure 5 shows the proposed RIB Demonstrator facility with the extended experimental room in which both nuclear and materials research experiments will be performed.

Similar to the negative-ion cyclotron vault which will produce ionising radiation, here the operation of the Demonstrator facility will be to bombard a uranium carbide target with a proton beam so it can fission. Part of the fission products are prompt neutrons at high energies.

- It is necessary to investigate whether the 3 m concrete shielding in this vault will be sufficient for areas outside the experimental room to be occupied safely by personnel.
- The vault is not completely closed and presumably neutrons will be isotropically distributed and thus a considerable amount will exit in the direction of the vault openings. One opening is connected to the entrance area of the spectrometer shown in the diagram. Locked doors prevent access into the various labyrinths during operation.

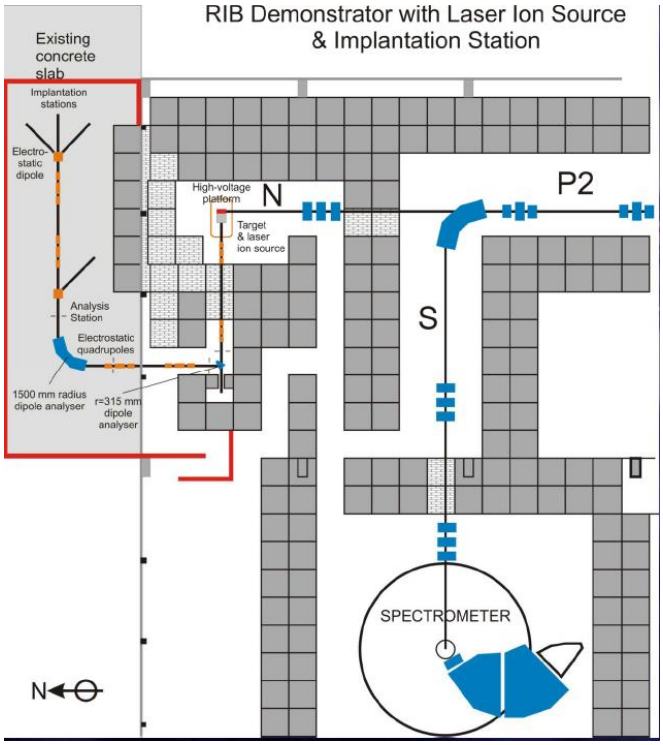

Figure 5: Plan view of the RIB Demonstrator vault, marked with N, where the target and laser ion source will be situated.

- The beamline extending from the vault to the experimental room allows neutrons to escape from the vault and make a beam towards the dipole analyser. These neutrons will increase radiation levels at the entrance and in the outside yard as well.

1.2 Research focus

1.2.1 Safety:

To ensure that ionising radiation is kept down to acceptable levels for different categories of personnel to access areas being investigated: (a) radiation workers, (b) general workers of iThemba LABS and (c) the general public visiting the facility.

1.2.2 Cost effectiveness:

Low activation rates avoid the need for replacements of radiation-damaged components.

The thickness of the shielding walls must be adequate, but an over-designed thickness does not provide any benefits, while additional money is spent.

1.3 Overall research aim and individual research objectives

1.3.1 To analyse radiation transport from all identified possible sources including the proton beam and activated beamline during emergency situations inside the new cyclotron vault.

1.3.2 To analyse transport of neutron and photon radiation arising from protons irradiating the UC_x target in the demonstrator facility.

1.3.3 To configure different thicknesses of the concrete shield of the new cyclotron vault and to recommend the thickness needed for radiation safety.

1.3.4 To configure different thicknesses of the concrete shield of the demonstrator vault and confirm that the current vault concrete thickness is adequate.

1.3.5 To classify the different areas and determine radiation safety levels in access areas for different categories of personnel to access those areas within or near the cyclotron vault and the Demonstrator facility.

1.3.6 To configure radiation absorber material in identified areas to meet safe levels.

1.4 Value of the research

- Safety: to ensure the shielding is sufficient and to verify the adequacy of protection against possible beam control accidents.

- Planning & improved design of the investigated facilities.
- Cost effectiveness of the RIB project:
- A baseline for future research for comparison with experimental investigations.

1.5 Dissertation Outline

CHAPTER 1: INTRODUCTION

- This provides the overall picture of the RIB project at iThemba LABS; in particular the rationale for Radiation Shielding calculations.

CHAPTER 2: LITERATURE REVIEW

- This chapter looks at the facilities similar to iThemba LABS which produce similar levels of ionising radiations. Some facilities exist and some are under design. Some facilities share the possible sources of ionising radiation with the anticipated RIB project. It thus investigates tools used to confirm or predict radiation safety levels. It appears that the Monte Carlo Neutral Particle eXtended (MCNPX) code is suitable to be used to perform calculations. Random Theory and Monte Carlo techniques as applied to particle transport are explained, MCNPX specifications that the user put in the input data set are described.

CHAPTER 3: METHODOLOGY

- This chapter explains the procedure of MCNPX, and how it was actually used to estimate radiation levels for facilities in question. Also, ways to ensure correct and accurate results are outlined.

CHAPTER 4: DATA ANALYSIS; FINDINGS AND DISCUSSION

- Here results are presented both as tabular or figural form; necessary comparisons and findings are discussed.

CHAPTER 5: CONCLUSIONS & RECOMMENDATIONS

- Results found and legal considerations relating to radiation shielding are analysed, and conclusions are drawn for the various scenarios that were considered.
- Further recommendations are made with regards to the current research for cases of future research and improving current results.

APPENDIX

- Useful documents are attached here for reference.

CHAPTER 2: LITERATURE REVIEW

2.1 Introduction

This chapter will consider radiation safety aspects at iThemba LABS and in other similar facilities. It explores the extent of the use of Monte Carlo codes for radiation transport, to estimate safety levels and its trustworthiness.

2.2 Radiation Shielding and Safety Systems

Radiation poses many challenges which are summarised in Johann van Rooyen's manual as follows [6]:

- Ionising radiation presents a health risk;
- Deontological ethics: the duty to protect people & the environment from excessive radiation health risk;
- Radiation protection recommendations by the ICRP; radiation protection standards set by the International Atomic Energy Agency (IAEA);
- National radiation protection legislation;
- The "international best practice" principle;
- Ionising radiation and radioactivity are emotional subjects that are politically sensitive.

Thus as a response to these challenges, Engineered Radiation Safety Systems are one component of Radiation Protection. Other components which will not be dealt with here include Management Controls and instilling Safety Culture in the workplace.

The Engineered Radiation Safety system may be subdivided into two sub-systems [6]:

- Access Control System, and
- Radiation Containment System

An Access Control System has to do with control and prevention of human entry into radiologically unsafe areas.

Radiation Containment, on the other hand, includes shielding (for big areas we use thick walls and for smaller radiation sources we used local shielding), labyrinths doors and beam dumps.

A Radiation Containment System is said to be "active" if it is movable and applicable when safe radiation levels have been exceeded, otherwise it is said to be "passive", like permanent shielding walls [6].

2.3 Criteria for judging radiation shielding

In order to decide on the adequate radiation shield, we need to quantify radiation at the possible radiologically unsafe areas. The biological threats to humans come from ionising radiation which transfers its energy (Joules) into the human body (kilograms). So, *absorbed dose* is the measure of the average amount of energy imparted to the medium per unit mass. The standard units of measurements are gray (symbol Gy) and sievert (symbol Sv) derived from 1 J / kg = 1 Gy = 1 Sv.
For different tissue organs, we have different radiation effects and the *equivalent dose* measures the effect for a specific tissue with unit of measurements of sievert.
Therefore, absorbed dose by a person is obtained by averaging over all irradiated tissues and this is called *effective dose* also measured in sievert.

The aim of this study is to decide on the thicknesses of the shielding necessary for the two facilities: new cyclotron vault & RIB Demonstrator vault so that dose rate limits received in the simulation is below dose rate limits as determined for different personnel accessing the these two facilities.
Table 1 lists the radiation limits to which personnel may be exposed to. Below are the assumptions that were adopted so as to deduce and project effective dose rates from Sieverts/year to Sieverts/hour of the Radiation worker and equivalently it was done for the Public and Non-Radiation Workers:

- Exposure time is 8 hours per day
- work only 5 days per week
- there are 4weeks per month
- there are 12 months in a year

This gives the total number of hours per year to be 1920 hours of possible exposure to radiation areas.
Therefore, for a Radiation Worker with the limit of 20mSv/yr, we convert this value into 20 000 µSv/hr. Using the factor of 1920 hours, the effective dose rate limit becomes 10.417 m Sv /hr. The same was done for the Public and Non-Radiation Worker personnel.

Table 1: Effective dose rate limits as recommended by ICRP 2007

Personnel	effective dose rates (mSv/year)	Projected effective dose rates (μSv/hour)
Radiation Worker	20	10.417
Public/ non-Radiation worker	1	0.521

This means that in areas where the dose rate is greater than specified amount, the corresponding personnel will be prohibited to access that specific area.

The next section discusses four (4) types of criteria used to judge the effectiveness of the shield in order to be within dose rate limits.

2.3.1 Design-base dose or dose budget

The International Commission on Radiological Protection (ICRP) recommends dose limits, which are thoroughly revised once every 15 to 20 years. Usually these limits are adopted as national legislation and to comply with this legislation, facilities have to introduce dose constraints. Based on dose constraints in force at a facility, e.g. the constraint on the annual effective dose, *derived dose constraints* may be calculated. Radiation shielding must be designed, and jobs involving exposure must be subject to management controls. Personnel accessing the facility are normally categorised as (1) radiation workers, (2) general workers, as well as (3) members of the public,

A *design-base dose constraint* or *dose budget* for the task is derived when, knowing the maximum realistic source-term as well as typical times that the above categories of personnel will spend performing specific jobs in radiation areas, we can design shields and develop working procedures that will maintain the total annual exposures of workers below a target dose constraint.

2.3.2 Maximum tolerable dose rate

Shielding design must consider the design-base doses. Given a budgeted design-base dose of D_{eff} (for annual budget, it is $annual\_D_{eff}$) and the period the worker must spend in a certain area, time t (year long period is $annual\_staytime$), then the tolerated dose rate is given by $\frac{D_{eff}}{t}$. In other words, shielding must be designed to ensure that dose rates on the personnel-side of the shields are lower than the value given by:

Annual based dose-rate constraint for the task = $\frac{annual\_D_{eff}}{annual\_staytime}$ ..... (1)

2.3.3 Dose attenuation factor

Radiation shields have a dose attenuation factor (DAF), defined as the ratio between transmitted dose rate with the shield in place and transmitted dose rate without the shield in place. If the shield has a DAF of 1/150, it means that the shield decreases the dose rate to a value 1/150 of the radiation level before the shield is applied.

2.3.4 Projected annual dose

Suppose the realistic annual staytime t_{yr} in a radiation area with the corresponding maximum realistic average dose rate of D_{av}.The projected annual dose that the worker will receive, is given by:

Projected annual dose = (D_{av}) x (t_{yr}) ..... (2)

2.4 Review of similar Accelerator Facilities & Vaults

As early as 1991, at iThemba LABS, radiation transport calculations have been done by Steyn et al. [3] for the local radiation shield of the target bombardment station at the Isotope Production Facility. The target is bombarded with a 66 MeV proton beam of 100 μA. The study looked at the radiation damage caused in the materials inside the vault by this high-intensity proton beam when irradiating the target which produces radiation fields. Thus the suitable local radiation shielding was designed to enclose the target shown in Figure 6. Using the realistic source term for the neutrons produced during bombardment in the target, radiation transport calculations could be done. Calculated neutron and gamma ray dose rates and DAFs were used to configure and optimize the shield. At the time, this study concluded that particularly for future local shields, complementary materials should be used at iThemba LABS, that is a 40 cm thick inner iron layer, 20 cm thick paraffin wax with 2.5% boron carbide and a 4 cm thick outer lead layer [3].

Note that the vault that confines this bombardment station has concrete walls of 4.5 ms thickness [3].

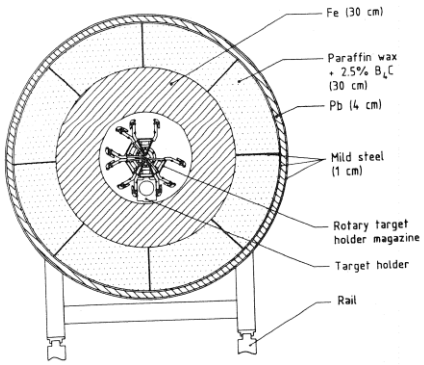

Figure 6: The cross sectional view of the target chamber in the bombardment station. Three complementary layers of materials were investigated for optimum shielding [3].

In 2006, F. M. Lukhele, did work for his MSc [4] on the horizontal target bombardment station, which was aimed at establishing activations of the vault and other components and keeping them as low as possible, as it is not only challenging to replace those activated components but expensive as well. Radiation sources were similar to those of Steyn et al. and MCNPX was used as the radiation transport calculation code. Primarily, dose attenuating factors (DAF) of complementary materials for different configurations were compared [4]. So MCNPX code proves to be reliable for this type of simulations.

In 2009, the project titled European Isotope Separation On-Line Radioactive Beam Facility (EURISOL) funded by the European Commission, aimed at increasing the radioactive ion beam intensities by several orders of magnitude using a proton beam of 1 GeV of up to 4 MW to bombard a multi-MW target. Now this will lead to levels approaching those of a reactor in terms of radioprotection safety as a result. This is one of the latest high profile projects, and the radiation transport calculation code MCNPX was used together with FLUKA [5].

Guided by the ICRP60, which stipulates the dose levels of 0.1 μSv/hr for public areas and 10 μSv/hr for controlled areas. The geometry of the materials used for shielding and thicknesses for EURISOL target is shown in Figure 7 and were examined as follows:
For the “direct” target, MCNPX was use to test the neutron/photon attenuations of two main shielding materials, i.e. concrete and iron, and results gave good confidence with only some deviation for the photon flux in iron, which was overestimated when compared to simulations of the CINDER’90 code [5], resulting in the estimation of concrete needed around the beam dumps to be 5 m thick.

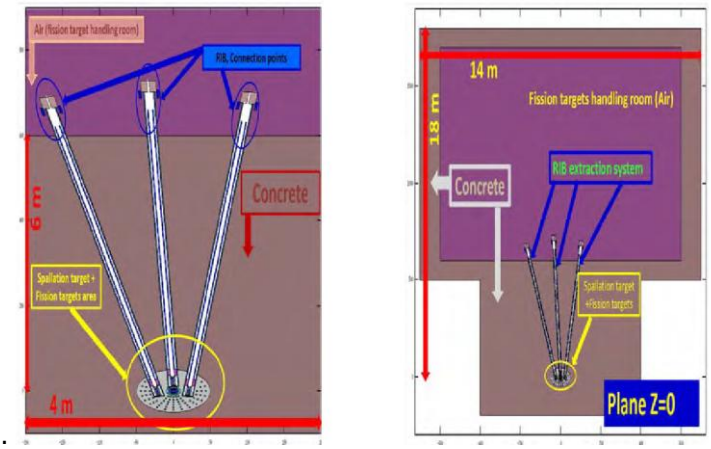

Figure 7: (Left) The geometry of the spallation target and fission target showing the RIB extraction tubes and connection points, in the z=0 plane, i.e. the level of the proton beam. (Right) On the same level, this figure extends to include the fission target-handling room [5].

Calculations for the multi-MW target to reach the ambient dose equivalent rate of 1 μSv/hr were performed and they led to the total shielding thickness of 6 m [5].

A project that has many aspects matching the iThemba LABS RIB project is the Selective Production of Exotic Species (SPES) project which is in progress in the Legnaro National Laboratory in Italy. Unlike the EURISOL, SPES will be using 70 MeV proton beam of 300 μA onto the UC_x target. The geometry of the SPES accelerator vault is shown in Figure 8 [7].

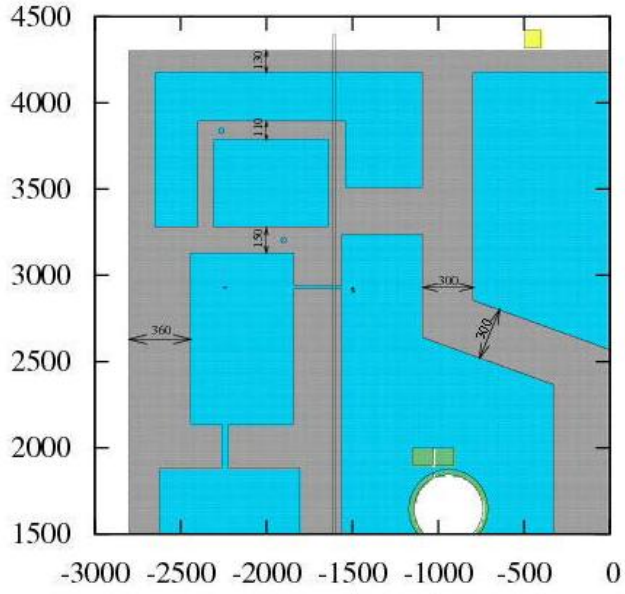

Figure 8: Concrete shielding in greyish colour with thicknesses labelled. The circular figure is the cyclotron. These thicknesses shown are final recommendations for shielding purposes [7].

Sources of radiation include the current of approximately 15% (112 μA) lost in the cyclotron during acceleration and extraction [7]. Another source is due to about 0.6% of the current (about 3 μA) being lost in the bending dipoles [7]. Another contribution to radiation is from secondary particles backscattered by the target; however, these are negligible [7]. The FLUKA Monte Carlo code was used to simulate radiation transport calculations and the following conclusions were reached.

Shielding walls made of 360 cm of concrete are suggested in the forward-direction of the proton beam to meet the maximum of 5μSv/hr for controlled classified areas and 0.3 μSv/hr for non-classified areas [7]. A thickness of 300 cm for the side walls will reduce the outside dose rate to be less than 1 μSv/hr. The calculation of this attenuation is shown in Figure 9.

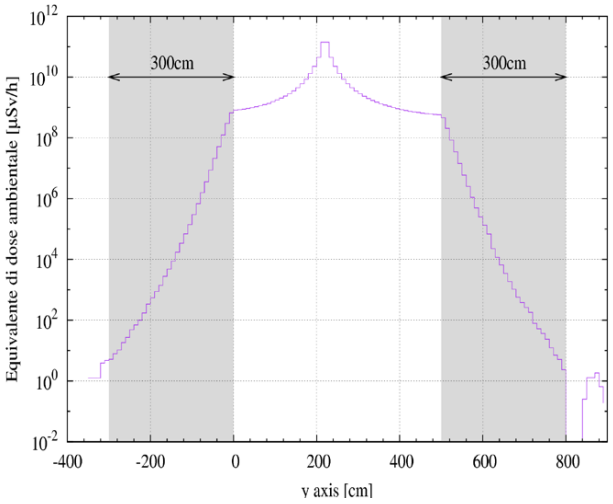

Figure 9: The dose-rate from the source centre which is highest at about 10^{11} μSv/hr. To the left of the wall surface it reads 10^{9} μSv/hr, or right to the wall surface it reads below 10^{9} μSv/hr, a two order decrease. At the wall surface outside of 300cm thick concrete, it reads about 5 μSv/hr whilst on the right it reads about 2 μSv/hr. [7]

In his MSc project, T. E. Sibiya [8] verified the radiation shielding design for both Stellenbosch insect sterilisation facility and High Energy Processing (Pty) Ltd (HEPRO) irradiation facilities. He also performed dose distribution calculations for these facilities.

The source of radiation in the Insect Sterile Facility is the Cobalt-60 source which decays by giving off two prompt gamma photons of 1.173 & 1.332 MeV [8]. Simulated radiation transport calculations were performed using MCNPX 2.5.0.

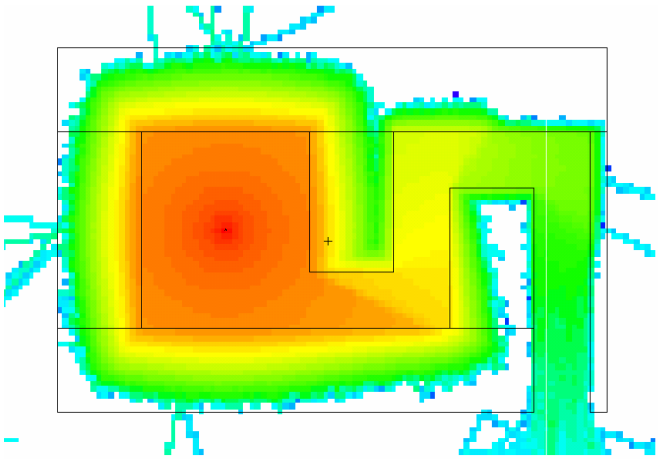

Figure 10: The layout of the Insect Sterile Facility concrete shielding area as seen from the top, including the spatial distribution of dose rates in μSv/hr. Note the effect of the labyrinth as the colour changes from red through to blue, expressing the decreasing dose rates [8].

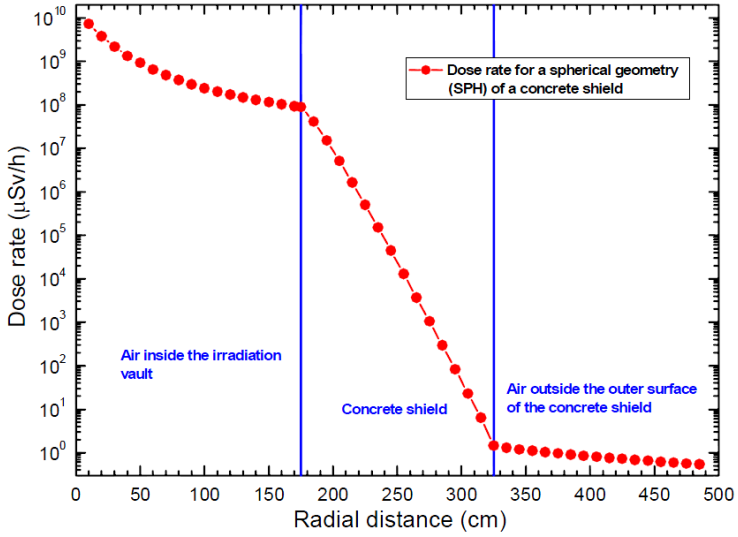

Figure 11: The dose rate distribution in the radial direction of the 150 cm thick spherical concrete shield. At the source point, the dose rate is 10^{10} μSv/hr, at the wall surface located 175cm from the source reads about 100 Sv/hr. On the outside wall surface the dose rate recorded is just above 1μSv/hr [8].

Figure 11 shows the calculation of the spherical concrete shield for the purposes of simplified and symmetrical geometry.

Sibiya et al. concluded that the MCNPX code is appropriate to perform dose distribution calculations, having compared it to calculations using other methods like MathCAD [8].

In conclusion, the above review of the facilities shows that Monte Carlo codes, particularly MCNPX, were used for radiation transport calculations for cases very similar to the one we are investigating in this project. Similarities include the radiation sources, particles and radiation transported (neutrons & photons) and shielding materials.

To return to my research objectives: radiation from incidental irradiation of the beam lines by protons will occur, in which case (p,n) and (p,$x\gamma$) reactions will take place, so that neutrons will be transported as well photons. Ordinary concrete will be investigated as a shielding material. Calculations will be guided by dose rates and safety levels (see Table 1) in access areas according to the criteria for the stay-time guidelines for the public, general workers and radiation workers of iThemba LABS.

In the same way, ground water contamination will also be prevented by having a thick concrete slab as the floor of the facility.

2.5 Monte Carlo, Random theory and particle transport

2.5.1 Particle transport

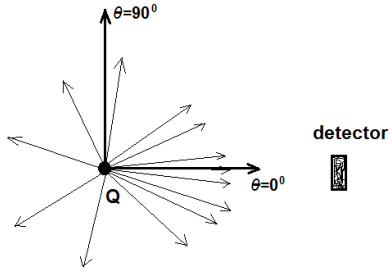

Let us evaluate the random transportation of particles from the point source Q to the detector as shown in the diagram at right. These particles are in state p undergoing $k\,(0,1,2,....k)$ collisions. Now we can define the general state p as $p=(\vec{r},\vec{v})$

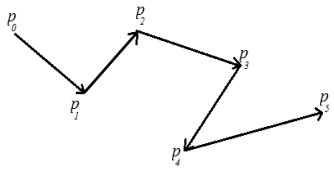

where $\vec{r}$ '= the initial position vector of the particle;

$\vec{v}$ '= the initial velocity vector of the particle

$\vec{r}$ = the next position vector of the particle;

$\vec{v}$ = the next velocity vector of the particle;

$Q(r',v')$ = source term, a function that represents the initial particle state (p_0), that is initial position $\vec{r}$ ' and velocity $\vec{v}$ '.

$\Psi(r,v)$ = particle density leaving the source or emanating from collisions in the medium;

$C(v'\rightarrow v,r')$ = the collision kernel, i.e. the probability of a change in velocity at a fixed position. It is used to estimate the velocity after the collision;

$T(r' \to r, v)$ = the transport kernel, probability of a change of position at a fixed velocity. It used to estimate the next point of collision.

The transition probability R from a state p' to a state p is given by the product of the collision and transport kernels:

$$R(p' \to p) = C(v' \to v, r') \cdot T(r' \to r, v)$$

The initial particle density $\Psi_0(p)$ depends on the particle source distribution and the probability of the next collision point, which is given by the integral of the product of the source term Q and the transport kernel T: $\Psi_0(p) = \int Q(r', v) \cdot T(r' \to r, v) dr'$

The particle density $\Psi_k(p)$ making the k^{th} collision is the integral of the product of the particle density $\Psi_{k-1}(p')$ in the previous $k-1$ collisions and the transition probability:

$$\Psi_k(p) = \int \Psi_{k-1}(p') \cdot R(p' \to p) dp' \quad \text{..... (3)}$$

This shows that the k^{th} particle density depends only on the $k-1^{th}$ collision and not any previous collisions.

We can thus gather all the histories (i.e. states p_0, p_1, p_2 ...) of the particle from the starting state (p_0) to the current state of after the k^{th} collision:

Thus we have:

$$\Psi_k(p) = \int \ldots \int \Psi_0(p_0) \cdot R(p_0 \to p_1) \cdot R(p_1 \to p_2) \ldots R(p_{k-1} \to p) dp_0 \ldots dp_{k-1} \quad \text{..... (4)}$$

This is a version of the Boltzmann transport equation (BTE). However, as a consequence of its mathematical complexity, it cannot be solved analytically for problems of practical interest; we have to resort to numerical techniques. The Monte Carlo method solves these integral problems, so we can use this method to find a solution to the linear BTE (Equation 4) for particle transport calculations [9].

The Monte Carlo method is a computational technique that uses algorithms based on random sampling to calculate results [6].

In the case of particle transport, particle trajectories are simulated individually according to the stochastic (non-deterministic and random) nature of the physical interactions. The treatment is in terms of probability distributions, for instance the probability that a given number of particles (in an energy & solid angle interval) traverse an element of area. The

stochastic approach (e.g. a Monte Carlo method) allows the calculation of any deterministic quantity as the average of the corresponding stochastic one over its probability distribution. The simulation of particle trajectories is performed with Monte-Carlo techniques.

2.5.2 Monte Carlo and Random theory

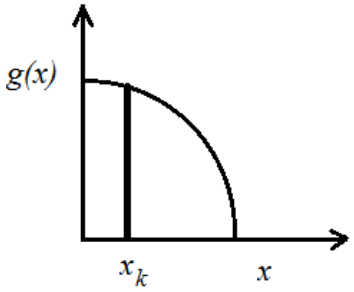

We begin with a simple example to illustrate the Monte Carlo technique. Here we want to estimate the area G under the curve given by $g(x)$. This curve is quarter of a circle with radius 1, so we need to evaluate

$$G = \int_0^1 g(x)dx \text{ with } g(x) = \sqrt{1-x^2} .$$

Analytic solution: The curve represents one quarter of the area of a unit circle, so $G = \frac{\pi}{4}$.

Monte Carlo solution: We can have a square shape of known area to estimate the area of the curve. The idea is to throw stones (points) randomly on the square and evaluate if the point falls within the curve (hit) or outside the curve (miss). The *ratio* of 'hits' to total number of trials constitutes an equivalent percentage of the area of the curve to that of the area of the square.

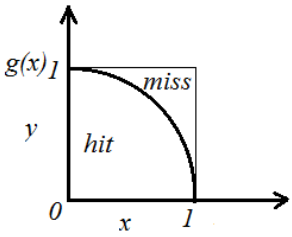

Clearly for a more accurate answer, a large number of trials '*k*' are needed. N is the total number of trials. The area under the curve is given by the area of a square with unit dimensions multiplied by this *ratio.*

For *k* = 1,.....,*N* we choose x_k y_k randomly between 0 and 1. Once the point is thrown onto the square, we need to evaluate whether it is a 'hit' or a 'miss' by testing whether $\hat{x}_k^2 + \hat{y}_k^2 \le 1$: if so, then we tally that point as a 'hit'.

Then $G =$[area under the curve] $\approx \frac{Number\_of\_hits}{N} \times$ area of a square..... (5)

With the simulation approach, the idea is as follows

- Generate a random point (between 0 and 1).
- Evaluate it mathematically ('hit' or 'miss').

- Register the outcome ('miss' is rejected whereas a 'hit' is accepted).
- Repeat until you have enough trials.

Monte Carlo for particle transport

Monte Carlo simulations are used for particle transport, random number generation, random sampling, collision physics, measuring quantities, statistics, and variance reduction. In the case of particle transport, the Monte Carlo technique does not solve the integral Boltzmann transport equation but approaches the solution using numerical simulations [9].

We want to simulate a neutron source, for example, and then to transport the neutrons through some medium to measure their fluence-rate at some point. We use the Monte Carlo technique to simulate the history of one particle at a time from birth to death and repeat this for as many particles as required for statistical purposes.

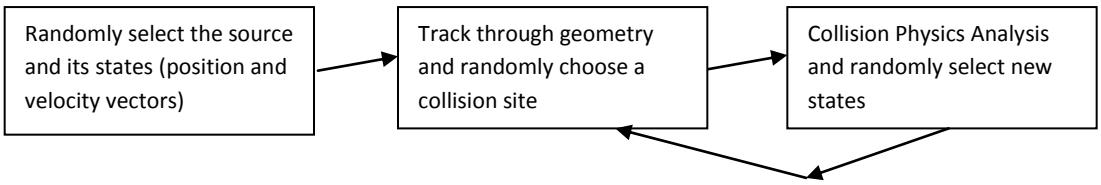

The above diagram shows that the process that one particle follows from the source until it is measured at the point of interest. F. B. Brown makes a list of assumptions in particle transport using Monte Carlo methods [9]. These include (but are not limited to) the following:

- Static, homogeneous medium
- Time-independent
- Markovian – next event depends only on current (*r,v,E*), not on previous events
- Particles do not interact with each other
- Neglect relativistic effects
- No long-range forces (particles fly in straight lines between events)
- Material properties are not affected by particle reactions [9].

The particle is randomly selected from the source with its initial position and velocity assigned. The next step is the random sampling of the target which this particle will collide with. The particle travels in a straight line to the next collision site. In the collision of these

particles, nuclear reactions take place and the results of the reactions are determined by probability distribution functions associated with cross sections saved in the code libraries. In all the particles that resulted from the reaction, only one particle will be further transported and the rest are saved in the particle transport code memory called ‘bank’ for later transport. For this one particle to be transported further, its position and velocity are randomly assigned. This particle is tracked until it reaches the area of interest in the geometry of the simulation and quantities of interest can be measured.

So in general there are three aspects of the simulation which can be understood to be interacting during the particle transport simulation routines are: Geometry; Collision Physics and Tallies [9].

With Geometry, we are concerned with the position of the particle; determining what particle it will hit next and knowing the material in which it travels, etc.

In Collision Physics we want to know the energy of the particle, what is it colliding with, what are the secondary particles and to determine the new direction(s), etc. Collision Physics models the particle’s physical interactions with the material through which it is transported. Random sampling is controlled by probability distribution functions (PDFs) determined by cross-section data kept within the particle transport code libraries.

During the process of random simulation of particle transport, the user may want to extract information about the particle being transported. The quantity being measured is called the “Tally”. Tallying involves performing measurements of number of collision events, energy binning for particles in a certain region and statistics, etc.

Depending on the quantity being calculated like exit energy, the estimate value of the exit energy may be derived from the states of defined history found in the particle transport code libraries.

Monte Carlo particle transport depends on random sampling. Random sampling models the outcome of physical events (e.g. neutron collisions, fission process, sources, etc.) These physical events have known probabilities of occurring. So mathematically the random variables used during sampling have to pass a randomness [14] before they can be adopted onto the particle transport code.

Random Variable:

This variable can have an associated discrete probability distribution (discrete random variable) or a continuous probability distribution (continuous random variable). Here discrete random variables sample specific values, each with some sort of probability greater than zero. Continuous random variables are considered with any of a range of values. An example will be to sample real numbers between 0 & 1. [14].

A continuous random variable is used to determine quantities like: flight distance, exit energy and direction, etc. And discrete random variables are used to select nuclide, interaction type, secondary particles, etc.

Discrete sampling: PDF $p(x)$ is the probability that the outcome of a random process is x.

Continuous sampling: PDF $p(x)dx$ is the probability that the outcome takes the value between x and $x+dx$. For both discrete and continuous probability density functions, when normalised, the probability of getting any of the possible outcomes is exactly 1.

Random Variables are generated using Random Number Generators (RNG) and details of the RNG are in Appendix 5

2.5.3 Interaction of neutrons with matter

Neutrons are uncharged, thus during nuclear reactions they can penetrate through to the nucleus without having to overcome the Coulomb barrier as charged particles do. This may even allow the neutron to interact at very low energies called thermal energies [13]. At room temperature the neutron energy $E_n = kT$ = 0.0025eV, where k = Boltzmann constant, and T = room temperature = 293K.

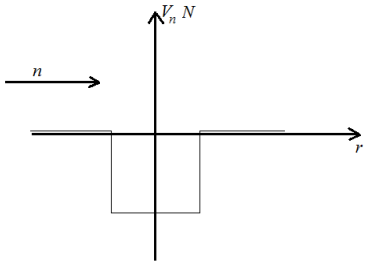

A charged particle will have to overcome the Coulomb barrier if it has to interact with the nucleus. Take an incident proton *p* on the nucleus *N.* For a successful impingement, the incident proton must have threshold energy, otherwise an elastic scattering reaction will occur.

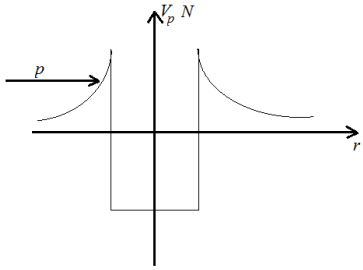

When the incident neutron reacts with the nucleus, it will either scatter elastically or form a Compound Nucleus (CN) provided the energy of the incident neutron is not too high. The probability of it to scatter is known as the scattering cross section (σ_s), whereas the probability for it to form a compound nucleus is the compound nucleus cross-section (σ_t^{CN}). Thus total cross section for the nuclear reaction by the incident neutron is [13]:

$$\sigma_t = \sigma_s + \sigma_t^{CN} \quad \text{..... (6)}$$

a) Scattering reaction

To express the scattering reaction illustrated by the diagram, we use the following notation:

$$n + {}^{A}X \rightarrow {}^{A}X + n \quad \text{..... (7)}$$

n - incident neutron
${}^{A}X$ - target nucleus
θ_L - scattering angle
i - incoming
o - outgoing

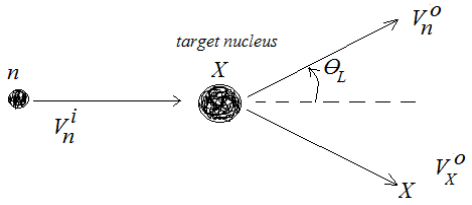

b) Compound Nucleus (CN) formation

In contrast to the scattering of the neutron is the phenomenon in which the neutron is absorbed by the target nucleus, forming the compound nucleus in an excited state:

$$n + {}^{A}_{Z}X_N \rightarrow {}^{A+1}_{Z}X^{*}_{N+1} \quad \text{..... (8)}$$

The kinetic energy of the neutron is distributed equally amongst all nucleons in the nucleus. In the exit channel of this type of reaction are many different possibilities.

The CN cross section is inversely proportional to the speed of the neutron, expressed as:

$$\sigma_t^{CN} \propto \frac{1}{v} \propto \frac{1}{\sqrt{E}}, \text{ where } (E = \frac{1}{2}mv^2) \quad \text{..... (9)}$$

where v and E are velocity and energy of the neutron respectively. [13]

This equation (9) means the slower the velocity of the incident neutron the higher the chance for the CN to be formed. This relationship is more dominant in light nuclei.

There are four possible exit channels when the Compound Nucleus is formed and we look at these below.

i) Inelastic scattering (σ_i)

After the CN is formed, the neutron is released with less energy leaving the original nucleus at the excited state and then this extra energy is released as a photon.

$$n + {}^{A}_{Z}X_{N} \rightarrow {}^{A+1}_{Z}X^{*}_{N+1} \rightarrow {}^{A}_{Z}X^{*}_{N} + n \quad \text{..... (10)}$$
$$\downarrow$$
$${}^{A}_{Z}X^{*}_{N} + \gamma \text{-emission}$$

ii) Radiative capture (σ_c)

There is a probability that the CN will not release the neutron, but instead decay through gamma emission. As the excited energy of the CN is about 8 MeV of the binding energy of the incident neutron, several photons will be emitted before ground state is reached.

$$X^{*}_{N+1} \rightarrow {}^{A+1}_{Z}X_{N+1} + \gamma \text{-emission} \quad \text{..... (11)}$$

iii) Emission of a light charged particle (σ_r)

This depends on the energy of the incident neutron, to supply the energy required to expel a charged particle like a proton from the nucleus. If the proton is released, then a new nuclide is formed. This reaction is expressed as follows:

$${}^{A+1}_{Z}X^{*}_{N+1} \rightarrow {}^{A}_{Z-1}X_{N+1} + p \quad \text{..... (12)}$$

iv) Fission (σ_f)

For heavy nuclides mostly, we include neutron-induced cross sections where the CN splits into lighter nuclei and free neutrons and photons.

$${}^{236}_{92}U^{*}_{144} \rightarrow {}^{147}_{57}La + {}^{87}_{35}Br + 2n \quad \text{..... (13)}$$

Therefore the total cross sections of the CN is expressed as follows:

$$\sigma_t^{CN} = \sigma_i + \sigma_c + \sigma_r + \sigma_f \quad \text{..... (14)}$$

Substituting (14) in (6), we have:

$$\sigma_t = \sigma_s + \sigma_i + \sigma_c + \sigma_r + \sigma_f \quad \text{..... (15)}$$

In a medium of material M through which the neutron is transported with N nuclides to possibly react with, then we can express the total macroscopic cross section as [9]:

$$\sigma_T = sum\ \ N^j \sigma_t^j \quad \text{..... (16)}$$

N^j = the number of nuclides of isotope *j*

σ_t^j = the total microscopic cross-sections of the nuclides of the isotope *j*

Here the assumption is that the material is uniform and homogenous.

If the material M has isotopes *j* and *k,* then the probability that the neutron interacts with isotope *j* is given by [9]*:*

$$p_j = \frac{N^j \sigma_t^j}{\sum_k N^k \sigma_t^k} \quad \text{..... (17)}$$

$\{p_j\}$ = the set of discrete probabilities for selecting collision isotope *j*

With the incoming particle, the sampling procedure is done, cross section tables are retrieved, processed and if the probability is highest for isotope *j* then it is chosen for the reaction.

Now consider equation (15) for probable reaction types: elastic scattering, radiative capture, etc. The probability that the reaction is elastic scattering in the isotope *j* is given by:

$$p_s = \frac{\sigma_s^j}{\sigma_t^j} \quad \text{..... (18)}$$

$\{p_s\}$ is the set of discrete probabilities for selecting scattering reaction *s.*

Again the sampling procedure is done, cross section tables are retrieved, processed and if the probability is highest for scattering reaction *s* then it is chosen for the reaction type.
The next process to consider is the emitted particle, for which we need to sample the free-flight distance (mean free path length) to the next collision.
Consider the total macroscopic cross section in the transport medium σ_T :

σ_T is the probability of any reaction per unit distance (p.u.d), with units of cm^{-1}

The PDF for the free-flight distance *s* is expressed as:

$f(s)$ = {probability reaction p.u.d} × {probability of travelling distance *s* without reaction}

$$f(s) = \sigma_T \exp(-\sigma_T s) \quad \text{..... (19)}$$

$s = \{0, \infty\}$

If the probability of travelling without reaction is $\exp(-\sigma_T s)$, then the probability for it to travel and react is: $1 - \exp(-\sigma_T s)$. Thus the sampling procedure is done and the next most probable free-flight distance is selected from the function given by:

$$F(s) = 1 - \exp(-\sigma_T s) \quad \text{..... (20)}$$

There are many sampling procedures explained in detail in [9] that will be done during the particle transport simulation, amongst them will be to select for the exit particle: its energy and direction.

2.5.4 Tallying

In the last section we have considered sequences of events that take place during the transport of one particle, at least from start to finish. We looked at the particle leaving the source and interacting with matter.

During the transport simulation the user may measure certain events. Let us take a detector placed in a radiation field described by the directional fluence-rate distribution function. The reaction rate at the detector point will depend on a linear interaction coefficient. The effects of a radiation field on the material can be described by the response function which describes how the detector material responds to the radiation field.

Tallying involves some of the following events and portions of phase space [9]:

– Range of energies, $E_1 - E_2$

– Range of particle times, $t_1 - t_2$

– Specified cells

– Specified surfaces

– Specified reaction cross-sections σ_X

– Secondary particle production

– Energy deposited in cell.

Below is a general equation used to generate an estimate of a specific quantity. This equation takes an average of a quantity A over p states for M histories.

$$A = \int A(p) \cdot \Psi(p) dp \approx \frac{1}{M} \cdot \sum_{m=1}^{M} \left(\sum_{k=1}^{\infty} A(p_{k,m}) \right) \quad \text{..... (21)}$$

Mathematically the average of that quantity is just its expectation value summed over all possible states. Inside a phantom we can tally A as the number of neutrons with energy range $E_1 - E_2$. Here k could define the energy range and M be the number of particle histories in this energy range.

2.5.5 Statistics of measurements

Just as in any experiment performed with outcomes x_j, after N trials, the sample mean is given by:

$$\text{(Mean)}\ \bar{x}_N = \frac{1}{N}\sum_{j=1}^{N} x_j \quad \text{..... (22)}$$

The Monte Carlo simulation that records the history of N transported particles will have a similar expression for the mean of the sample, which becomes the expected value of the sample.

To investigate how each value varies from this expected value, the difference between each measurement (x_j) and mean ($\bar{x}$) is calculated.

The variance (σ^2) is simply the average of the squared differences of x_j and $\bar{x}$:

$$\text{(Variance)}\ \sigma^2 = \frac{1}{N}\sum_{j=1}^{N} x_j^2 - \left(\frac{1}{N}\sum_{j=1}^{N} x_j\right)^2 = \frac{1}{N}\sum_{j=1}^{N} x_j^2 - \bar{x}^2 \quad \text{..... (23)}$$

This is also called the “population variance” in transport codes.

Variance of the mean: $\sigma_{\bar{x}}^2 = \frac{\sigma^2}{N}$ ..... (24)

The standard deviation (σ) is the square root of the variance i.e. $\sqrt{\sigma^2}$.

The third component of statistical analysis to be considered is the confidence level on the estimated mean.

We may want to compare the standard deviation of the mean ($\sigma_{\bar{x}}$) to the mean value ($\bar{x}$) by taking their ratio, called the relative error (RE):

$$RE = \frac{\sigma_{\bar{x}}}{\bar{x}} \quad \text{..... (25)}$$

The overall quantity to characterise the usage and performance of the Monte Carlo code is called the figure of merit (FOM):

$$FOM = \frac{1}{RE^2 \cdot T} \quad \text{..... (26)}$$

where RE = the relative error defined above,

T = the total simulation time required for the specified number of trials.

Improvement of these quantities improves the accuracy and precision of any Monte Carlo calculation [14].

Clearly, to reduce the variance, thereby making statistically acceptable results when tallying, we need the number of trials N to be very big, which leads us to the next section.

2.5.6 Variance Reduction Technique

The simulation code tracks one particle at a time from start to finish. In cases where the particle takes a long time to reach tally points (areas of interest), an even longer time will be needed to reach acceptable statistics.

The variance reduction technique (VRT) may then be used not only to get good statistics but to get them more quickly. The VRT may be necessary in order to sample rare events. The user may then include the following operations in the input data:

- Use 'biased' PDFs so that physics interactions favour events of interest
- Use geometry splitting/roulette to increase particles in certain regions of interest
- Track only particles in the regions on interest and kill other particles in uninteresting regions.

We would want the variance reduction not to change or affect the expected mean score when improving the statistics and reducing the tallying time T.
Variance reduction may contribute to the increase of FOM by either reducing RE or T.

MCNPX has about 20 variance reduction techniques [12] which some will be discussed in section 2.7.1.3 (c). The list includes the following VRTs

- Time and energy cutoffs
- Geometry splitting & roulette
- Weight windows
- Exponential transform
- Forced collisions
- Energy splitting & roulette
- Time splitting & roulette
- Point and ring detectors
- DXTRAN contribution
- Implicit capture
- Weight cutoff
- General source biasing
- Secondary particle biasing
- Bremsstrahlung energy biasing

Let us consider geometry splitting which is dependent on the VRT called “importance biasing”. Geometry splitting increases the number of particles in the (important) regions of interest and thus decreases the number of particles in other (unimportant) regions.
This technique involves assigning higher “importances” in regions of higher interest. Those regions correspond to certain ‘cells’ in the geometry of the problem. Thus, the higher the value of the cell, the more important is that region. These importances must not change the Monte Carlo calculation; they must always be greater than zero as zero kills the particle and declares the region to be unimportant.

Let us consider the geometry that is split into two regions:
The figure on the right shows Cell 1 and Cell 2 with corresponding importances I_1 =*1* and I_2 =2. We declare Cell 2 to be the more important as it is on the side of the detector and we want more particles to reach it. Thus Cell 2 has a higher importance than Cell 1, i.e. $I_2 > I_1$.

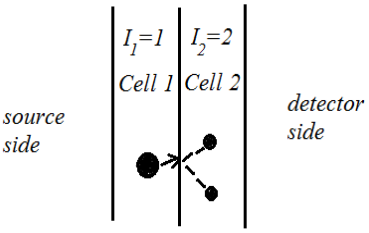

Now consider the splitting ratio *r* for a particle moving between the two importances: $r = \frac{I_2}{I_1}$

and let n be the number of particles it splits into : $n = [r]$

When the particle is transported from Cell 1 to Cell 2, if n >1 then we say that the particle must split into n particles. In the case shown here n =2/1 which is 2, therefore the particle will split into 2. It is clear that this is a biased consideration and as it stands the mean value of the score will be affected. To achieve the unbiased mean we need to assign statistical weights (w_{e-p}) to each particle, determined from the original total weight (w) of the particle before splitting.

In this case the weight of each particle after splitting becomes: $w_{e-p} = \frac{w}{n}$

Some things to be noted with this operation is that [9]:

- all the n particles born due to geometry splitting have identical attributes (e.g., *x, y ,z, E,* etc) including $w_{e-p} = \frac{w}{n}$
- these n particles are of the same history and are treated as such, hence their contribution to tallies are combined.

Transport codes simulate one particle history from start to finish, so when n particles are born then only one particle will be tracked until it dies while $n-1$ particles are banked. The next particle is removed from the bank and tracked until all particles in the bank are finished.

A warning that must be given here is that the user must be careful of over-splitting the geometry, and the total weight of the splitting particle (w) must be conserved otherwise VRT can achieve the opposite of what is aimed at, i.e. reducing the time for the simulation and unbiased results. Therefore the splitting ratio must not be greater than 4: i.e.

$$(r = \frac{I_2}{I_1} \leq 4).$$

There are a number of VRTs to be considered; however we will limit our argument to the geometry splitting as it will be used in this work. Next to consider is the particle transport code that will be used.

2.7 Tips for correct and efficient problems

For the optimal use of MCNPX in the particle transport calculations, we will consider the three-phased checklist: Problem definition and set up, preparing for the long computer runs that you may require, and making the runs that will give you results.[12] Not all items in the checklist will be used; however it serves as a guide for further advanced problems.

Problem Setup

- Do not set up all geometry at once.
- Model the geometry and source distribution in enough detail as needed for accuracy.
- Use simple cells.
- Use the simplest surfaces.
- Always plot the geometry to see if it is correctly defined and what was intended.
- Know and compare calculated mass and volumes/surf areas.
- Use the VOID card when checking geometry.
- Look at print tables 10, 110, and 170 to check the source.
- Be aware of physics approximations, problem cutoffs, and default cross-sections.
- Cross-section sets matter!
- Use separate tallies for the fluctuation chart.
- Use the most conservative variance reduction techniques.
- Do not use too many variance reduction techniques.
- Balance user time with computer time.
- Study all warning messages.
- Generate the best output (consider PRINT card).
- RECHECK the INP file (materials, densities, masses, sources, etc.)
- GARBAGE into code = GARBAGE out of code.

Preproduction

- DO NOT USE MCNP/ MCNPX AS A BLACK BOX.
- Run some short jobs.
- Examine the outputs carefully.
- Study the summary tables.

- Study the statistical checks on tally quality and the sources of variance.
- Compare the figures of merit and variance of the variance.
- Consider the collisions per source particle.
- Examine the track populations by cell.
- Scan the mean free path column.
- Check detector diagnostic tables.
- Understand large tally contributions (with event logs).
- Strive to eliminate unimportant tracks.
- Check secondary particle production.
- Do a back-of-the-envelope check of the results.

Production

- Save RUNTPE for expanded output printing, continue run, tally plotting.
- Look at figure of merit stability.
- Make sure answers seem reasonable.
- Examine statistical checks.
- Form valid confidence intervals.
- Make continue runs if necessary.
- See if stable errors decrease by $1/\sqrt{N}$
- Remember, accuracy is only as good as the nuclear data, modelling, MCNP sampling approximations, etc.
- Adequately sample all cells.

2.8 Emerging Issues

Considering the literature review section, I would like to conclude that MCNPX code is suitable for this study outlined in the section 1.3.

The next chapter looks at the method that this code was actually applied in this study.

CHAPTER 3: METHODOLOGY

EXPERIMENTAL TECHNIQUES AND EQUIPMENTS

3.1 Introduction

This section considers step-by-step actions taken to arrive at the recorded results. It discusses the techniques employed to ensure that correct and accurate results were achieved and thus build confidence with regard to any judgement that may arise in considering these results.

3.1.1 Assumptions and definitions

Beam losses in the cyclotron are not considered: in the SPES project, the beam lost in the cyclotron during acceleration and extraction is estimated to be at 15% of the total beam [7]. These lost particles impinge onto the cyclotron – mainly made of steel – which then add to cyclotron activation. However, self-shielding is part of the commercial cyclotron accelerator.

We assumed that there are no openings in the concrete walls of the cyclotron vault: in my geometry cards for input data in the MCNPX, I used the macrobodies to define the vault. (see Appendix 1s) There is no opening through which radiation may penetrate.

Activation of other systems was not considered: the C70 cyclotron has cooling systems in which water and copper materials, for example, can be activated by neutrons and photons.

Radiation from radioactive ions was not considered: the MCNPX code does not transmutate nuclides, so in the RIB demonstrator, once the UC_x fissions and radioactive nuclides are formed, they add to the neutron/ photon count inside the RIB demonstrator vault. However they are unaccounted for in this simulation.

The angle of incidence of the proton beam onto the target is 0°: The required thickness of stainless steel beamstop was calculated using The Stopping and Range of Ions on Matter (SRIM) software [15]. This thickness allows the maximum number of product neutrons, as self-shielding does not take place as in the case of a thicker target. We simulate a person by placing the phantom in front of the target, although outside of the shielding, knowing that neutrons are forward peaked: thus the normal angle of incidence is zero to simulate the worst-case scenario. see figure 12.

Source definition: Source information (si), is a proton beam of 70 MeV of 350 μA current with radial spread of 0.5 cm maximum. Source probability (sp), the radial intensity distribution is given by the power law (called by the function -21 in the MCNPX code and the parameter is 1, see section 2.7.1.3 (d) (iii)). Parameter 1 means the radial intensity distribution of the beam is linear and uniform. [See Appendix 1 under Source Definition cards for our calculation.]

Mode card specifies H N P, this card specifies the particle types to be transported in the simulation. For all simulations in this project, proton (H) particles irradiate the target and secondary neutrons particles, (N) and photons (P) are born and are actually the items of interest. A proton is a charged particle which interacts electromagnetically thus; computer time is increased in tracking each proton particle which will eventually not threaten radiation safety; thus once it has produced secondary particles we are more interested in, protons can be switched off by using H=0 which kills its importance and MCNPX code stops tracking it [6]. H is switched off immediately after it has irradiated the target (H=0 to improve runtime). [See Appendix 1 under Physics Card.]

There are four parameters for neutrons in the physics card:

- Emax (75 MeV) this is the neutron maximum energy for which neutron data can be recorded in the memory.
- EMCNF (0 MeV) defines whether below this energy is analogue capture or above this is implicit capture.
- IUNR (0=default) default calls for an active treatment of unresolved resonance range of probability in the presence of data tables. [10] [See Appendix 1 under Physics Card.]

Materials used (air; concrete; Tissue Equivalent Material (TEM) for phantom, stainless steel and UC_x): for the purpose of shielding calculations; I have protons irradiating the target of stainless steel (SS-304L – low carbon) in the case of a new cyclotron vault, and irradiating UC_x for the case of the RIB demonstrator vault. Neutrons and photons as secondary objects are transported in the normal dry air at STP before reaching the concrete shielding. Ordinary concrete shielding is used with specifications of “15 years after initial mix” so that it is dry and represents the worst-case scenario in which concrete will not be damp, thus holds less water, and subsequently less hydrogen which moderates neutrons. This kind of calculation can miscalculate the efficiency of the shield for the period when the concrete is dry. Material compositions are adopted from J. Van Rooyen’s MCNPX training manual [6].

3.1.2 Precautions to ensure correct results

MCNPX does extensive input checking but is not foolproof.

- First, the geometry of the calculation must be plotted and checked from different views. X-Server is a good geometry plotter compatible with MCNPX
- Secondly, one should surround the entire geometry with a sphere and flood the geometry with particles from this spherical source using an inward cosine distribution on the spherical surface. The idea is to use a VOID card to remove all materials specified in the problem then do the trial run. If there are any incorrectly specified places in the geometry, this procedure will usually find them. Importances inside the source should not be zero. Tally outputs must be checked to see if they are reasonable with what is calculated. [12]

3.2 Tallies and Results

This section describes what we wanted to calculate and how did we come to achieve that.

3.2.1 New Cyclotron Vault

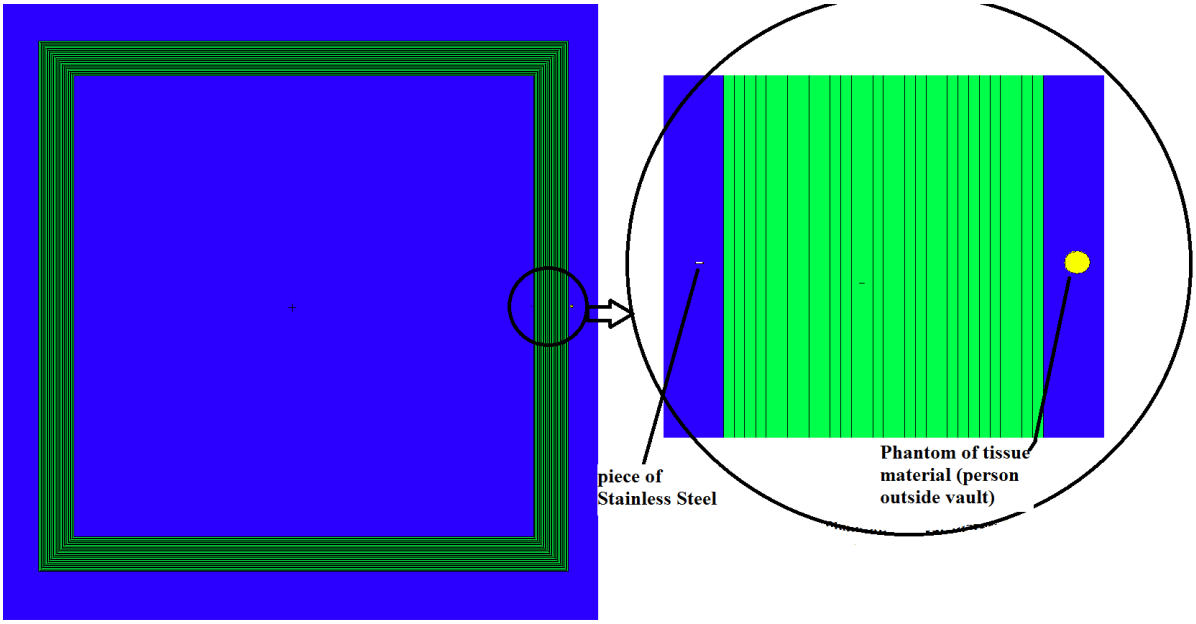

Figure 12: The top view plan of the simplified negative-ion cyclotron vault. The beamline (piece of Stainless Steel) to be activated by incidental proton beams is shown together with concrete shielding with geometry split as a means for Variance Reduction Technique. The phantom is placed where fluence-rate of radiation is investigated Incidental beam onto the target is towards the phantom as neutrons are forward peaked so as to have a worse scenario in which neutron fluence-rate is high

Calculations in the new cyclotron vault involved concrete shielding of 3 m and 4 m in thickness. Now this is deep penetration transport and capture of neutrons makes it difficult for transported particles to reach the phantom, which means the statistics are not satisfactory. As described in the literature review section, we then need the Variance Reduction Technique (VRT) to force particles towards the point where we need more particles, specifically we used geometry splitting and cell importance biasing.

This technique requires a single block of concrete shielding wall to be separated into subsections, as described in the literature review. In this case the 3 m thickness was cut into 30 subsections of 10 cm thickness each. [In Appendix 1 in the input file under Cell Cards, the inner subsection (inside vault) is numbered 11 whereas the outer subsection is numbered 40. Correspondingly, in the Surface Cards (macrobody RPP), they are numbered with the inner surface as 01 with outer surface as 31.]

To get the VRT correctly, the population of particles that are transported must be constant in the subsequent cells towards the point of interest, e.g. towards the detector or phantom. This means both neutron & photon flux must evidently be constant throughout from surface 01 to surface 31. In the input file, we start by having all these “importances” of particles be 1 throughout the concrete sections and run the simulation for a short time, i.e. 30 minutes of computer time. The number of neutrons decreases as we approach surface 31 because of shielding by the concrete. A spreadsheet with a formula for importance setting was used to feed the population of neutrons & photons and thus calculate the new importance to be entered in the input file. Once these new importances were calculated, they were then copied to the input file as the new importance across the subsections. The simulation was then run with these new importances for another 30 minutes. In the output file, what is observed again is the distribution of particles as populated towards the outer surface. If the population is still not constant, the last population is used to calculate the latest importances. These will be copied to become the latest importances in the new input file. The following tables show the populations of neutrons and photons before and after VRT was done.

Table 2: Showing population of neutrons and photons before using the Variance Reduction Technique: much more computer time will be needed for enough particles to reach the detector side (cell 81).

Cell	Importances	Tracks entering	Neutron population	importances	Tracks entering	Photon population
1	1.00E+00	153307	153126	1	378041	377911
2	1.00E+00	46	153170	1	42	432227
3	1.00E+00	638210	184689	1	692746	469883
11	1.00E+00	978568	222279	1	839534	710894
12	1.15E+00	792396	269631	1	373922	475688
13	1.32E+00	592750	233928	2	389434	499219
14	1.52E+00	412504	170984	4	389751	475342
15	1.75E+00	269651	114861	8	378562	441701
16	2.01E+00	169830	73605	16	362955	390525
17	2.31E+00	103952	45786	16	174674	183647
18	2.66E+00	62468	27881	16	87762	93808
19	3.06E+00	37004	16593	16	45582	49556
20	3.52E+00	22183	10175	16	24319	26879
21	4.05E+00	13287	6086	16	13287	14674
22	4.65E+00	8012	3687	16	7383	8195
23	5.35E+00	4836	2262	16	4180	4709
24	6.15E+00	2768	1329	16	2304	2667
25	7.08E+00	1783	860	16	1408	1595
26	8.14E+00	1232	552	16	833	1011
27	9.36E+00	909	419	16	529	678
28	1.08E+01	611	286	16	373	441
29	1.24E+01	457	204	16	247	306
30	1.42E+01	338	137	16	157	191
31	1.64E+01	266	112	16	123	149
32	1.88E+01	202	83	16	83	106
33	2.16E+01	155	62	16	44	63
34	2.49E+01	107	43	16	24	39
35	2.86E+01	65	32	16	26	34
36	3.29E+01	35	22	16	16	21
37	3.79E+01	18	12	16	9	12
38	4.35E+01	16	8	16	5	5
39	5.01E+01	8	4	16	2	4
40	5.76E+01	2	1	16	0	0
81	5.76E+01	0	0	30	0	0
91	5.76E+01	0	0	30	0	0

To gauge the effectiveness of the shield, one method is to track particles passing through each surface from the inner to the outer surface. We need to calculate a particle current integrated over a surface, thus we need a tally and in the MCNPX we call this the F1 tally.

Table 3: Showing population of neutrons and photons after Variance Reduction Technique is constant towards the detector side (Cell 81), i.e. enough particles are reaching it.

Cell	importances	Tracks entering	Neutron population	importances	Tracks entering	Photon population
1	1.00E+00	6175584	6168311	1.00E+00	12611863	12607079
2	1.00E+00	1517	6169831	1.00E+00	1419	14459954
3	1.00E+00	25805958	6491713	1.00E+00	23221224	15834903
11	1.00E+00	39545193	6841440	1.00E+00	27502850	25125946
12	1.00E+00	27784503	7041165	1.63E+00	19919326	24367132
13	1.00E+00	17992463	7165680	3.19E+00	18490858	22075830
14	1.49E+00	16055256	9218881	6.17E+00	17025401	20350195
15	2.59E+00	15817405	10068086	1.20E+01	16300846	19599624
16	4.58E+00	15196541	9924463	2.36E+01	16238830	19470554
17	8.33E+00	14572991	9740070	4.61E+01	16259758	19390238
18	1.58E+01	14260761	9732789	8.92E+01	16287178	19374498
19	3.05E+01	14120331	9747944	1.72E+02	16367510	19435651
20	5.92E+01	14058437	9737352	3.26E+02	16387611	19448539
21	1.14E+02	13945211	9635690	6.14E+02	16390200	19441042
22	2.17E+02	13788109	9510287	1.14E+03	16349677	19393859
23	4.10E+02	13751710	9490171	2.12E+03	16316894	19373180
24	7.77E+02	13979436	9599842	3.91E+03	16285781	19402633
25	1.43E+03	14000803	9504133	7.19E+03	16365772	19518857
26	2.56E+03	13960781	9407369	1.32E+04	16442798	19627588
27	4.56E+03	14057507	9409573	2.40E+04	16480317	19700325
28	7.94E+03	14077672	9336217	4.35E+04	16498664	19751248
29	1.37E+04	14123881	9314008	7.81E+04	16444858	19708736
30	2.32E+04	14201049	9315369	1.39E+05	16313831	19590736
31	3.91E+04	14320432	9332333	2.44E+05	16034082	19307531
32	6.50E+04	14368477	9293743	4.23E+05	15668632	18914061
33	1.07E+05	14323520	9213296	7.19E+05	15142629	18318525
34	1.74E+05	14337610	9201382	1.19E+06	14345673	17422041
35	2.83E+05	14342886	9186310	1.90E+06	13345094	16312680
36	4.58E+05	14358013	9188898	2.95E+06	12182277	15020952
37	7.42E+05	14352904	9223110	4.34E+06	10813416	13509794
38	1.21E+06	14225618	9256068	6.14E+06	9362084	11938688
39	2.02E+06	13523345	9270712	8.56E+06	7957409	10473155
40	4.01E+06	11963055	9217797	1.29E+07	6215444	9008179
81	4.01E+06	493372	460488	1.29E+07	312325	576605

To correct for these particles, we need to consider the source strength, thus evoking the FM1 tally for multiplication factor. We can again convert using Dose Conversion Function (DF card), this card converts FM1 tally into dose-rate in Sv/hr. The F1 tally, FM1 tally and DF cards were done separately for neutrons and photons in each surface. The dose-rates for neutrons and photons were summed to have a single dose-rate for each surface. These readings were then plotted against the distance in centimetres so as to establish the

effectiveness of attenuation by the concrete. [See Appendix 1 under Tally cards & Dose Conversion Functions cards as it was coded.]

To simulate a person on the outside of the shield and the registered dose-rate, the flux of particles averaged over a cell is tallied. This is the F4 tally. Here the phantom with a tissue equivalent material (TEM) was placed directly adjacent to the outer surface of the shield. It was placed 20 cm from the outer surface and 340 cm from where the accidental irradiation of stainless steel is simulated in the case of 300 cm shielding and 440cm in the case of 400cm shielding. Again to correct for these tallies, we need to consider the source strength, thus evoke FM4 tally for multiplication factor. We also converted using Dose Conversion Function (DF card), this card converts FM4 tally into dose-rate in Sv/hr. The F4 tally, FM4 tally and DF cards were done separately for neutrons and photons for the phantom. The dose-rates for neutrons and photons were summed to have a single dose-rate for the phantom.

In the phantom, one would like to measure absorbed dose-rate as it gives an indication of the rate at which ionising radiation damages materials, particularly hydrogenous carbon-chain polymers, as there is a very good correlation between radiation-induced damage of such materials with the absorbed dose-rate [6]. To do this we need to tally the energy deposited by neutrons and photons, averaged over the phantom. Thus one of the tallies we used is the F6 tally. This tally was done for neutrons and photons combined [see Appendix 1 under Tally Cards] and again to correct for the source strength the FM6 tally for multiplication factor was used.

It may be of advantage to be able to establish the energy spectra for both neutrons and photons in every tally. This is known as “energy binning”, where particles are grouped into specified energy groups. In this case we wanted to have the binning for every tally thus an E0 tally energy card was used and binning was between E_{min} = 1E-11 MeV to E_{max} = 70 MeV. This allows us to tell the maximum energy of particles reaching the outer surface and eventually reaching the phantom. [See Appendix 1 under Tally Cards]. Energy spectra for both neutrons & photons were plotted for the inner surface, outer surface and the phantom.

Dose-rate profiles can be represented graphically in 2-dimensional plots (xy and yz planes). This profile is called the “mesh” and is calculated using a mesh tally. In this tally particles are tracked through the independent mesh as part of the simulation [11]. Contours are colour coded, in this case according to particle dose-rate (mesh tally type 1). Where the

dose-rate is more intense the region is red and less intense regions are blue. We did a rectangular mesh tally in the xy plane. In the z-direction between +119 cm and +121 cm, this covers the height of the beamline, i.e. 120 cm. In the x-direction it spans over -2410 cm to +2400 cm which covers the whole vault, including the phantom. [See Appendix 1 under Mesh tally Plot.]

3.2.2 RIB Demonstrator

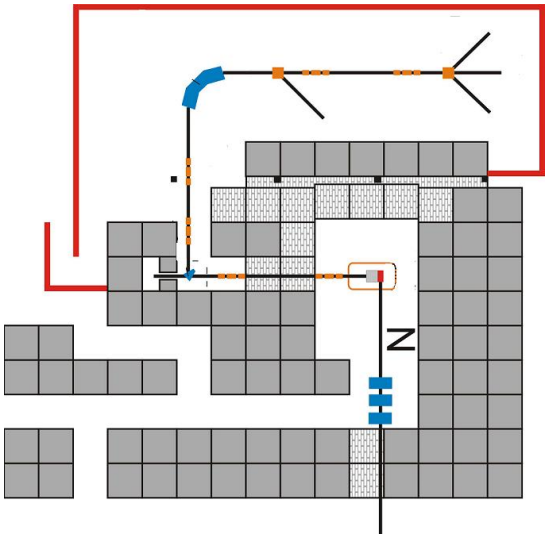

Figure 13: A smaller plan view of the RIB Demonstrator vault compared to the one in Figure 5. This will be the geometry of the simulation in MCNPX. Each grey square represents a 150 cm x 150 cm concrete block. (Each block is 300 cm tall.)

The actual geometry of the RIB Demonstrator vault is shown in Figure 13. Complete dimensions of the plan were available and were thus used in the input file of the calculation. However, as a means of variance reduction, two geometries were used for the simulation. Below, in Figure 14, the geometry plotting option was used to produce and check if the geometry is correct for the first geometry. It shows the vault open. Areas of interest are shown with phantoms 153; 154; 155; 156; 157 and 158. The aim was to check if the area of the corridor leading to the spectrometer (at left) will be accessible during beam operations; also that on the areas on top of the spectrometer and on top of the vault will be safe as well. However, when geometry splitting is done, the ‘air’ material in the opening imposed artificial biasing on the simulation and more neutrons were transported towards phantom 154, 155, 156 and 157 and unrealistic results were found in phantoms 150, 152 and 152, which are shown in the second geometry, Figure 15. The interest in the second geometry is on the radiation threat posed by the beampipe transporting RIBs from the vault to the experimental room. For realistic results these regions of interests had to be considered separately. Thus

in the second simulation the vault is closed, and geometry splitting was used to improve statistics though the beampipe.

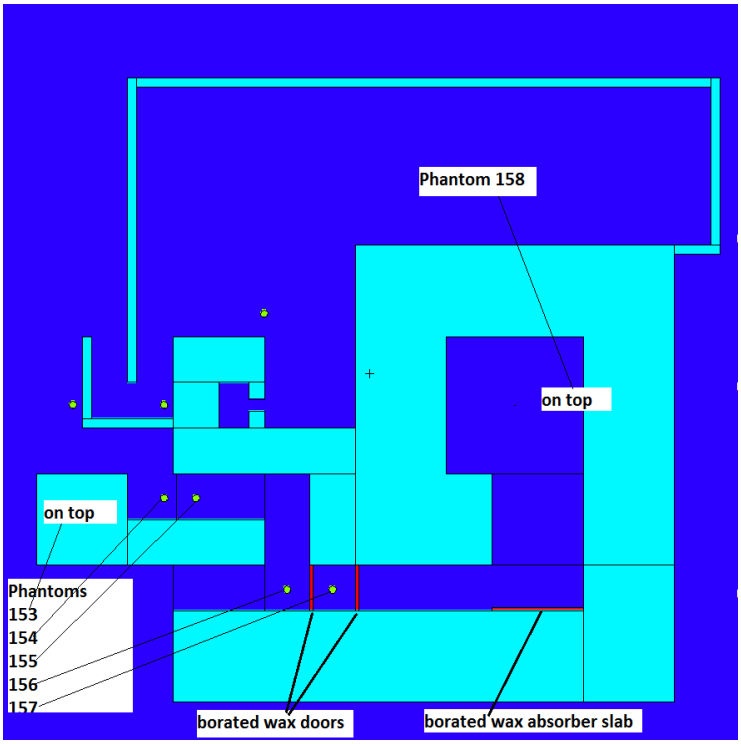

Figure 14: The geometry of the plan view of the RIB Demonstrator vault as plotted with MCNPX. Here notice that the opening into the vault is left as in the real vault.

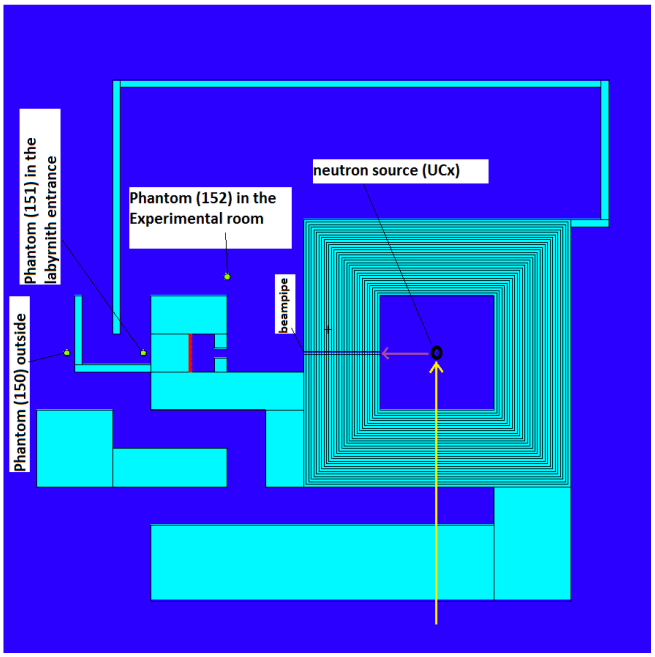

Figure 15: The geometry of the plan view of the RIB Demonstrator vault as plotted by MCNPX. In the centre of the vault will be a lead (Pb) sphere irradiated from its centre with point source of proton beam of 350 µA at 70 MeV. The purple arrow shows the beampipe through which radioisotopes and neutrons will be transported towards the experimental room.

Simulating the neutron source

In the RIB demonstrator, the UC_x target will be irradiated to produce radionuclides. In order to investigate if the vault walls will provide effective shielding, again neutrons and photons have to be transported. Johann van Rooyen MCNPX expert [6] suggested that because MCNPX code, for safety reasons, has limitations that it does not transmute nuclides at high energy protons, while we need to work with 70MeV of proton. Thus irradiating UC_x might not yield high enough neutron yields to pose radiation threats. This might then undermine the radiation source strength. The source that will come very close to the practical case will be a neutron source that is irradiated by protons of 70 MeV and 350 μA current. To achieve an isotropic distribution of neutrons from the target, these protons must be a point source placed in the centre of spherical material. This material must be a high neutron emitter, and the choice was between beryllium (Be); copper (Cu); stainless steel (Fe); lead (Pb) and tungsten (W). Because we do not want self-shielding to take place (in which case we will have less neutrons emitted), then the radius of the spherical target must be the stopping length of that particular material for a proton beam of 70 MeV of 350 μA current. SRIM was used to determine this length.

Our interest was the neutron flux per second passing through the outer surface of the spherical target, thus the simulation had an F1 tally. Simulations were done for all five materials. [See Appendix 2 for the complete input file with lead (Pb) as the target.]

Radiation simulations:

(a) Open vault with a beamline opening leading to the experiment room

For the case where the area of interest pertaining to radiation safety levels is along the passage from the vault entrance, then this is where we put phantoms. See Figure 14. To achieve close-to-reality calculations, the RIB demonstrator vault is simulated with the entrance labyrinth.

Along the passage, high dose-rates were calculated and we therefore decided to put borated paraffin wax doors to protect the corridor towards the spectrometer. At first only one was placed and dose-rates were still high and it was then rearranged for a final simulation as shown in Figure 14.

Again the F1 tally for neutron and photon particles was calculated for phantoms along the passage, including one on top of the spectrometer. These tallies were converted to dose-rates as well.

An E0 card was added for energy binning in the tallies with particular interest in the phantoms, so as to reveal the energy spectra of neutrons reaching the phantoms.
For the reasons explained in section 3.2.1, the F6 tally was calculated for neutrons and photons combined for the energy deposited into every phantom.

The rectangular mesh tally in the xy-plane was calculated with parameters exactly as for the closed vault. See Figure 31.

(b) Closed vault with a beamline opening leading to the experiment room

The RIB demonstrator vault is an existing structure, while the complete RIB demonstrator will be an extended facility to this vault. Dimensions of the vault are thus available and it has an entrance passage as shown in figure 13.

The thickness of concrete shielding walls is 3 metres and roof also 3 metres. Again this is deep penetration of radiation transport and so VRT was used to run simulations for which the interest was investigating whether a 3-metre thickness is sufficient all around. The entrance to the vault will mean air with a much lower density than that of ordinary concrete, thus less scattering will take place and thus particles will travel further before getting absorbed. As MCNPX tracks each particle, more computer time is required for the concrete than for air. If there is any opening, results may be misleading as more particles may be transported through the air and thus reach phantoms then when there is no opening. Thus, we had to simulate with a completely closed vault, just as we did for the new cyclotron vault.

However, as there is a beamline through which radionuclides will be transferred from the UC_x target chamber to the experimental room, this will have to be open to ensure sensible results – i.e. safety levels – as the opening will be there during operation. The beam pipe is estimated to be 10 cm in diameter and this vault will have this opening. Areas in which we want to investigate radiation safety levels for personnel are indicated with the phantom as shown in Figure 14 &15.

Again the F4 tally for neutron and photon particles was calculated for each surface from the inner to the outer surface and for phantoms adjacent to the experimental room and the outside field. These were converted to dose-rates as well.

An E0 card was added for energy binning in the tallies with more interest on the inner & outer surfaces of the vault and phantoms.

For the reasons explained in section 3.2.1, the F6 tally was calculated for neutrons and photons combined for the energy deposited into every phantom.

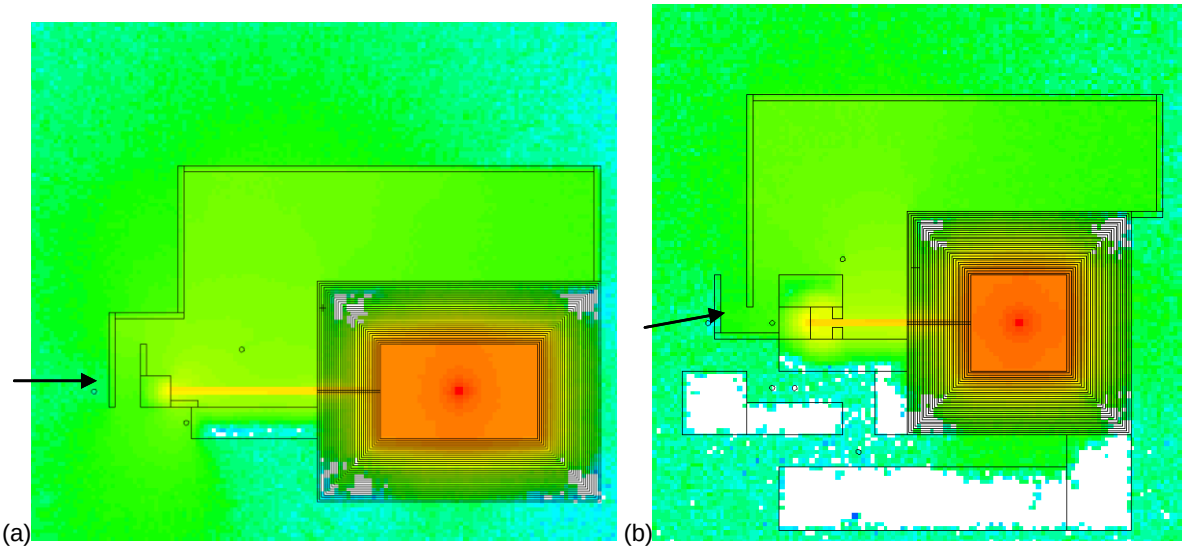

Figure 16: On the left (a), we have the labyrinth (as shown by the arrow) before modified to cater for high neutron flux escaping out to the yard. On the right (b), the modified labyrinth with a beam dump. Small circles indicate phantom positions.

The simulation was first run in the geometry of Figure 16(a). High doses were recorded and we became aware that the labyrinth must be reconfigured to have less neutrons escaping to the outside areas. The revised labyrinth with a new beam dump is shown in Figure 14 &16(b). Having changed the labyrinth we still had to deal with high dose-rates in the experimental room, for which we recognised that the escaping neutrons need to be dumped into a neutron absorber. This neutron absorber is made of borated paraffin-wax, so as to ensure both high- and low-energy neutrons are absorbed. This dump could be placed behind the 90^0 bending magnet which diverts the beamline coming out of the vault. (See Figure 3.3).

A rectangular mesh tally in the xy & yz planes. For the xy pane, the z-direction between +119 cm to +121 cm covers the height of the beamline, i.e. 120cm. In the x-direction it spans from -2500 cm to +2500 cm which covers the whole vault, including the phantom. For the yz plane, in the x-direction between -5 cm to +5 cm, this covers the beamline surface yz plane as the target is at x=0 cm. In the y-direction it spans from -1910 cm to +1900 cm which covers the whole vault and in the z-direction -350 cm to + 1300 cm, which includes the phantom. [See Appendix 1 under Mesh tally Plot.]

3.3 Conclusion and techniques for improving results

Geometry splitting as a Variance Reduction Technique proved to be very useful, as enough particles reached the detector (phantom) making the results trustworthy and statistically sound.

CHAPTER 4: DATA ANALYSIS, FINDINGS AND DISCUSSION

4.1 Introduction

This chapter is dedicated to looking at the results found for the two vaults under investigation:

- ordinary concrete walls of 3-metre thickness for the negative-ion cyclotron vault
- ordinary concrete walls of 4-metre thickness for the negative-ion cyclotron vault
- ordinary concrete walls of 3-metre thickness for the RIB Demonstrator vault.

4.2 Description of results

Negative-ion Cyclotron Vault

Neutrons generated by irradiating an Fe target with a 70 MeV proton beam of 350 µA:

Table 4: Average number of neutrons leaving the stainless steel target when irradiated by proton beam

Neutron counts (particle/cm^2)	relative error (%)
4.04E+13	0.0004

Table 5: Neutron energy bins averaged in the stainless steel target

n_energy (MeV)	Counts	Relative error (%)
1.00E-11	0.00E+00	0
1.00E-07	5.07E+08	0.0958
1.00E-03	2.84E+09	0.0531
1.00E-01	6.56E+11	0.0033
1.00E+00	6.86E+12	0.001
2.00E+00	8.49E+12	0.0008
3.00E+00	5.88E+12	0.001
4.00E+00	3.78E+12	0.001
5.00E+00	2.51E+12	0.0015
6.00E+00	1.72E+12	0.0018
7.00E+00	1.23E+12	0.0021
8.00E+00	9.12E+11	0.0025
9.00E+00	7.10E+11	0.0028
1.00E+01	5.82E+11	0.0031
1.20E+01	9.39E+11	0.0024
1.40E+01	7.57E+11	0.0027
1.60E+01	6.51E+11	0.0029
1.80E+01	5.74E+11	0.0031
2.00E+01	5.10E+11	0.0033
2.50E+01	1.04E+12	0.0023
3.00E+01	7.86E+11	0.0027
3.50E+01	6.13E+11	0.003
4.00E+01	4.74E+11	0.0035
4.50E+01	3.45E+11	0.0041
5.00E+01	2.28E+11	0.0051
5.50E+01	1.27E+11	0.0069
6.00E+01	4.95E+10	0.0111
6.50E+01	7.48E+09	0.0284
7.00E+01	1.63E+08	0.1902

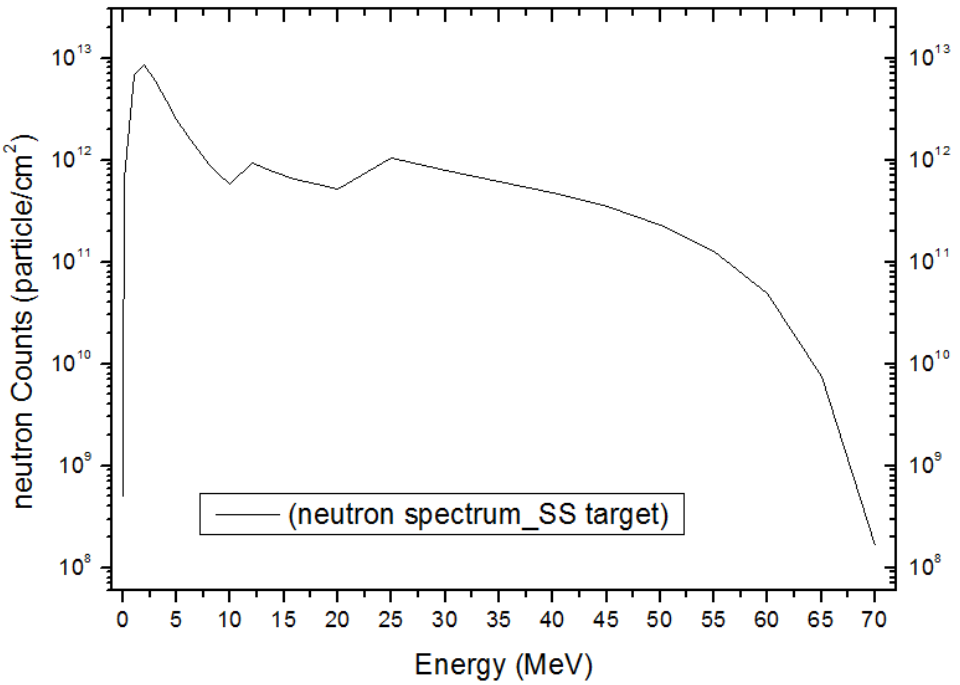

Figure 17: Neutron energy spectra averaged inside the stainless steel target as it is irradiated by the proton beam.

This spectrum shows a definite considerable number of prompt neutrons from the accidental irradiation and thus a suitable shield is a prime requirement. Neutrons were even created at 70 MeV energy. These will be most challenging to attenuate.

4.2.1 Results of the cyclotron vault with 3 metre wall thickness

Table 6: Neutrons dose-rates at each surface from the inner surface of the vault (0 cm) to the outer surface of the vault (300 cm). The particle flux is also reflected in the table.

Thickness(cm)	Dose rate(Sv/hr)	Relative error (%)		Flux(particles/cm^2)	Relative error (%)
0	1.26E+08	0.0006		2.21E+14	0.0006
10	5.38E+07	0.0009		1.62E+14	0.0008
20	2.68E+07	0.0013		1.10E+14	0.001
30	1.37E+07	0.0017		6.78E+13	0.0012
40	7.21E+06	0.0023		3.93E+13	0.0016
50	3.87E+06	0.0031		2.19E+13	0.0019
60	2.11E+06	0.0038		1.19E+13	0.0022
70	1.17E+06	0.0046		6.42E+12	0.0025
80	6.62E+05	0.0054		3.45E+12	0.0028
90	3.82E+05	0.0063		1.87E+12	0.0032
100	2.22E+05	0.0072		1.02E+12	0.0038
110	1.31E+05	0.008		5.62E+11	0.0044
120	7.79E+04	0.0089		3.14E+11	0.0051
130	4.69E+04	0.0097		1.78E+11	0.0059
140	2.85E+04	0.0106		1.02E+11	0.0067
150	1.74E+04	0.0114		5.95E+10	0.0076
160	1.07E+04	0.0122		3.51E+10	0.0085
170	6.59E+03	0.013		2.09E+10	0.0093
180	4.09E+03	0.0138		1.26E+10	0.0102
190	2.54E+03	0.0146		7.64E+09	0.0111
200	1.58E+03	0.0153		4.66E+09	0.012
210	9.91E+02	0.0161		2.87E+09	0.0128
220	6.20E+02	0.0168		1.77E+09	0.0136
230	3.90E+02	0.0175		1.10E+09	0.0144
240	2.45E+02	0.0183		6.83E+08	0.0151
250	1.54E+02	0.019		4.26E+08	0.0159
260	9.74E+01	0.0198		2.67E+08	0.0167
270	6.06E+01	0.0186		1.67E+08	0.0175
280	3.80E+01	0.0193		1.05E+08	0.0182
290	2.33E+01	0.0199		6.62E+07	0.019
300	1.28E+01	0.0209		4.17E+07	0.0197

The table shows that for the first 50 cm of concrete the neutron flux is reduced by 2 orders of magnitude, and after that 50 cm reduces by a single order. In terms of flux, from the start 50 cm reduces the flux by an order of magnitude.

Table 7: Photon dose-rates at each surface. from inner surface of the vault (0 cm) to outer surface of the vault (300 cm). The particle flux is also reflected in the table.

Thickness(cm)	Dose rate(Sv/hr)	Relative error (%)		Flux(particles/cm^2)	Relative error (%)
0	4.19E+06	0.0005		2.21E+14	0.0006
10	1.88E+06	0.0008		1.62E+14	0.0008
20	1.14E+06	0.001		1.10E+14	0.001
30	7.34E+05	0.0013		6.78E+13	0.0012
40	4.72E+05	0.0014		3.93E+13	0.0016
50	2.96E+05	0.0016		2.19E+13	0.0019
60	1.80E+05	0.0017		1.19E+13	0.0022
70	1.07E+05	0.0019		6.42E+12	0.0025
80	6.28E+04	0.002		3.45E+12	0.0028
90	3.64E+04	0.0022		1.87E+12	0.0032
100	2.10E+04	0.0025		1.02E+12	0.0038
110	1.20E+04	0.0027		5.62E+11	0.0044
120	6.90E+03	0.0031		3.14E+11	0.0051
130	3.97E+03	0.0034		1.78E+11	0.0059
140	2.29E+03	0.0039		1.02E+11	0.0067
150	1.33E+03	0.0044		5.95E+10	0.0076
160	7.74E+02	0.0049		3.51E+10	0.0085
170	4.54E+02	0.0055		2.09E+10	0.0093
180	2.68E+02	0.0062		1.26E+10	0.0102
190	1.59E+02	0.0068		7.64E+09	0.0111
200	9.53E+01	0.0075		4.66E+09	0.012
210	5.72E+01	0.0082		2.87E+09	0.0128
220	3.46E+01	0.0089		1.77E+09	0.0136
230	2.10E+01	0.0097		1.10E+09	0.0144
240	1.28E+01	0.0104		6.83E+08	0.0151
250	7.85E+00	0.0111		4.26E+08	0.0159
260	4.81E+00	0.0119		2.67E+08	0.0167
270	2.94E+00	0.0126		1.67E+08	0.0175
280	1.77E+00	0.0132		1.05E+08	0.0182
290	1.01E+00	0.0136		6.62E+07	0.019
300	4.97E-01	0.0137		4.17E+07	0.0197

The table shows that for every 50 cm of concrete the photon flux is reduced by a single order of magnitude, with a similar behaviour for flux measurements. This shows that while neutrons are attenuated, secondary photons are produced, adding to the flux.

Table 8: Total dose rates for each surface as added from neutron and photon doses from inner surface of the vault (0 cm) to outer surface of the vault (300 cm)

Thickness(cm)	Neutron Dose rate(Sv/hr)	Photon Dose rate(Sv/hr)	Total
0	1.26E+08	4.19E+06	1.30E+08
10	5.38E+07	1.88E+06	5.57E+07
20	2.68E+07	1.14E+06	2.79E+07
30	1.37E+07	7.34E+05	1.45E+07
40	7.21E+06	4.72E+05	7.69E+06
50	3.87E+06	2.96E+05	4.17E+06
60	2.11E+06	1.80E+05	2.29E+06
70	1.17E+06	1.07E+05	1.28E+06
80	6.62E+05	6.28E+04	7.25E+05
90	3.82E+05	3.64E+04	4.18E+05
100	2.22E+05	2.10E+04	2.43E+05
110	1.31E+05	1.20E+04	1.43E+05
120	7.79E+04	6.90E+03	8.48E+04
130	4.69E+04	3.97E+03	5.09E+04
140	2.85E+04	2.29E+03	3.08E+04
150	1.74E+04	1.33E+03	1.87E+04
160	1.07E+04	7.74E+02	1.14E+04
170	6.59E+03	4.54E+02	7.05E+03
180	4.09E+03	2.68E+02	4.35E+03
190	2.54E+03	1.59E+02	2.70E+03
200	1.58E+03	9.53E+01	1.68E+03
210	9.91E+02	5.72E+01	1.05E+03
220	6.20E+02	3.46E+01	6.55E+02
230	3.90E+02	2.10E+01	4.11E+02
240	2.45E+02	1.28E+01	2.58E+02
250	1.54E+02	7.85E+00	1.62E+02
260	9.74E+01	4.81E+00	1.02E+02
270	6.06E+01	2.94E+00	6.35E+01
280	3.80E+01	1.77E+00	3.97E+01
290	2.33E+01	1.01E+00	2.43E+01
300	1.28E+01	4.97E-01	1.33E+01

Adding together the fluxes of neutrons and photons gives an idea that neutrons dominate transport calculations; thus they control the population of particles towards the phantom.

In the plot below (Figure 18) the total dose rate is almost the same as the neutron dose rate, which is obscured by the total dose rate.

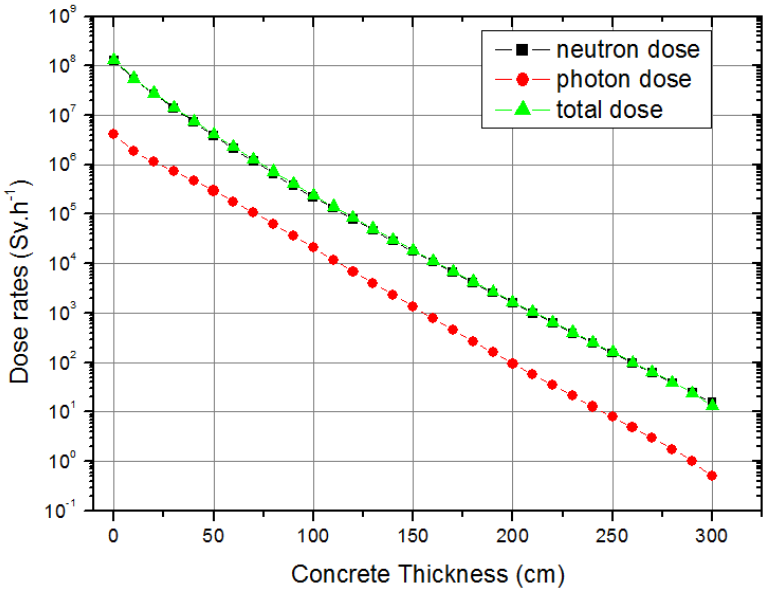

Figure 18: Attenuation of neutron, photon and total dose rates from the inner surface of the vault (0 cm) to the outer surface of the vault (300 cm). Doses were recorded at every 10 centimetres up to the 300 cm thickness of concrete shielding.

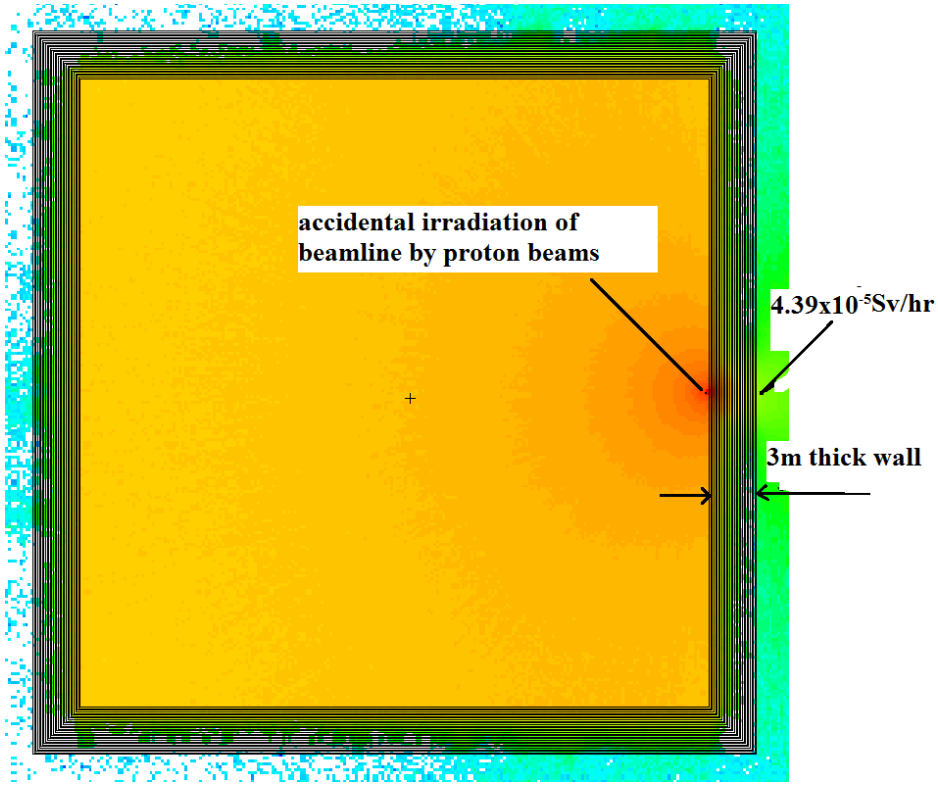

Figure 19: Mesh tally plot in the xy-plane showing the intensity distribution of neutron dose rates from the incident point through ordinary concrete of 3 metre thickness. The recorded total effective dose rate is shown.

In Figure 19, we can see that the effective dose rate recorded at the phantom is 43.9µSv/hr. This is the worst possible value for such an accident around the cyclotron vault considering its position to that of the radiation source.

Below in Figure 20, we observe the penetration of radiation towards the ground as the beam is 120 cm high from the floor. This gives an idea of what should be thickness of the slab to protect against underground contamination of ground-water.

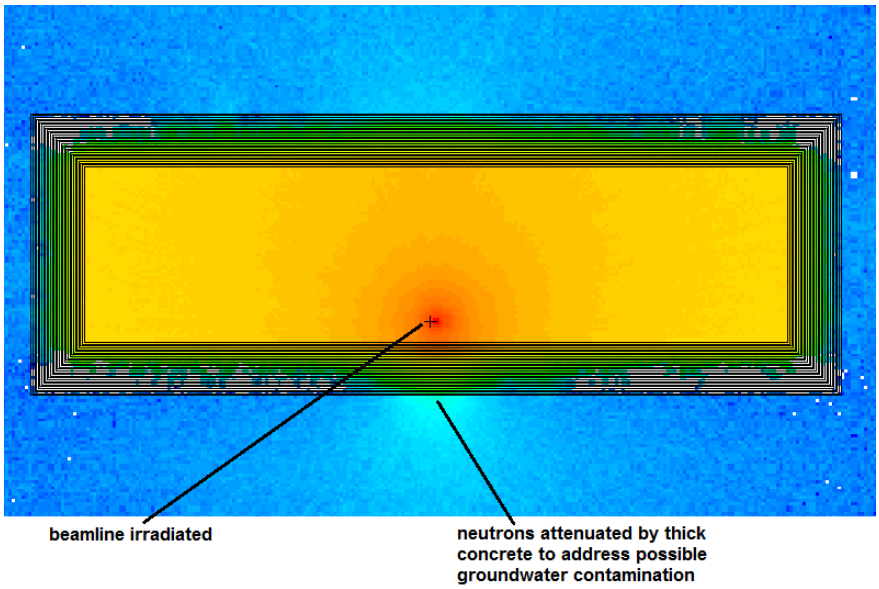

Figure 20: Mesh tally plot in the yz-plane showing the intensity distribution of neutron dose rates from the incident point through ordinary concrete of 3 m thickness.

Table 9 below shows dose rates for neutrons and photons as well as the total dose rate which is calculated by summing the two dose rates.

Table 9: Doses for neutrons and photons in the phantom which is placed 20 cm behind the 300 cm thick shielding wall. Doses registered here are the most severe ones around the outside of the vault for a simulated irradiation of the beamline by the proton beam.

Particles	Dose-rate (Sv/hr)	Relative error (%)
Neutrons	4.14E-05	0.0264
Photons	2.47E-06	0.0173
Total	4.39E-05	

The energy of ionising radiation per unit mass was also calculated. For the effective dose rate of 43.9 μ Sv/hr, absorbed dose rate was measured to be 6.74 μ Gy/hr shown in Table 10.

Table 10: Absorbed dose rate on the phantom in MeV/g.s and multiplying by factor 5.77×10^{-7} it was converted to Gy/hr, units used in the Radiation Protection literature.

Absorbed dose-rate (MeV/g.s)	**Relative error (%)**	**Absorbed. dose-rate (Gy/hr)**
1.17E+01	0.064	6.74E-06

4.2.2 Results of the cyclotron vault with 4 metre thickness

Table 11: Neutron dose rates and corresponding fluxes at each surface of a 4 m thickness of concrete shielding.

Thickness (cm)	Dose (Sv/hr)	Relative error (%)	Flux (particles /cm^2)	Relative error (%)
0	1.26E+08	0.0006	2.21E+14	0.0006
10	5.39E+07	0.0009	1.62E+14	0.0008
20	2.68E+07	0.0013	1.10E+14	0.001
30	1.37E+07	0.0017	6.78E+13	0.0012
40	7.21E+06	0.0024	3.93E+13	0.0016
50	3.87E+06	0.003	2.19E+13	0.0019
60	2.11E+06	0.0037	1.19E+13	0.0022
70	1.17E+06	0.0044	6.42E+12	0.0025
80	6.62E+05	0.0052	3.45E+12	0.0028
90	3.82E+05	0.006	1.87E+12	0.0032
100	2.22E+05	0.0068	1.02E+12	0.0038
110	1.31E+05	0.0076	5.62E+11	0.0044
120s	7.79E+04	0.0084	3.14E+11	0.0051
130	4.69E+04	0.0091	1.78E+11	0.0059
140	2.85E+04	0.0099	1.02E+11	0.0067
150	1.74E+04	0.0106	5.95E+10	0.0076
160	1.07E+04	0.0113	3.51E+10	0.0085
170	6.59E+03	0.012	2.09E+10	0.0093
180	4.09E+03	0.0127	1.26E+10	0.0102
190	2.54E+03	0.0134	7.64E+09	0.0111
200	1.58E+03	0.014	4.66E+09	0.012
210	9.91E+02	0.0147	2.87E+09	0.0128
220	6.20E+02	0.0154	1.77E+09	0.0136
230	3.90E+02	0.016	1.10E+09	0.0144
240	2.45E+02	0.0167	6.83E+08	0.0151
250	1.54E+02	0.0173	4.26E+08	0.0159
260	9.74E+01	0.018	2.67E+08	0.0167
270	6.15E+01	0.0186	1.67E+08	0.0175
280	3.88E+01	0.0193	1.05E+08	0.0182
290	2.45E+01	0.0199	6.62E+07	0.019
300	1.55E+01	0.0209	4.17E+07	0.0197
310	9.83E+00	0.0236	2.63E+07	0.0204
320	6.23E+00	0.0244	1.66E+07	0.0212
330	3.95E+00	0.0252	1.05E+07	0.022
340	2.51E+00	0.026	6.61E+06	0.0227
350	1.59E+00	0.0268	4.18E+06	0.0235
360	1.01E+00	0.0276	2.64E+06	0.0243
370	6.42E-01	0.0284	1.66E+06	0.025
380	4.05E-01	0.0292	1.01E+06	0.0257
390	2.50E-01	0.0301	5.50E+05	0.0264
400	0.139	0.0312	1.71E+05	0.0275

Adding 100 cm to the 300 cm to give 400 cm thickness of concrete made a significant effect in further reducing the neutron fluency by a total of two orders magnitude. The inner surface started with 2.19×10^{14} particles/cm^2 and on the outside we recorded at least 1.75×10^5 particles/cm^2.

Table 12: Photon dose rates and corresponding fluxes at each surface of a 4 m thickness of concrete shielding

Thickness (cm)	Dose (Sv/hr)	Relative error (%)	Flux Particles /cm^2	Relative error (%)
0	4.19E+06	0.0005	2.67E+14	0.0004
10	1.88E+06	0.0008	1.32E+14	0.0007
20	1.14E+06	0.001	7.46E+13	0.0009
30	7.35E+05	0.0012	4.58E+13	0.0011
40	4.72E+05	0.0014	2.87E+13	0.0013
50	2.95E+05	0.0016	1.77E+13	0.0015
60	1.80E+05	0.0018	1.07E+13	0.0017
70	1.07E+05	0.0019	6.33E+12	0.0018
80	6.29E+04	0.0021	3.68E+12	0.002
90	3.64E+04	0.0023	2.12E+12	0.0022
100	2.10E+04	0.0026	1.21E+12	0.0025
110	1.21E+04	0.0029	6.94E+11	0.0028
120	6.92E+03	0.0032	3.96E+11	0.0032
130	3.98E+03	0.0036	2.27E+11	0.0036
140	2.30E+03	0.0041	1.31E+11	0.0042
150	1.33E+03	0.0046	7.54E+10	0.0047
160	7.77E+02	0.0052	4.39E+10	0.0054
170	4.55E+02	0.0059	2.57E+10	0.0061
180	2.69E+02	0.0066	1.52E+10	0.0068
190	1.60E+02	0.0073	9.00E+09	0.0076
200	9.55E+01	0.0081	5.38E+09	0.0084
210	5.74E+01	0.0089	3.23E+09	0.0092
220	3.47E+01	0.0097	1.96E+09	0.01
230	2.11E+01	0.0105	1.19E+09	0.0109
240	1.29E+01	0.0113	7.27E+08	0.0117
250	7.87E+00	0.0121	4.46E+08	0.0125
260	4.85E+00	0.013	2.75E+08	0.0134
270	3.00E+00	0.0138	1.70E+08	0.0142
280	1.86E+00	0.0147	1.06E+08	0.015
290	1.16E+00	0.0155	6.57E+07	0.0159
300	7.20E-01	0.0163	4.10E+07	0.0167
310	4.50E-01	0.0171	2.57E+07	0.0175
320	2.81E-01	0.018	1.61E+07	0.0183
330	1.76E-01	0.0188	1.01E+07	0.0191
340	1.11E-01	0.0196	6.32E+06	0.02
350	6.94E-02	0.0204	3.97E+06	0.0208
360	4.34E-02	0.0213	2.49E+06	0.0216
370	2.71E-02	0.0221	1.55E+06	0.0224
380	1.66E-02	0.0228	9.48E+05	0.023
390	9.63E-03	0.0233	5.43E+05	0.0236
400	4.70E-03	0.0234	2.16E+05	0.0238

Secondary photons were attenuated by the added 100 cm concrete as expected by an order of magnitude. The energy of neutrons at this point is still high enough for photon production.

Table 13: Total dose rates at each surface of a 4 m thickness of concrete shielding

Thickness (cm)	Neutron dose rate (Sv/hr)	Photon dose rate (Sv/hr)	Total dose rate (Sv/hr)
0	1.26E+08	4.19E+06	1.30E+08
10	5.39E+07	1.88E+06	5.58E+07
20	2.68E+07	1.14E+06	2.79E+07
30	1.37E+07	7.35E+05	1.44E+07
40	7.21E+06	4.72E+05	7.68E+06
50	3.87E+06	2.95E+05	4.17E+06
60	2.11E+06	1.80E+05	2.29E+06
70	1.17E+06	1.07E+05	1.28E+06
80	6.62E+05	6.29E+04	7.25E+05
90	3.82E+05	3.64E+04	4.18E+05
100	2.22E+05	2.10E+04	2.43E+05
110	1.31E+05	1.21E+04	1.43E+05
120	7.79E+04	6.92E+03	8.48E+04
130	4.69E+04	3.98E+03	5.09E+04
140	2.85E+04	2.30E+03	3.08E+04
150	1.74E+04	1.33E+03	1.87E+04
160	1.07E+04	7.77E+02	1.15E+04
170	6.59E+03	4.55E+02	7.05E+03
180	4.09E+03	2.69E+02	4.36E+03
190	2.54E+03	1.60E+02	2.70E+03
200	1.58E+03	9.55E+01	1.68E+03
210	9.91E+02	5.74E+01	1.05E+03
220	6.20E+02	3.47E+01	6.55E+02
230	3.90E+02	2.11E+01	4.11E+02
240	2.45E+02	1.29E+01	2.58E+02
250	1.54E+02	7.87E+00	1.62E+02
260	9.74E+01	4.85E+00	1.02E+02
270	6.15E+01	3.00E+00	6.45E+01
280	3.88E+01	1.86E+00	4.07E+01
290	2.45E+01	1.16E+00	2.57E+01
300	1.55E+01	7.20E-01	1.62E+01
310	9.83E+00	4.50E-01	1.03E+01
320	6.23E+00	2.81E-01	6.51E+00
330	3.95E+00	1.76E-01	4.13E+00
340	2.51E+00	1.11E-01	2.62E+00
350	1.59E+00	6.94E-02	1.66E+00
360	1.01E+00	4.34E-02	1.05E+00
370	6.42E-01	2.71E-02	6.69E-01
380	4.05E-01	1.66E-02	4.22E-01
390	2.50E-01	9.63E-03	2.60E-01
400	0.139	4.70E-03	1.44E-01

400 cm thickness reduced the effective dose rate by total of nine orders of magnitude from the inner surface of the vault wall to the outside. Figure 21 below shows the flux reduction. Beyond

the first 50 cm there was a slight increase of secondary photon population compared to the neutrons. Otherwise the population for both neutrons and photons was of same magnitude, with the last surface recording a flux of the order of 10^5 particles/cm^2.

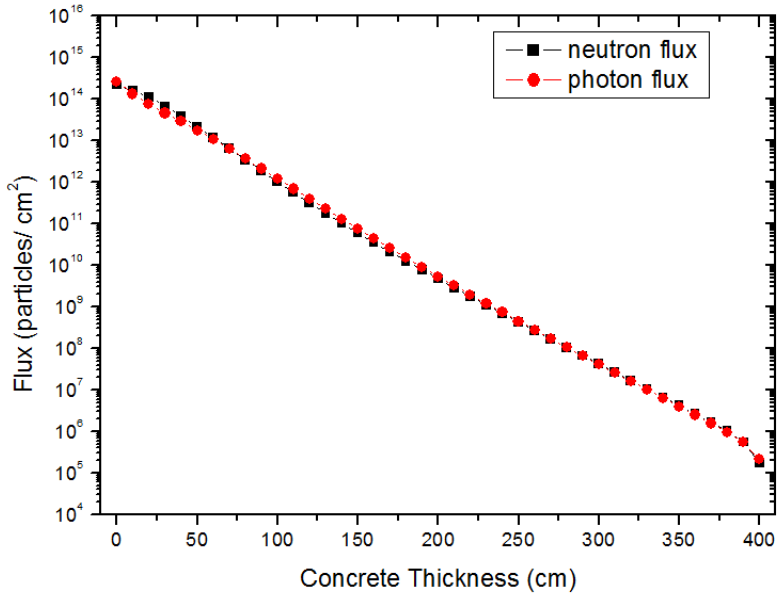

Figure 21: Attenuation of neutron and photon flux from the inner surface of the vault (0 cm) to the outer surface of the vault (400 cm). Doses were recorded at every 10 centimetres up to the 400 cm thickness of concrete shielding

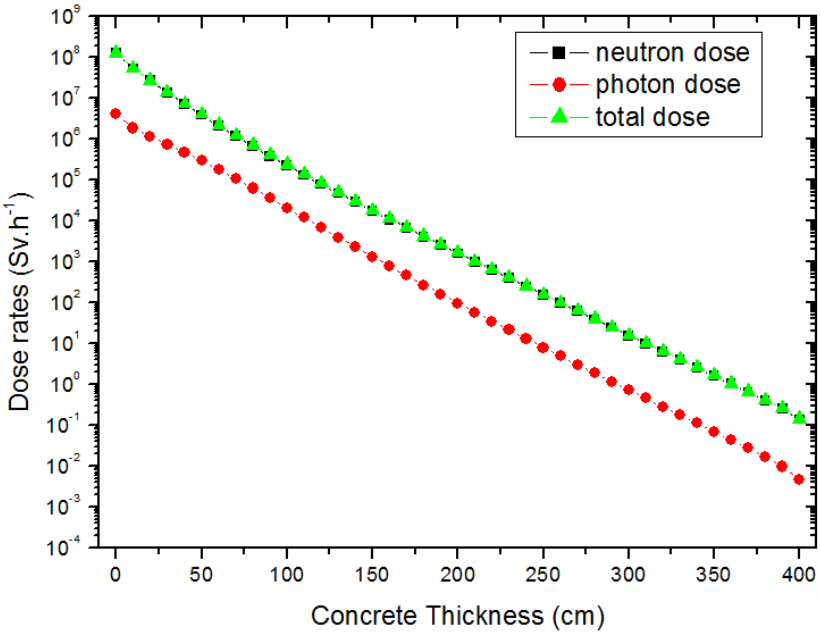

Figure 22: Attenuation of neutron; photon and total dose rates from the inner surface of the vault (0 cm) to the outer surface of the vault (400 cm). Doses were recorded at every 10 centimetres up to the 400 cm thickness of concrete shielding

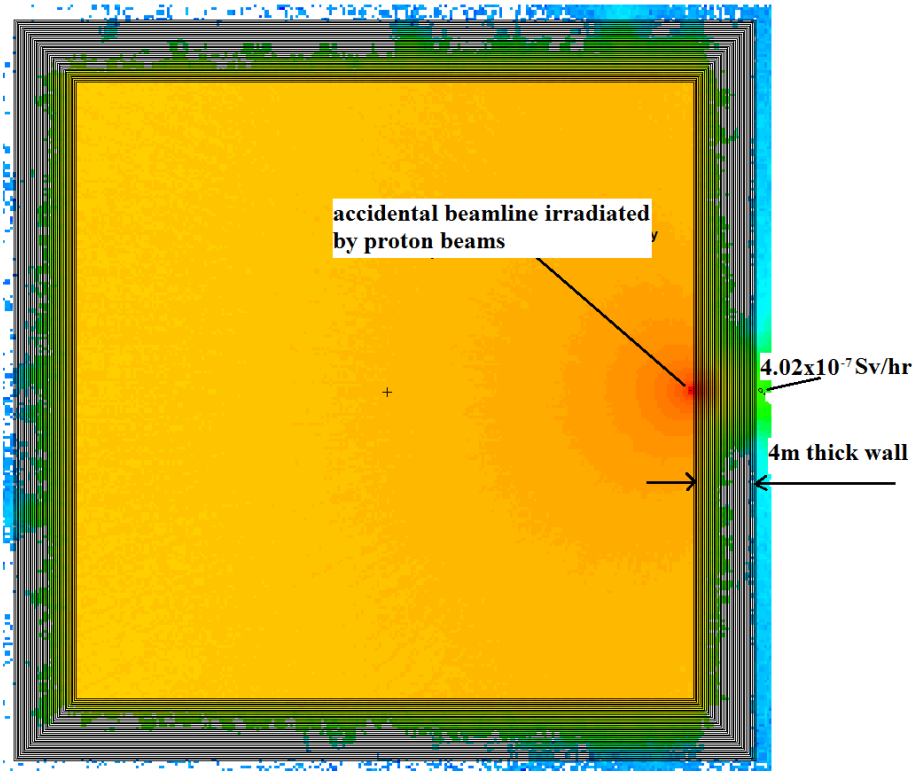

Figure 23: Mesh tally plot in the xy-plane showing the intensity distribution of neutron dose rates from the incident point through ordinary concrete of 4 metre thickness. The recorded total effective dose rate is shown

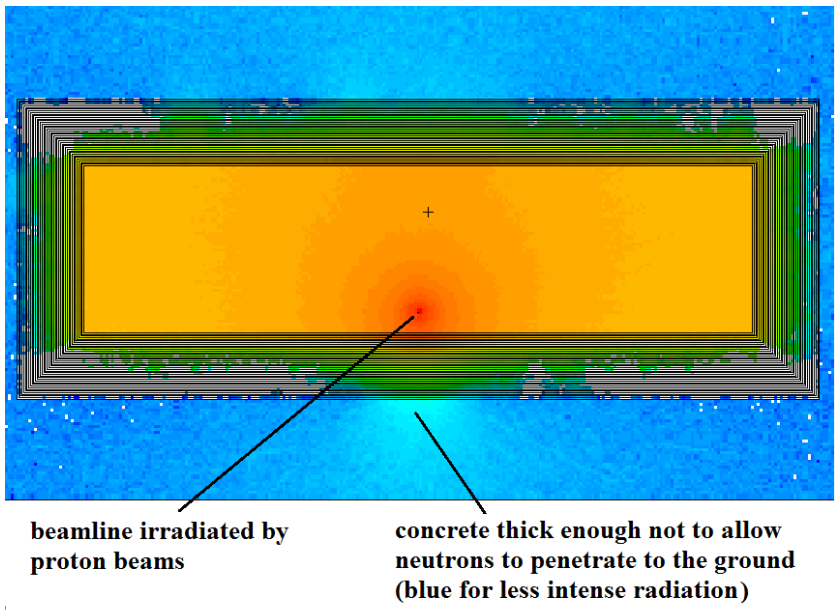

Figure 24: Mesh tally plot in the yz-plane showing the intensity distribution of neutron dose rates from the incident point through ordinary concrete of 4 metre thickness.

In Figure 23, we recorded an effective dose of 0.4 µSv/hr at the phantom. This value is much less compared to 43.9 µSv/hr that was received in the 3 metre thick concrete.
Should the ground floor concrete slab be 4 m thick as well, the flux towards underground will be effectively reduced.

Table 14: Doses for neutron and photons in the phantom which is placed 20 cm behind the 400 cm thick shielding wall. Doses registered here are the most severe ones around the outside of the vault for a simulated irradiation of the beamline by the proton beam

Particles	Dose-rate (Sv/hr)	Relative error (%)
Neutrons	3.81E-07	0.0381
Photons	2.07E-08	0.0282
Total	4.02E-07	

For the 4 metre thick concrete calculation, phantom dose rate of 0.4 µSv/hr was registered and corresponding to this is the absorbed dose rate of 0.6 x 10^{-7}Gy/hr (see Table 15).

Table 15: Absorbed dose rate on the phantom in MeV/g.s and multiplying by factor 5.77x10^{-7} it was converted to Gy/hr, the units used in the Radiation Protection literature.

Absorbed dose-rate (MeV/g.s)	Relative error (%)	Absorbed dose-rate (Gy/hr)
1.04E-01	0.0333	5.98E-08

Table 16: Neutron energy bins recorded at the inner surface of the shield of the vault (0 cm); at the middle of the shielding (200 cm) and at the outer surface of the shield (400 cm).

Inner surface (0cm)		
Energy Spectra		
n_energy(MeV)	Counts (particles/cm^2)	Relative error (%)
1.00E-11	0.00E+00	0.00E+00
1.00E-07	2.62E+13	1.30E-03
1.00E-03	2.89E+13	1.30E-03
1.00E-01	2.26E+13	1.40E-03
1.00E+00	4.44E+13	1.00E-03
2.00E+00	2.84E+13	1.10E-03
3.00E+00	1.93E+13	1.20E-03
4.00E+00	1.05E+13	1.60E-03
5.00E+00	6.82E+12	1.90E-03
6.00E+00	4.53E+12	2.30E-03
7.00E+00	3.17E+12	2.70E-03
8.00E+00	2.35E+12	3.20E-03
9.00E+00	1.90E+12	3.50E-03
1.00E+01	1.56E+12	3.90E-03
1.20E+01	2.54E+12	3.10E-03
1.40E+01	2.08E+12	3.40E-03
1.60E+01	1.80E+12	3.70E-03
1.80E+01	1.61E+12	3.90E-03
2.00E+01	1.44E+12	4.10E-03
2.50E+01	2.97E+12	2.90E-03
3.00E+01	2.28E+12	3.30E-03
3.50E+01	1.79E+12	3.70E-03
4.00E+01	1.37E+12	4.30E-03
4.50E+01	9.82E+11	5.00E-03
5.00E+01	6.41E+11	6.20E-03
5.50E+01	3.51E+11	8.30E-03
6.00E+01	1.34E+11	1.35E-02
6.50E+01	2.02E+10	3.47E-02
7.00E+01	5.82E+08	2.04E-01

Mid surface (200cm)		
Energy Spectra		
n_energy(MeV)	Counts (particles/cm^2)	Relative error (%)
1.00E-11	6.87E+02	0.7605
1.00E-07	2.12E+09	0.0108
1.00E-03	9.74E+08	0.0121
1.00E-01	3.67E+08	0.013
1.00E+00	3.55E+08	0.0133
2.00E+00	1.46E+08	0.0133
3.00E+00	1.30E+08	0.0132
4.00E+00	4.64E+07	0.0143
5.00E+00	3.81E+07	0.0143
6.00E+00	2.63E+07	0.0146
7.00E+00	2.06E+07	0.0149
8.00E+00	1.28E+07	0.0162
9.00E+00	1.13E+07	0.0164
1.00E+01	9.83E+06	0.017
1.20E+01	1.52E+07	0.0158
1.40E+01	1.34E+07	0.0165
1.60E+01	1.21E+07	0.0165
1.80E+01	1.29E+07	0.0165
2.00E+01	1.20E+07	0.0168
2.50E+01	2.94E+07	0.0149
3.00E+01	3.73E+07	0.0145
3.50E+01	4.67E+07	0.015
4.00E+01	5.66E+07	0.0168
4.50E+01	5.88E+07	0.0204
5.00E+01	5.51E+07	0.0259
5.50E+01	3.99E+07	0.0373
6.00E+01	1.76E+07	0.0699
6.50E+01	1.52E+06	0.1938
7.00E+01	4.06E+04	0.7211

Outer surface (400cm)		
Energy Spectra		
n_energy(MeV)	Counts (particles/cm^2)	Relative error (%)
1.00E-11	0.00E+00	0
1.00E-07	4.95E+04	0.0256
1.00E-03	2.95E+04	0.0266
1.00E-01	1.20E+04	0.0274
1.00E+00	1.26E+04	0.0277
2.00E+00	7.05E+03	0.0277
3.00E+00	7.71E+03	0.0275
4.00E+00	2.75E+03	0.0284
5.00E+00	2.45E+03	0.0283
6.00E+00	1.84E+03	0.0285
7.00E+00	1.56E+03	0.0279
8.00E+00	9.81E+02	0.0293
9.00E+00	8.80E+02	0.0293
1.00E+01	7.77E+02	0.0292
1.20E+01	1.23E+03	0.0288
1.40E+01	1.14E+03	0.029
1.60E+01	1.04E+03	0.0292
1.80E+01	1.13E+03	0.0291
2.00E+01	1.09E+03	0.0287
2.50E+01	2.62E+03	0.028
3.00E+01	3.28E+03	0.0268
3.50E+01	4.15E+03	0.0253
4.00E+01	5.19E+03	0.0243
4.50E+01	6.31E+03	0.0264
5.00E+01	6.81E+03	0.0327
5.50E+01	5.37E+03	0.0489
6.00E+01	2.17E+03	0.1001
6.50E+01	1.57E+02	0.2902
7.00E+01	1.10E+00	1

To find the energy of neutrons as they penetrate concrete, energy binning was performed in three successive surfaces: the inner surface of the vault wall, the middle and the outer surface.

From the behaviour observed in Figure 25, which displays the neutron energy spectra in these surfaces, it seems that while the flux of neutrons was reduced, their energy distribution remained fairly constant. Even in the last surface there were still fast neutrons of 6 MeV making 2.17×10^3 particles/cm^2.

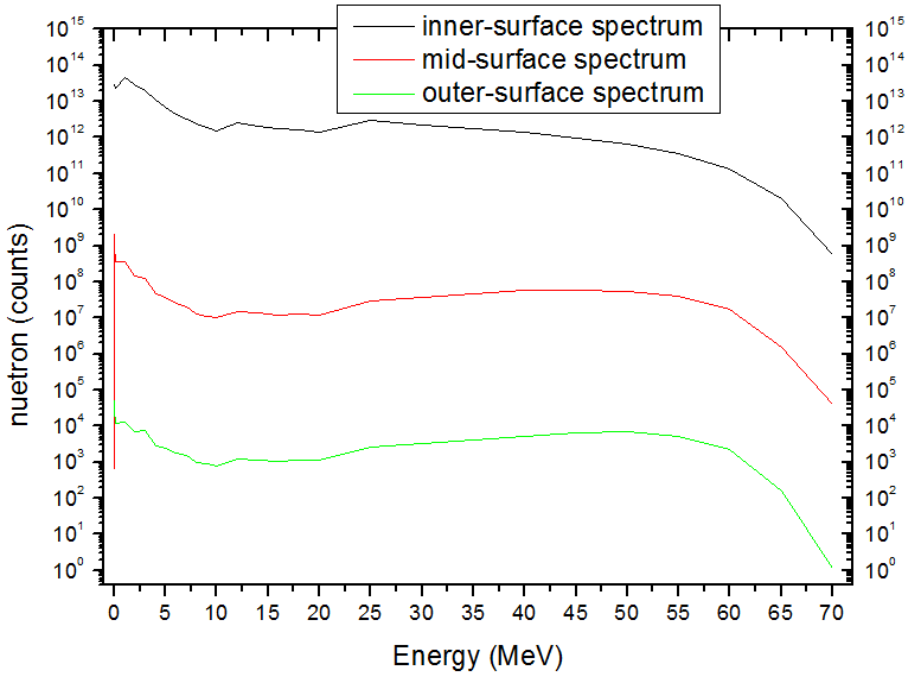

Figure 25: Neutron energy spectra for three surfaces of the concrete shielding wall. The inner surface is from the source side, where high counts of neutrons are registered (about 10^9 neutrons at 70 MeV). The mid-surface is 200 cm deep into the concrete. The outer surface is on the phantom side at 400 cm, where the average count for all energies is of order of 10^3.

Table 17: Neutron energy bins recorded at the phantom (81) placed 20 cm outside the 4 m concrete wall thickness

Energy Spectra		
n_energy (MeV)	Counts (particles/cm^2)	Relative error (%)
1.00E-11	2.12E-08	0.1271
1.00E-07	2.01E-01	0.0247
1.00E-03	5.73E-02	0.025
1.00E-01	1.84E-02	0.0254
1.00E+00	2.12E-02	0.0256
2.00E+00	1.21E-02	0.026
3.00E+00	1.05E-02	0.0263
4.00E+00	6.30E-03	0.0266
5.00E+00	5.76E-03	0.027
6.00E+00	4.96E-03	0.0275
7.00E+00	4.27E-03	0.0275
8.00E+00	3.34E-03	0.0294
9.00E+00	3.03E-03	0.0292
1.00E+01	2.72E-03	0.0291
1.20E+01	4.86E-03	0.0282
1.40E+01	4.42E-03	0.0296
1.60E+01	4.02E-03	0.0288
1.80E+01	4.16E-03	0.0292
2.00E+01	3.95E-03	0.0296
2.50E+01	9.33E-03	0.0276
3.00E+01	1.08E-02	0.0271
3.50E+01	1.25E-02	0.026
4.00E+01	1.53E-02	0.0256
4.50E+01	1.74E-02	0.0274
5.00E+01	1.78E-02	0.0328
5.50E+01	1.38E-02	0.0489
6.00E+01	5.97E-03	0.095
6.50E+01	4.27E-04	0.3077
7.00E+01	0.00E+00	0

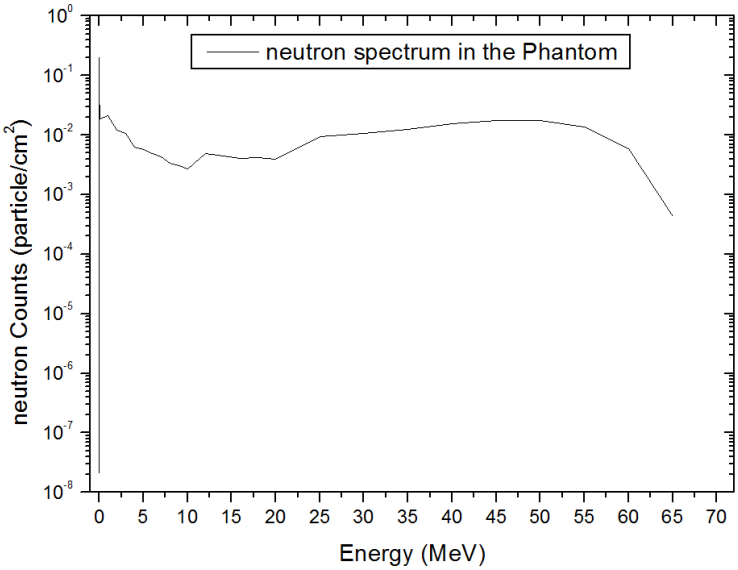

Figure 26: Neutron energy spectra as recorded in the phantom (81) placed 20 cm outside the 4m concrete wall thickness

4.2.2 Results of the RIB Demonstrator vault

This section will look into the neutron source used to simulate neutrons from the fissioning of UC_x. Secondly we look at the effectiveness of the 3 m thick walls of the vault in making sure that ionising radiation is at reasonable levels during beam operations, particularly in the entrance to the experimental room and also the experimental room itself.

a) Proton irradiation of different materials and neutron flux

To choose the material with the most neutron flux leaving the spherical source, we performed an F1 current tally (flux) tally for beryllium (Be), beryllium oxide (BeO), copper (Cu), stainless steel (Fe), lead (Pb) and tungsten (W) when irradiated by proton point source of 70MeV of 350μA current. Comparing the neutron flux from these materials, Pb gave the highest flux of $3.15x10^{14}$ particles/cm^2. Therefore lead was used in the RIB demonstrator vault to simulate a very high neutron yield source. Table 18 shows neutron yields.

Table 18: Neutron yields calculated as neutron flux leaving the outer surface of the spherical target material

Material	Flux (particle/cm^2)	Relative error (%)
Be	2.57E+14	0.0007
BeO	1.15E+14	0.0013
Cu	2.25E+14	0.0273
Fe	1.23E+14	0.0047
Pb	3.15E+14	0.0032
W	2.90E+14	0.0034

b) for the closed vault with a beamline opening leading to the experiment room

Table 19: Neutron yield from lead (Pb), calculated to be higher than that from the other materials considered.

Material	Neutron flux	Relative error (%)
Pb	3.15E+14	0.0032

The energy binning of the neutrons leaving the lead sphere is shown in the table below. As explained in section 3.2.2 why lead can be used instead of UC_x to estimate dose levels, the neutron flux calculated 3.15E+14 is high enough to give confidence that when we have phantom readings, we can make reliable conclusions regarding radiation safety in the RIB Demonstrator facility.

Table 20: Neutron energy bins recorded in the lead (Pb) target. This shows that fast neutrons indeed are emitted.

Energy Spectra		
n_energy (MeV)	Counts (particles/cm^2)	Relative error (%)
1.00E-11	0.00E+00	0.00E+00
1.00E-07	2.35E+09	1.27E-01
1.00E-03	4.78E+10	2.72E-02
1.00E-01	7.08E+12	2.20E-03
1.00E+00	7.85E+13	7.00E-04
2.00E+00	1.01E+14	6.00E-04
3.00E+00	5.96E+13	8.00E-04
4.00E+00	2.97E+13	1.10E-03
5.00E+00	1.41E+13	1.50E-03
6.00E+00	7.07E+12	2.20E-03
7.00E+00	4.06E+12	2.90E-03
8.00E+00	2.69E+12	3.50E-03
9.00E+00	2.01E+12	4.10E-03
1.00E+01	1.64E+12	4.50E-03
1.20E+01	2.69E+12	3.50E-03
1.40E+01	2.23E+12	3.90E-03
1.60E+01	1.95E+12	4.20E-03
1.80E+01	1.70E+12	4.40E-03
2.00E+01	1.49E+12	4.70E-03
2.50E+01	3.04E+12	3.30E-03
3.00E+01	2.36E+12	3.80E-03
3.50E+01	1.84E+12	4.30E-03
4.00E+01	1.44E+12	4.80E-03
4.50E+01	1.06E+12	5.60E-03
5.00E+01	7.21E+11	6.80E-03
5.50E+01	4.23E+11	8.90E-03
6.00E+01	1.75E+11	1.39E-02
6.50E+01	3.64E+10	3.03E-02
7.00E+01	1.68E+08	4.47E-01

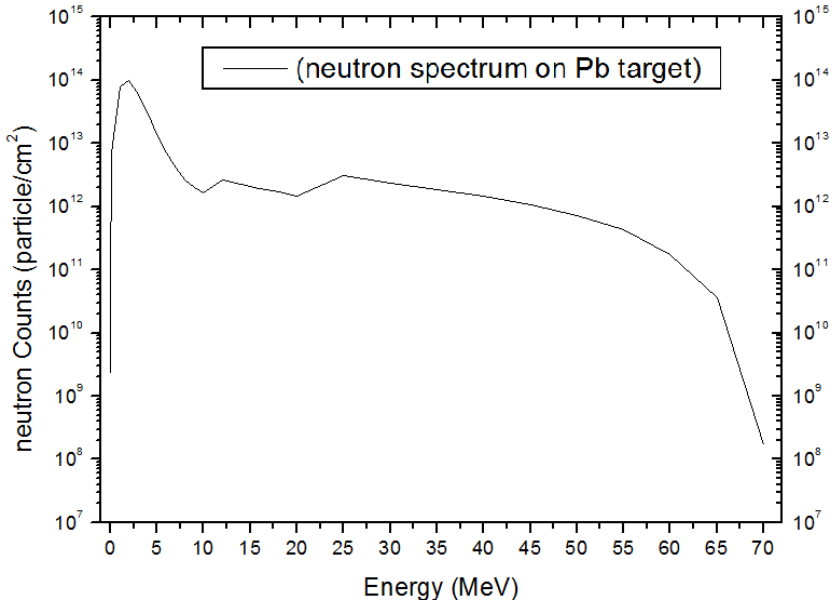

Figure 27: Neutron energy spectra as recorded in the lead (Pb) target. About 10^8 of fast neutrons at 70 MeV were produced when a 70 MeV proton beam of 350μA current irradiates a spherical lead ball of stopping-length radius

Table 21: Neutron dose rates and corresponding fluxes at each surface of the 3 m thickness of the RIB Demonstrator concrete shielding

Thickness(cm)	Dose (Sv/hr)	Relative error (%)	Flux (particles/cm^2)	Relative error (%)
0	8.08E+07	0.0007	3.36E+14	0.0005
10	3.52E+07	0.0012	2.28E+14	0.0008
20	1.54E+07	0.0017	1.35E+14	0.0011
30	6.99E+06	0.0026	7.34E+13	0.0015
40	3.24E+06	0.0037	3.76E+13	0.0020
50	1.55E+06	0.0051	1.85E+13	0.0024
60	7.58E+05	0.0067	8.96E+12	0.0030
70	3.80E+05	0.0088	4.26E+12	0.0036
80	1.96E+05	0.0112	2.03E+12	0.0044
90	1.05E+05	0.0140	9.61E+11	0.0053
100	5.79E+04	0.0172	4.66E+11	0.0065
110	3.24E+04	0.0206	2.28E+11	0.0080
120	1.86E+04	0.0240	1.14E+11	0.0099
130	1.07E+04	0.0273	5.81E+10	0.0122
140	6.44E+03	0.0307	3.06E+10	0.0150
150	3.88E+03	0.0341	1.66E+10	0.0183
160	2.36E+03	0.0376	9.28E+09	0.0218
170	1.43E+03	0.0412	5.27E+09	0.0251
180	8.90E+02	0.0446	3.02E+09	0.0287
190	5.54E+02	0.0478	1.76E+09	0.0324
200	3.43E+02	0.0511	1.04E+09	0.0364
210	2.14E+02	0.0548	6.31E+08	0.0402
220	1.35E+02	0.0590	3.90E+08	0.0441
230	8.51E+01	0.0614	2.40E+08	0.0476
240	5.35E+01	0.0649	1.48E+08	0.0510
250	3.38E+01	0.0691	9.26E+07	0.0549
260	2.12E+01	0.0731	5.73E+07	0.0588
270	1.35E+01	0.0761	3.59E+07	0.0627
280	8.61E+00	0.0793	2.21E+07	0.0643
290	5.36E+00	0.0823	1.31E+07	0.0607
300	3.05E+00	0.0830	7.69E+06	0.0380

Comparing this 3 metre thickness of the Demonstrator vault to the 3 metre thickness of the cyclotron vault, there is agreement in the attenuation of particle flux and the decrease of orders of magnitude for both cases.

Table 22: Photon dose rates and corresponding fluxes at each surface of the 3 m thickness of the RIB demonstrator concrete shielding.

Thickness(cm)	Dose (Sv/hr)	Relative error (%)	Flux (particles/cm^2)	Relative error (%)
0	2.25E+06	0.0008	1.54E+14	0.0006
10	1.63E+06	0.0010	1.08E+14	0.0009
20	1.16E+06	0.0013	7.30E+13	0.0011
30	7.77E+05	0.0015	4.77E+13	0.0014
40	4.89E+05	0.0018	2.96E+13	0.0016
50	2.92E+05	0.0021	1.75E+13	0.0019
60	1.68E+05	0.0024	9.97E+12	0.0021
70	9.37E+04	0.0027	5.53E+12	0.0024
80	5.12E+04	0.0030	3.00E+12	0.0028
90	2.76E+04	0.0034	1.60E+12	0.0031
100	1.48E+04	0.0039	8.47E+11	0.0036
110	7.94E+03	0.0044	4.50E+11	0.0041
120	4.23E+03	0.0051	2.38E+11	0.0047
130	2.27E+03	0.0058	1.26E+11	0.0055
140	1.22E+03	0.0067	6.71E+10	0.0064
150	6.62E+02	0.0078	3.63E+10	0.0076
160	3.61E+02	0.0091	1.96E+10	0.0090
170	1.98E+02	0.0105	1.07E+10	0.0106
180	1.10E+02	0.0123	5.93E+09	0.0125
190	6.18E+01	0.0141	3.31E+09	0.0145
200	3.49E+01	0.0163	1.87E+09	0.0169
210	1.99E+01	0.0188	1.07E+09	0.0196
220	1.15E+01	0.0212	6.15E+08	0.0223
230	6.68E+00	0.0241	3.58E+08	0.0256
240	3.92E+00	0.0273	2.12E+08	0.0289
250	2.32E+00	0.0307	1.25E+08	0.0325
260	1.38E+00	0.0340	7.44E+07	0.0362
270	8.28E-01	0.0379	4.48E+07	0.0399
280	4.89E-01	0.0409	2.66E+07	0.0427
290	2.83E-01	0.0420	1.53E+07	0.0435
300	1.54E-01	0.0374	7.86E+06	0.0321

Table 23: Total dose rates at each surface of 3 m thickness of concrete shielding

Thickness(cm)	Neutron dose rate (Sv/hr)	Photon dose rate (Sv/hr)	Total dose rate (Sv/hr)
0	8.08E+07	2.25E+06	8.30E+07
10	3.52E+07	1.63E+06	3.68E+07
20	1.54E+07	1.16E+06	1.66E+07
30	6.99E+06	7.77E+05	7.76E+06
40	3.24E+06	4.89E+05	3.73E+06
50	1.55E+06	2.92E+05	1.84E+06
60	7.58E+05	1.68E+05	9.26E+05
70	3.80E+05	9.37E+04	4.73E+05
80	1.96E+05	5.12E+04	2.47E+05
90	1.05E+05	2.76E+04	1.33E+05
100	5.79E+04	1.48E+04	7.27E+04
110	3.24E+04	7.94E+03	4.03E+04
120	1.86E+04	4.23E+03	2.28E+04
130	1.07E+04	2.27E+03	1.30E+04
140	6.44E+03	1.22E+03	7.66E+03
150	3.88E+03	6.62E+02	4.54E+03
160	2.36E+03	3.61E+02	2.72E+03
170	1.43E+03	1.98E+02	1.63E+03
180	8.90E+02	1.10E+02	1.00E+03
190	5.54E+02	6.18E+01	6.15E+02
200	3.43E+02	3.49E+01	3.78E+02
210	2.14E+02	1.99E+01	2.34E+02
220	1.35E+02	1.15E+01	1.47E+02
230	8.51E+01	6.68E+00	9.18E+01
240	5.35E+01	3.92E+00	5.74E+01
250	3.38E+01	2.32E+00	3.62E+01
260	2.12E+01	1.38E+00	2.26E+01
270	1.35E+01	8.28E-01	1.43E+01
280	8.61E+00	4.89E-01	9.10E+00
290	5.36E+00	2.83E-01	5.64E+00
300	3.05E+00	1.54E-01	3.21E+00

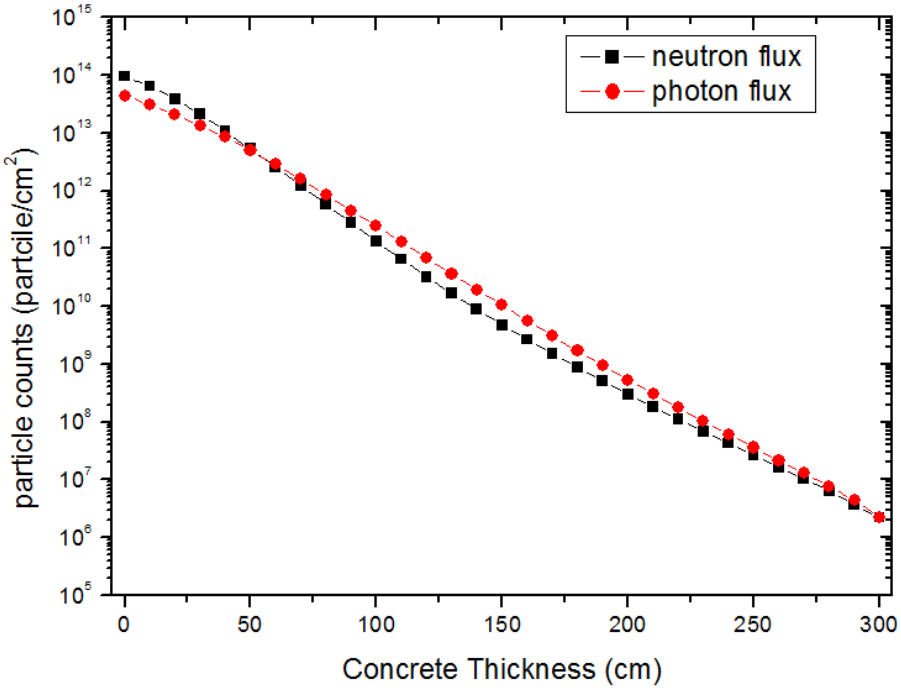

Figure 28: Attenuation of neutron and photon flux from the inner surface of the vault (0 cm) to the outer surface of the vault (300 cm). Doses were recorded at every 10 cm up to 300 cm thickness of the RIB Demonstrator concrete shielding.

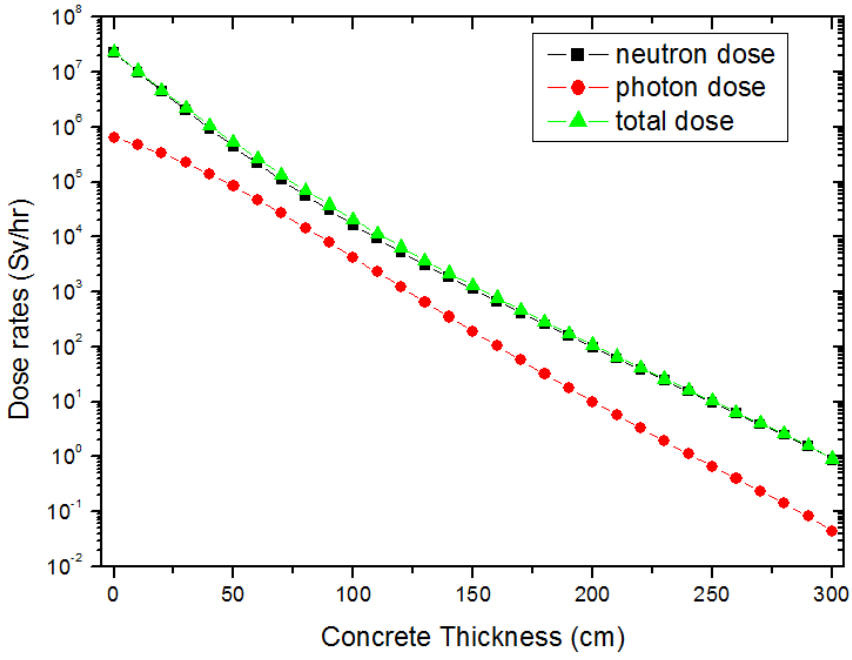

Figure 29: Attenuation of neutron, photon and total dose rates from the inner surface of the vault (0 cm) to the outer surface of the vault (300 cm). Doses were recorded at every 10 cm up to 300 cm thickness of the RIB Demonstrator concrete shielding

Figure 28 shows a noticeable behaviour of secondary photons being produced beyond 50 cm concrete. As neutrons loose energy (at lower energy) more secondary photons are produced. However in the outer surface of the vault (300 cm) the flux of neutrons and photons is of the same magnitude.

Figure 29 shows the attenuation of dose rates for both neutrons and photon as well as total dose rate which shows neutron dominating.

Neutron energy binning at the three surfaces of the concrete is presented below in Table 24.

Table 24: Neutron energy bins recorded at the inner surface of the shield of the RIB Demonstrator vault (0 cm); at the middle of the shielding (150 cm) and at the outer surface of the shield (300 cm).

Inner surface (0 cm)

Energy Spectra		
n_energy (MeV)	Counts (particles/cm^2)	Relative error (%)
1.00E-11	2.59E+07	1.00E+00
1.00E-07	8.34E+13	8.00E-04
1.00E-03	7.16E+13	9.00E-04
1.00E-01	4.52E+13	1.10E-03
1.00E+00	6.85E+13	9.00E-04
2.00E+00	3.27E+13	1.20E-03
3.00E+00	1.73E+13	1.50E-03
4.00E+00	6.83E+12	2.30E-03
5.00E+00	3.09E+12	3.30E-03
6.00E+00	1.50E+12	4.70E-03
7.00E+00	8.44E+11	6.20E-03
8.00E+00	5.42E+11	7.70E-03
9.00E+00	4.13E+11	8.80E-03
1.00E+01	3.31E+11	9.80E-03
1.20E+01	5.11E+11	8.00E-03
1.40E+01	4.12E+11	8.90E-03
1.60E+01	3.47E+11	9.70E-03
1.80E+01	3.01E+11	1.05E-02
2.00E+01	2.61E+11	1.13E-02
2.50E+01	5.20E+11	8.00E-03
3.00E+01	4.01E+11	9.10E-03
3.50E+01	3.10E+11	1.04E-02
4.00E+01	2.45E+11	1.17E-02
4.50E+01	1.78E+11	1.37E-02
5.00E+01	1.19E+11	1.67E-02
5.50E+01	7.19E+10	2.15E-02
6.00E+01	3.00E+10	3.33E-02
6.50E+01	6.02E+09	7.43E-02
7.00E+01	6.65E+07	7.07E-01

Mid surface (150 cm)

Energy Spectra		
n_energy (MeV)	Counts (particles/cm^2)	Relative error (%)
1.00E-11	0.00E+00	0.00E+00
1.00E-07	3.03E+11	5.80E-03
1.00E-03	8.70E+10	8.60E-03
1.00E-01	2.27E+10	1.41E-02
1.00E+00	2.02E+10	1.51E-02
2.00E+00	8.57E+09	1.74E-02
3.00E+00	7.70E+09	1.81E-02
4.00E+00	1.76E+09	2.86E-02
5.00E+00	1.49E+09	3.11E-02
6.00E+00	1.07E+09	3.68E-02
7.00E+00	8.70E+08	4.16E-02
8.00E+00	4.79E+08	5.06E-02
9.00E+00	3.93E+08	5.37E-02
1.00E+01	3.59E+08	5.82E-02
1.20E+01	5.28E+08	5.01E-02
1.40E+01	4.25E+08	5.31E-02
1.60E+01	4.51E+08	5.83E-02
1.80E+01	4.31E+08	5.94E-02
2.00E+01	3.56E+08	6.73E-02
2.50E+01	1.03E+09	4.56E-02
3.00E+01	1.28E+09	4.68E-02
3.50E+01	1.45E+09	5.12E-02
4.00E+01	1.50E+09	5.20E-02
4.50E+01	1.42E+09	5.75E-02
5.00E+01	1.04E+09	7.12E-02
5.50E+01	6.41E+08	9.81E-02
6.00E+01	3.26E+08	1.49E-01
6.50E+01	6.30E+07	4.12E-01
7.00E+01	0.00E+00	0.00E+00

Outer surface (300 cm)

Energy Spectra		
n_energy (MeV)	Counts (particles/c	Relative error (%)
1.00E-11	0.00E+00	0.00E+00
1.00E-07	3.17E+06	3.13E-02
1.00E-03	2.01E+06	3.86E-02
1.00E-01	6.30E+05	4.22E-02
1.00E+00	4.01E+05	5.23E-02
2.00E+00	1.84E+05	6.40E-02
3.00E+00	1.74E+05	7.35E-02
4.00E+00	6.09E+04	7.55E-02
5.00E+00	5.60E+04	8.44E-02
6.00E+00	3.96E+04	8.84E-02
7.00E+00	3.36E+04	1.02E-01
8.00E+00	2.00E+04	1.16E-01
9.00E+00	1.80E+04	1.10E-01
1.00E+01	1.68E+04	1.15E-01
1.20E+01	2.83E+04	1.00E-01
1.40E+01	2.42E+04	1.16E-01
1.60E+01	2.38E+04	1.09E-01
1.80E+01	2.09E+04	1.14E-01
2.00E+01	2.43E+04	1.07E-01
2.50E+01	6.09E+04	9.30E-02
3.00E+01	7.50E+04	9.07E-02
3.50E+01	8.34E+04	8.60E-02
4.00E+01	1.17E+05	8.64E-02
4.50E+01	1.15E+05	9.69E-02
5.00E+01	1.21E+05	1.14E-01
5.50E+01	1.14E+05	1.59E-01
6.00E+01	5.64E+04	3.06E-01
6.50E+01	9.74E+03	8.76E-01
7.00E+01	0.00E+00	0.00E+00

Again the neutron energy spectra in selected surfaces show that the concrete merely reduced the flux of particles; however the energy distribution remained the same. Fast neutrons can escape from the vault, judging by those recorded in the outer surface (300 cm).

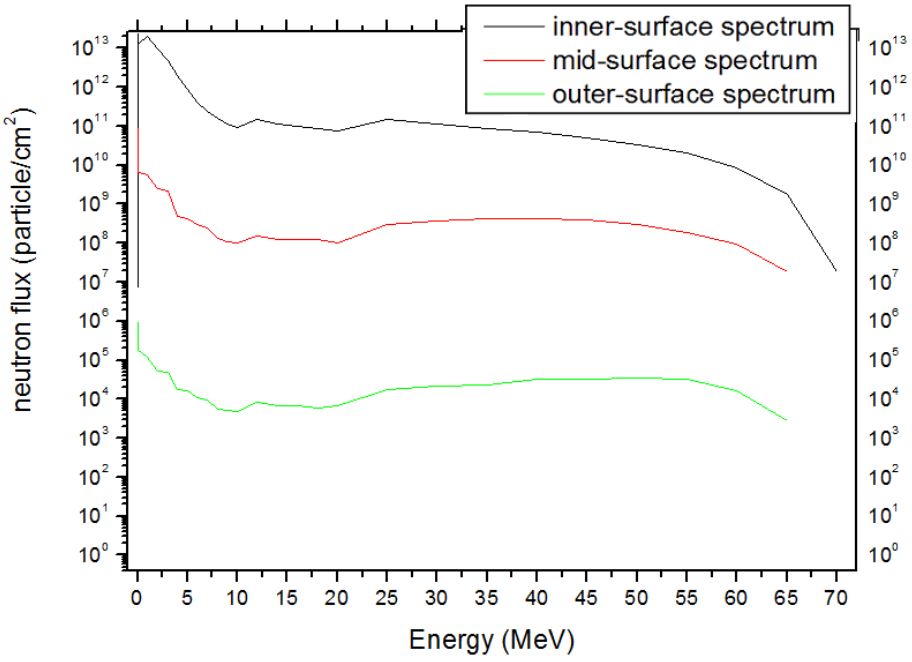

Figure 30: Neutron energy spectra for three surfaces of the RIB Demonstrator concrete shielding wall. The inner surface is from the source side, high counts of neutrons are registered (about 10^7 neutrons at 70 MeV counted). The mid-surface is 150 cm deep into the concrete. The outer surface is on the phantom side at 300 cm, where the count of all energies is between 10^3 and 10^4.

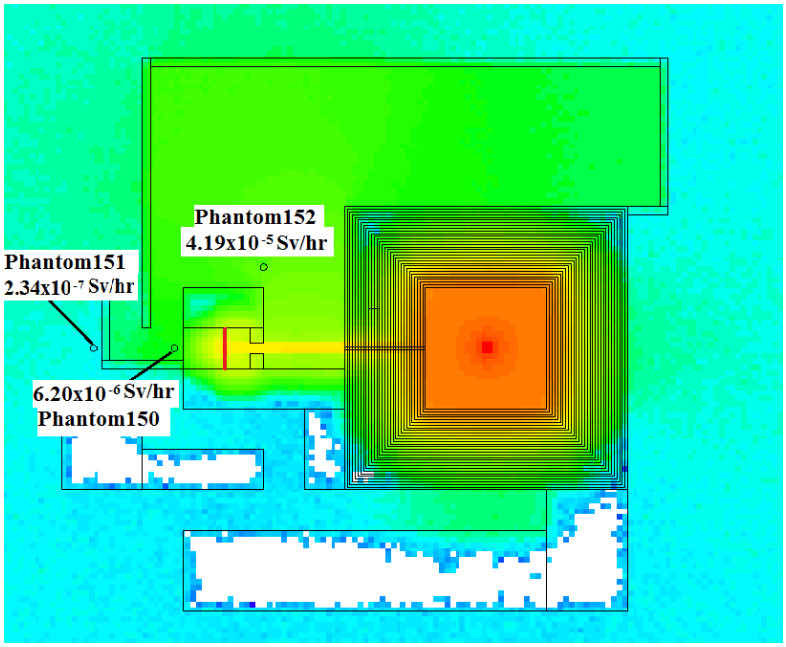

Figure 31: Mesh tally plot in the xy-plane showing the intensity distribution of neutron dose rates from the target point through ordinary concrete of 3 metre thickness. The recorded total effective dose rates are shown for different areas of interest.

Table 25: Neutron energy bins recorded at the phantoms (152, 150 and 151) placed in the RIB Demonstrator.

Phantom 152

Energy Spectra		
n_energy (MeV)	Counts (particles/cm^2)	Relative error (%)
1.00E-11	3.04E-05	0.2252
1.00E-07	2.71E+02	0.0817
1.00E-03	7.91E+01	0.0874
1.00E-01	2.19E+01	0.1
1.00E+00	2.04E+01	0.1116
2.00E+00	8.21E+00	0.1407
3.00E+00	5.04E+00	0.2179
4.00E+00	1.73E+00	0.2814
5.00E+00	6.80E-01	0.2752
6.00E+00	4.93E-01	0.2929
7.00E+00	4.02E-01	0.355
8.00E+00	2.31E-01	0.4019
9.00E+00	2.01E-01	0.4343
1.00E+01	1.97E-01	0.4551
1.20E+01	2.84E-01	0.3998
1.40E+01	2.79E-01	0.3821
1.60E+01	2.74E-01	0.59
1.80E+01	5.03E-01	0.7263
2.00E+01	1.47E-01	0.3396
2.50E+01	3.51E-01	0.3447
3.00E+01	2.93E-01	0.4275
3.50E+01	3.29E-01	0.4972
4.00E+01	2.02E-01	0.7177
4.50E+01	3.31E-01	0.7754
5.00E+01	9.89E-02	0.4703
5.50E+01	2.54E-02	0.56
6.00E+01	2.64E-02	0.4352
6.50E+01	1.94E-03	1
7.00E+01	0.00E+00	0

Phantom 150

Energy Spectra		
n_energy (MeV)	Counts (particles/cm^2)	Relative error (%)
1.00E-11	3.18E-06	0.4738
1.00E-07	1.01E+01	0.1999
1.00E-03	2.34E+00	0.2409
1.00E-01	4.89E-01	0.3542
1.00E+00	4.43E-01	0.4187
2.00E+00	2.08E-01	0.4958
3.00E+00	1.77E-01	0.507
4.00E+00	9.54E-02	0.5215
5.00E+00	8.05E-02	0.6137
6.00E+00	7.91E-02	0.5178
7.00E+00	7.93E-02	0.5732
8.00E+00	5.56E-02	0.5731
9.00E+00	4.26E-02	0.6328
1.00E+01	4.77E-02	0.662
1.20E+01	7.58E-02	0.656
1.40E+01	7.63E-02	0.6314
1.60E+01	6.92E-02	0.7157
1.80E+01	6.84E-02	0.6318
2.00E+01	5.71E-02	0.5913
2.50E+01	1.07E-01	0.4808
3.00E+01	1.48E-01	0.5307
3.50E+01	2.24E-01	0.446
4.00E+01	1.29E-01	0.6497
4.50E+01	1.41E-01	0.9273
5.00E+01	2.82E-01	1
5.50E+01	2.60E-01	1
6.00E+01	0.00E+00	0
6.50E+01	0.00E+00	0
7.00E+01	0.00E+00	0

Phantom 151

Energy Spectra		
n_energy (MeV)	Counts (particles/cm^2)	Relative error (%)
1.00E-11	0.00E+00	0
1.00E-07	5.42E-01	0.1356
1.00E-03	1.37E-01	0.1701
1.00E-01	2.37E-02	0.3092
1.00E+00	1.78E-02	0.5392
2.00E+00	1.25E-02	0.6087
3.00E+00	8.36E-03	0.7145
4.00E+00	1.40E-03	0.7132
5.00E+00	2.37E-03	0.5831
6.00E+00	3.49E-03	0.9316
7.00E+00	1.49E-03	0.7173
8.00E+00	2.82E-03	0.8691
9.00E+00	2.10E-03	0.7077
1.00E+01	4.90E-04	1
1.20E+01	3.68E-03	1
1.40E+01	1.62E-03	1
1.60E+01	6.46E-03	0.9841
1.80E+01	4.36E-03	0.9603
2.00E+01	9.98E-04	1
2.50E+01	1.11E-02	0.8215
3.00E+01	6.10E-03	1
3.50E+01	1.05E-02	0.8595
4.00E+01	2.82E-03	1
4.50E+01	1.05E-03	1
5.00E+01	9.70E-03	1
5.50E+01	8.20E-03	1
6.00E+01	0.00E+00	0
6.50E+01	0.00E+00	0
7.00E+01	0.00E+00	0

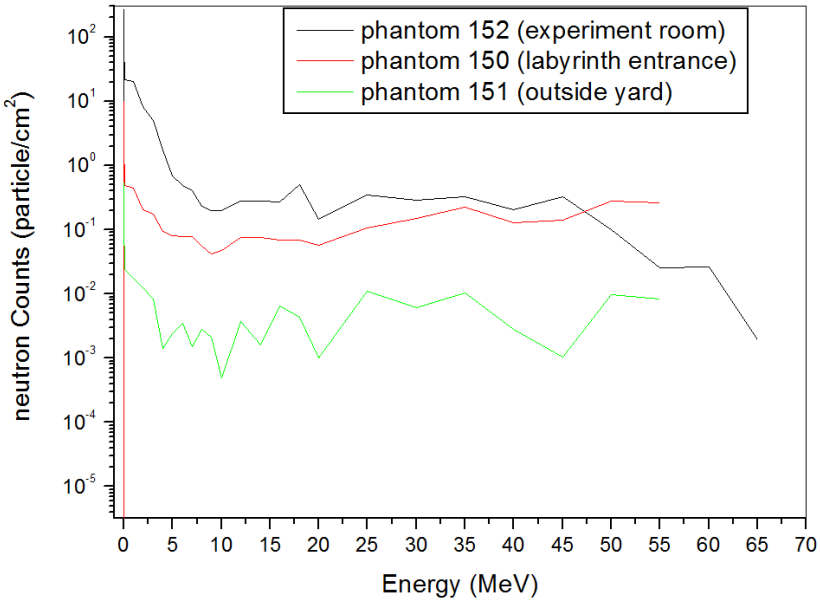

Figure 32: Neutron energy spectra as recorded in the phantoms (152, 150, and 150) placed outside the closed RIB demonstrator vault

Figure 31 confirms the beamlike exit of neutrons from the RIB Demonstrator vault through the beamline. This escape is the main contributor to that of the high dose rates in the experimental room where Phantom 152 is placed. This figure with its colour-coding also shows the effectiveness of the beam dump in achieving radiation containment, particularly of neutrons.

Figure 32 shows neutron spectra of listed phantoms. Phantom 152 which was placed in the experimental room registered a high neutron count compared to the Phantom 150 & 151 which is expected. Neutron energies as well reflect a realistic situation as neutrons of 70MeV were recorded in Phantom 152 whereas Phantom 150 & 151 recorded a maximum of about 55MeV. However, Phantom 150 was placed behind the beam dump as neutrons are forward peaked it is expected that at high energies (higher than 45MeV) more neutrons are recorded in Phantom 150 compared to Phantom 152 which was adjacent to the beam dump.

It may be interesting to learn what is the energy deposited by the ionising radiation into the material per unit mass for the tissue equivalent material (TEM) that was used in the phantom emulating a person. Tables (26, 27 & 28) below show that for different phantoms.

Table 26: Absorbed dose rate on the phantom 150

Absorbed dose-rate (MeV/g.s)	Relative error (%)	Absorbed dose-rate (Gy/hr)
2.60E+00	0.3367	1.50E-06

Table 27: Absorbed dose rate on the phantom 151

Absorbed dose-rate (MeV/g.s)	Relative error (%)	Absorbed dose-rate (Gy/hr)
9.12E-02	0.4393	5.26E-08

Table 28: Absorbed dose rate on the phantom 152

Absorbed dose-rate (MeV/g.s)	Relative error (%)	Absorbed dose-rate (Gy/hr)
2.53E+01	0.0921	1.46E-05

c) Open vault with a beamline opening leading to the experiment room

Now that we have examined dose rates by the side of the experimental room, we now look at the entrance side of the vault. Figure 33 shows the allocation of phantoms in areas of interest with corresponding dose rates. The aim is to see whether the corridor will be accessible during the RIB experiments as the corridor leads to the entrance of the spectrometer.

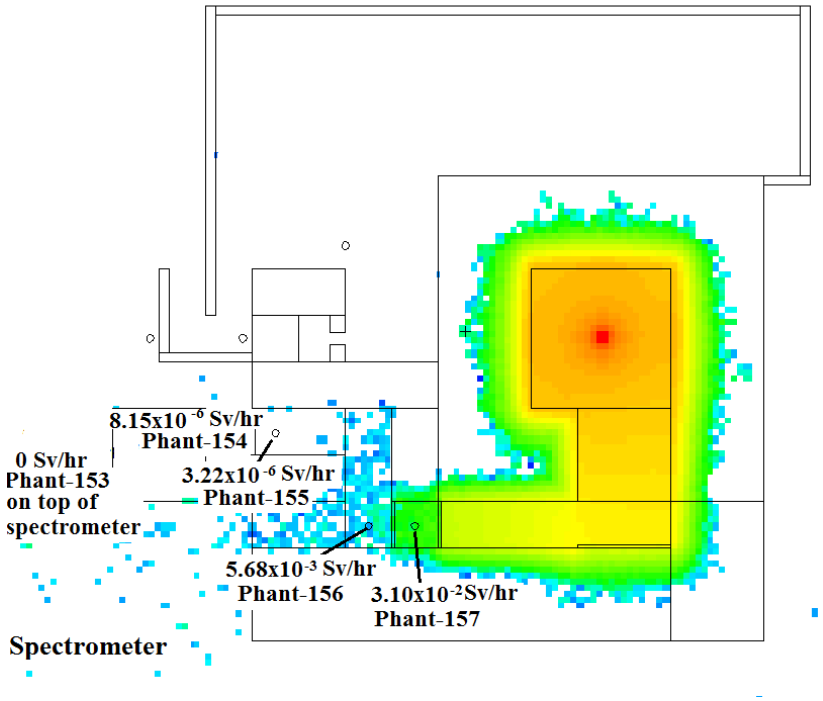

Figure 33: Mesh tally plot in the *xy*-plane showing the intensity distribution of neutron dose rates from the target point through an open vault to show the effectiveness of the borated wax doors. The recorded total effective dose rate is shown.

Table 29: Doses for neutrons and photons in the phantom 154

Particle	Dose-rate (Sv/hr)	Relative error (%)
neutron		
photon	8.15E-06	0.7991
total	8.15E-06	

Table 30: Doses for neutrons and photons in the phantom 155

particle	Dose-rate (Sv/hr)	Relative error (%)
neutron	2.12E-07	0.6137
photon	3.01E-06	0.3037
total	3.22E-06	

Table 29 and 30 shows dose rate of Phantom 155 to be higher than that of Phantom 154 as 155 recorded low energy neutrons and are more harmful than by biological effect conventions dose rate is estimated higher, whereas 154 did not record any neutrons only photons.

Table 31: Doses for neutrons and photons in the phantom 156

particle	Dose-rate (Sv/hr)	Relative error (%)
neutron	7.41E-04	0.5374
photon	4.93E-03	0.0566
total	5.68E-03	

Table 32: Doses for neutrons and photons in the phantom 157

particle	Dose-rate (Sv/hr)	Relative error (%)
neutron	6.97E-03	0.1852
photon	2.41E-02	0.0368
total	3.10E-02	

Table 33: Absorbed dose rate on the phantom 154

Absorbed dose-rate (MeV/g.s)	Relative error (%)	Absorbed dose-rate (Gy/hr)
1.46E+01	0.8263	8.44E-06

Table 34: Absorbed dose rate on the phantom 155

Absorbed dose-rate (MeV/g.s)	Relative error (%)	Absorbed dose-rate (Gy/hr)
4.79E+00	0.2993	2.77E-06

Table 35: Absorbed dose rate on the phantom 156

Absorbed dose-rate (MeV/g.s)	Relative error (%)	Absorbed dose-rate (Gy/hr)
8.87E+03	0.0576	5.11E-03

Table 36: Absorbed dose rate on the phantom 157

Absorbed dose-rate (MeV/g.s)	Relative error (%)	Absorbed dose-rate (Gy/hr)
4.38E+04	0.0373	2.53E-02

We are interested in the neutron counts and their corresponding energies reaching the phantoms placed in Figure 33. The figure below shows that phantom 155 registered insignificant number of neutrons and energy. Phantom 156 registered neutrons with maximum energy of about 15MeV. Phantom 157 registered a higher count of neutrons compared to phantom 156 with higher energy as well. Phantom 154 did not register any neutrons, however in registered secondary photons and it is shown in Figure 35.

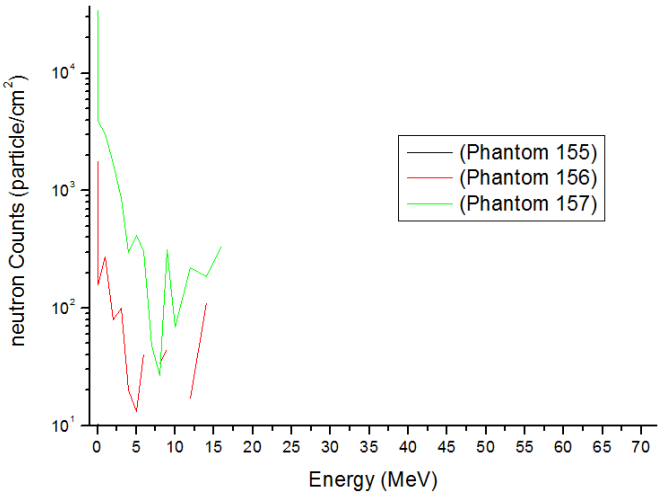

Figure 34: Neutron energy spectra averaged inside the phantoms shown. These are neutrons that reached phantoms having been transported from the source. Neutrons that reached Phantom 155 are negligible because of their energy and low counts

Phantom 154 registered the following photons with maximum energy of about 2 MeV.

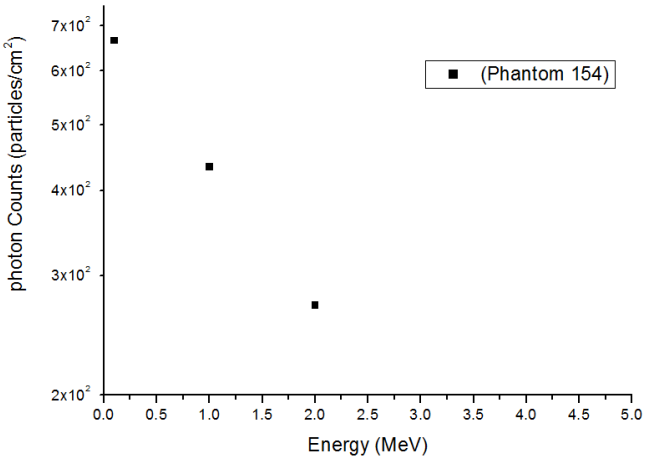

Figure 35: secondary photon energy spectra averaged inside phantom 154 shown. These are photons that reached the phantoms having been produced from (n, γ) reactions.

4.3 Limitations & Challenges

New Cyclotron Vault

Material activations not accounted for which will increase the dose rate in the phantom side.

Geometry of the vault does not reflect the real design, it was modified to achieve symmetry so that the geometry splitting as a VRT may be applied.

Beam loss activation inside the cyclotron not included which might increase dose rate as well, however the casing of the C70 cyclotron which is earmarked for use, has precautions taken in the design and self-shielding is included.

Activation of water in the cooling systems is not included, which will increase the secondary photon count.

RIB Demonstrator

for the open vault with a beamline opening leading to the experiment room

It is possible that not enough particles reached the phantoms, this may be caused by the asymmetry of the geometry

4.4 Analysis against Literature review

The SPES calculations when compared to my calculation for a 3 m thickness of concrete have agreed. It must be noted that the SPES calculation was done using FLUKA code and the dose-rate dropped 8 orders of magnitude, so did the RIB Demonstrator for 3 m thickness. (See Figure 9 and Figure 29). For both calculations the attenuation rate for the first 50 centimetre dropped by 2 orders of magnitude , with SPES dropping from 10^9 µSv/hr to 10^7 µSv/hr and Demonstrator vault dropping from 10^8 Sv/hr to 10^6 Sv/hr. The rest of 50 cm dropping by a magnitude up to 300cm gave a similar behaviour as well for both.

4.5 Evaluation of results

The aim of this section is to take results on radiation obtained in the two facilities: new cyclotron vault & RIB Demonstrator vault and compare them with the effective dose rate limits recommended for different personnel accessing the facility.
The table below is Table 1, it lists the radiation limits to which personnel may be exposed to.

Personnel	effective dose rates (mSv/yr)	Projected effective dose rates (µSv/hr)
Radiation Worker	20	10.417
Public/ non-Radiation worker	1	0.521

Table 37: Effective dose rate recorded in the phantoms in the Cyclotron and RIB Demonstrator vault

Effective dose rates (µSv/hr)	Effective dose rates (µSv/hr)
Phantom (81) cyclotron	0.4
phantom (150) RIB labyrinth	1.5
phantom (151) RIB outside yard	0.053
phantom (152) RIB exp room	14.6
phantom (154) RIB exit/entrance passage	8.15
phantom (155) RIB exit/entrance passage	3.22
phantom (156) RIB after 2nd boron door	5680
phantom (157) RIB after 1st boron door	31000

New Cyclotron

The registered total dose rate for the 4m thick concrete at the phantom was 0.4 mSv/hr, which is just below the limit for the Public and Non-Radiation Workers. This value is clearly safe for Radiation Workers as well. Where the phantom was placed will actually be a target station which will not be accessible by anyone when the beam is running. This value can now benchmark for offices which be adjacent to the New Cyclotron vault that they will be safer for both the Public and Non-Radiation Workers as well.

RIB demonstrator vault

Phantom 152 which was placed in the experimental room registered 14.6 µSV/hr which is higher than the acceptable limit. However this reading is for during the experiment which is out of bound even for Radiation Workers.

Phantom 150 which was placed in the labyrinth entrance to the experimental room registered 1.5micro Sieverts/hour which is higher than the Public/Non-Radiation Worker limits.

Phantom 151 which was placed in the yard to specifically assess if the Public/Non-Radiation Workers will be able to access it, registered 0.053 µSV/hr of effective dose rate. However, its location compared to Phantom 154 suggests that at 70MeV and 350µA current of proton, the area is not safe for the Public.

Phantoms 154 & 155 which were placed in the entrance of the passage to the spectrometer registered dose rates of 8.15 µSV/hr and 3.22 µSV/hr respectively. This is definitely not for Public/Non-Radiation Workers; however Radiation Workers may access this area in cases of emergency.

Phantom 156 & 157 were placed to assess the effectiveness of putting borated wax doors and the registered dose rates are very high as the can be seen. This is a no-go area for Radiation Workers as well, during beam-on periods.

CHAPTER 5: CONCLUSION & RECOMMENDATIONS

5.1 Introduction

This chapter gives closing remarks regarding results obtained. It uses outlined research objectives to reach necessary conclusions. Recommendations are made for future considerations relating either to the current study or safety aspects during the operation of the facility.

5.2 Research objectives:

Below are prime objectives that this study was addressing: Safety and Cost-effectiveness.

5.2.1 Safety

Conclusion on New Cyclotron Vault

Dose rate levels that were registered for the worse case give confidence that a 4 m thickness of concrete shielding walls will make the facility safe during beam operations as per specifications of beam energy and current.

Conclusion the RIB demonstrator

Guided by Phantom 154, safety levels are NOT met with 3 m walls for the RIB Demonstrator vault operated at 350 µA current of 70 MeV proton beam for Public/Non-Radiation Workers to access the area where Phantom 151 is located. This area should be out of bounds during experiments. It will be safer if the vault is operated only at 100 µA current of 66 MeV proton beam, as currently envisaged. This means the calculated absorbed doses will be reduced by a factor of at least 0.3 in magnitude.

5.2.2 Cost-effectiveness

Conclusion on New Cyclotron Vault

A 4 m thickness of concrete shield instead of the 5 m which was earlier proposed means a huge cut in the budget.

Conclusion on the RIB demonstrator

No major additional construction will be needed for the RIB demo vault, which is a big saving. However, some additional roof shielding will be needed to provide the required thickness.

Putting two consecutive borated-wax doors will reduce dose levels towards the corridor (compare phantoms 156 &157) .

A boron strip against the wall will reduce dose rates, especially for absorbing high energy neutrons that have longer ranges.

5.2.3 Access areas

Conclusion on New Cyclotron Vault

A highly unlikely accidental event was simulated and dose rate levels well below the limits were registered, giving confidence that corridors and offices can be accessed maximally during operation of the cyclotron.

Conclusion on the RIB demonstrator

The corridor will have to be closed off, preventing access to the spectrometer.

The yard area outside the building will not be out of bounds to the public during experiments, so sufficient shielding and access labyrinths have to be provided, as suggested.

Access to the experiment room will be out of bounds during RIB experiments, even for radiation workers.

5.3 Recommendations

5.3.1 On Results

Results may be improved by considering activations of beam diagnostics and water.

FLUKA can be used for Cyclotron activations due to beam loss.

FLUKA would be better as it transmutes materials so the target can be UC_x for the RIB demonstrator.

Additional physical controls (e.g. locked doors, fences, etc.) can be incorporated in areas surrounding the shielding to ensure that occupancy in these areas is controlled as necessary [9].

Localised shielding is required at pronounced higher beam-loss points like collimators, beam windows and stripping foils.

5.3.2 On Future Research

Experimental measurements as MSc research to validate my numerical calculations

Adequate model combinations for different observables are recommended instead of using MCNPX only.

Safety studies on dismantling of the RIB demonstrator will need to be conducted.

REFERENCES

[1] R. Bark, iThemba LABS Radioactive Ion Beam Project Workshop presentations, iThemba LABS, Western Cape, South Africa, 20 to 26 September 2011 (http://www.tlabs.ac.za/rib.htm: 23/12/2011)

[2] *NRF Annual Performance Report*, National Research Foundation, Pretoria South Africa 2010/11

[3] G.F. Steyn, T.J. van Rooyen, J.H. Hough, F.M. Nortier, S.J. Mills, *Design calculations for a local radiation shield of a radioisotope production target bombardment station*, Nuclear Instruments and Methods in Physics Research Section A: Accelerators, Spectrometers, Detectors and Associated Equipment", Volume 316, Issues 2-3, 1 June 1992, Pages 128-133

[4] F. M. Lukhele, E. Z. Buthelezi, O. M. Ndwandwe, *Radiation Shielding calculations by means of MCNPX*, MSc Thesis, University of Zululand, South Africa, January 2006

[5] The EURISOL Design Study (GANIL, Caen, France) 2009

[6] J. van Rooyen, *Handbook for Transport and Shielding of Ionising Radiation*, unpublished, January 2011

[7] L. Sarchiapone, D. Zafiropoulos*, Radiation Protection Aspects of SPES Project - Phase Alpha,* SPES 2010 International Workshop*,* Legnaro National Laboratory, Italy, 12-15 November 2010.

[8] T. E. Sibiya, T. Nam, J. Van Rooyen, *Radiation shielding design, verification and dose distribution calculations for industrial and insect irradiation facilities*, MSc Thesis, University of Witwatersrand, South Africa, August 2010

[9] F. B. Brown, *Fundamentals of Monte Carlo Particle Transport, Lecture notes for Monte Carlo course* Los Alamos National Laboratory, USA, LA-UR-05-4983

[10] J. K. SHULTIS; R. E. FAW, *An MCNP Primer*, Kansas State University, Manhattan, USA, 2006

[11] X-5 Monte Carlo Team, *MCNP Version 5 Volume11 User's Guide*, LA-CP-03-0245, Los Alamos National Laboratory, USA , 24 July 2003

[12] D.B. Pelowitz, editor. *MCNPX Version 2.6.0 User's Manual,* Report LA-CP-07-1473, Los Alamos National Laboratory, USA, April 2008.

[13] R. Lieder, *Introduction to Nuclear Reactor Physics*, lecture notes, MaNuS programme, University of the Western Cape, South Africa, 2010.

[14] Z. Zibi, A. Albornoz, *Benchmarking of MCNP Modelling of HTR Cores against Experimental Data from the ASTRA Critical Facility*, MSc Thesis, North-West University, South Africa, May 2010

[15] J. M. Ziegler, The Stopping and Range of Ions in Matter software, (http://www.srim.org : 11/01/2012)

[16] *The American Heritage® Science Dictionary*. (http://www.thefreedictionary.com/modulus: 11/01/2012)

APPENDICES

Appendix 1: Explanation of MCNPX code

MCNPX

MCNPX is the acronym for Monte Carlo Neutral Particle eXtended. With the MCNPX code, source term specification has become much simpler, and the user simply models the primary beam of incident, monoenergetic, mono-directional protons. The MCNPX code uses cross section tables and nuclear models that contain (p,nX) and (p,γX) cross sections, i.e. the cross sections for nuclear reactions with protons in the entrance channel and neutrons and ionising photons in the exit channel. That is, the production of neutrons and ionising photons are modelled by the code, using information in cross section libraries and in nuclear reaction models. There are available benchmark validations that have been done before.
MCNPX is appropriate for high-energy sources which we will be investigating, and for their activities and related radiations they produce. It is regularly updated, so its cross sections and other physics properties are updated built-in cards and its accuracy is improved. The structure of the MCNPX Input file will provide guidance in the design of the computer simulation.

INPUT file

The INPUT (INP) file is the document in which the user supplies specifications of the problem to be run (calculated). Various software editors s are available for coding the INP file, for an example Notepad++. Generally there are two forms of the INP file: Initiate-Run and Continue-Run [11]. A single line of input in the INP file is called ‘card’ and this line is up to 80 characters [12]. A user has the option to use a message block before the problem identification title card in the INP file.

Initiate-Run

Message Block {optional}
blank line delimiter {optional}
One Line Problem Title Card
Cell Cards [Block 1]
blank line delimiter
Surface Cards [Block 2]
blank line delimiter
Data Cards [Block 3]
blank line terminator {optional}

Continue-run

Let us say the job was run for 5 hours and results are statistically unsatisfying due to less particle history. To run for an additional hour to have more histories, the Continue-run is used to continue that problem that was terminated [12].

Message Block (optional)
Blank Line Delimiter (optional)
CONTINUE
Data Cards
.
.
Blank Line Terminator (Recommended)
Anything else (Options)

Not all data cards in the Initiate-Run are allowed in the Continue-Run input file The allowed Continue-Run data cards are:

- Print Hierarchy (FQ)
- detector and DXTRAN diagnostics and contribution (DD)
- History Cutoff Card (NPS)
- Computer Time Cutoff (CTME)
- integer array available for user-modified code (IDUM)
- real array available to the user (RDUM)
- print, dump, TFC, and rendezvous control (PRDMP)
- lost particle abort/debug print control (LOST)
- debug information card (DBCN)
- control the printing of optional tables to the OUTP file (PRINT)
- define a criticality eigenvalue (k_{eff}) problem (KCODE)
- produce plots of tallies while the problem is running (MPLOT)
- and separate cards for inputting user data to user-modified code (ZA, ZB, ZC) [11].

The Continue Run INP file is only required if the above cards are to be changed. Depending on the computing environment, otherwise only the run file RUNTPE and the C/ CN option on the MCNP execution line are necessary A very convenient feature is that if none of the above items are to be changed (and if the computing environment allows execution line messages), the Continue-Run input file is not required [12].

Card Format

All INP file cards are limited to 80 columns. There are no restrictions on alphabetic characters; they can be upper, lower, or mixed case. The input format is entered in horizontally (up to 80 columns); however, a vertical input format is allowed for data cards. A comment can be added to any input card other than Mesh tally Card after a $ (dollar sign) which terminates data entry. Blank lines are used as delimiters and terminators. Data entries are separated by one or more blanks [12].

Example of a horizontal input file format:

```
phys:h   75  0   -1   J   0   J   0
```

Vertical input file format:

```
phys:h   75
          0
         -1
          J
          0
          J
          0
```

See Appendix 1 under Physics Cards.

CELL CARDS

Cell cards allow the user to specify the geometry of the problem together with Surface cards. Cell cards in particular define specific regions in the geometry [6].

Form: *j* *m* *d* geometry parameters

j = cell number.

m = material number if the cell is not a void, 0 if the cell is a void. This material entry *m* is specified on the M*m* card.

d = material density. Here a positive entry represents the atomic density in units of 10^{24} atoms/cm^3.and a negative entry is the mass density in units of g/cm^3. If absent, then the cell is a void.

geometry = specification of the geometry of the cell. Here surface numbers with signs and Boolean operators specify how the regions bounded by the surfaces are to be combined.

parameters = optional specification of cell parameters by entries in the keyword, here the *keyword* = value form, like particle importance of 1 in a cell (IMP = 1)

SURFACE CARDS

Surfaces Defined by surfaces or planes

Form: j n a list

j = surface number: 1≤ j ≤ 99999. , with asterisk for a reflecting surface or plus for a white boundary. If surface defines a transformed cell (TRCL card) then with TRCL, 1≤ j ≤ 999.

n = specifies surface j is periodic with surface n, 0, specifies number of Transformation (TRn) card absent for no coordinate transformation.

a = equation or Boolean operators

list = one to ten entries.

Surfaces Defined by Macrobodies

Macrobodies allow geometrical bodies to be described with a single keyword and a combination of surfaces and planes. Below is the list of available bodies [12]:

BOX	Arbitrarily oriented orthogonal box
RPP	Rectangular Parallelepiped
SPH	Sphere
RCC	Right Circular Cylinder
RHP or HEX	Right Hexagonal Prism
REC	Right Elliptical Cylinder
TRC	Truncated Right-angle Cone
ELL	Ellipsoid
WED	Wedge
ARB	Arbitrary polyhedron

BOX: Arbitrarily oriented orthogonal box (all corners are 90°).

BOX *Vx Vy Vz A1x A1y A1z A2x A2y A2z A3x A3y A3z*

where *Vx Vy Vz* = *x,y,z* coordinates of corner

A1x A1y A1z = vector of first side

A2x A2y A2z = vector of second side

A2x A3y A3z = vector of third side

RPP: Plane X_{min} Plane X_{max} Plane Y_{min} Plane Y_{max} Plane Z_{min} Plane Z_{max}

Example: RPP -2000 +2000 -2000 +2000 0 +1000 $ (this is a cube centered at *x* = *y* = 0; z = 500cm, 4000 cm x 4000cm and 1000cm height);

RCC: Plane normal to beginning of *Hx Hy Hz;* Plane normal to end of *Hx Hy Hz;* Cylindrical surface of radius *R*

Example: RCC 0 0 0 0 0 300 +12 $ (this is a cylinder with its circular base centred at *x* = *y* = z =0; height is 300 cm and radius of 12 cm.

DATA CARDS

Data cards are entered after the blank card delimiter following the surface card block. The mnemonic must begin anywhere within the first five columns. Available data cards are listed below according to categories:

(a) Problem type (MODE) Card
(b) Geometry Cards
(c) Variance Reduction Technique (VRT)
(d) Source Specification
(e) Tally Specification
(f) Material Specification
(g) Energy and Thermal Treatment Specification
(h) Problem Cutoff Cards
(i) User Data Arrays
(j) Peripheral Cards

(a) Problem Type (MODE) Card

This card specifies particle type to be transported in the calculation.

Form: MODE x_1.....x_i

x_i = N for neutron transport
P for photon transport
E for electron transport

Default: If the MODE card is omitted, MODE N is assumed.

Example: MODE H N P (i.e. Protons (H) irradiating stainless steel thus neutrons (N) and photons (P) are generated. So, in the target all three particles must be transported).

(b) Geometry Cards

	Mnemonic	**Card Type**
i)	VOL	Cell Volume
ii)	AREA	Surface Area
iii)	U	Universe
iv)	TRCL	Cell Transformation
v)	LAT	Lattice
vi)	FILL	Fill
vii)	TRn	Coordinate Transformation

For our calculations we did not use these geometry cards under the data cards as they are optional [11], and thus we shall not expand on them further.

(c) Variance Reduction

This technique can be applied to get statistically meaningful results more quickly [6]. The following cards define parameters for variance reduction (VR) cards.

i)	IMP	Cell Importance
ii)	ESPLT	Energy Splitting and Roulette
iii)	TSPLT	Time Splitting and Roulette
iv)	PWT	Photon Weight
v)	EXT	Exponential Transform
vi)	VECT	Vector Input
vii)	FCL	Forced Collision
viii)	WWE	Weight Window Energies or Times
ix)	WWN	Cell-Based Weight Window Bounds
x)	WWP	Weight Window Parameter
xi)	WWG	Weight Window Generation
xii)	WWGE	Weight Window Generation Energies or Times
xiii)	MESH	Superimposed Importance Mesh for Mesh-Based Weight Window Generator
xiv)	PDn	Detector Contribution
xv)	DXC	DXTRAN Contribution
xvi)	BBREM	Bremsstrahlung Biasing

Either an IMP or a WWN card is required; most of the other cards are optional for VRT.

i) IMP Cell importance cards

Use: An IMP:n card is required with an entry for every cell unless a WWN weight window bound card is used.

Form: IMP:n x_1 x_2 x_i x_I

n = N for neutrons, P for photons, E for electrons. N,P or P,E or N,P,Eis allowed if importances are the same for different particle types.

x_i = importance for cell i

I = number of cells in the problem

Default: If an IMP:P card is omitted in a MODE N P problem, all photon cell importances are set to unity (=1) unless the neutron importance is 0. In that case the photon importance is set 0. [See Appendix 1 under Cell Cards to see importance cards for MODE H N P.]

This was the only card we used for our VRT and thus we shall limit our discussion to it.

(d) Source Specification

MCNPX problems must have one of four sources: general source (SDEF card), surface source (SSR card), criticality source (KCODE card), or user-supplied source (default if SDEF, SSR, and KCODE are all missing). These sources can be specified by distribution functions on SIn, SPn, SBn, and DSn cards.

Below are source specification cards:

	Mnemonic	**Card Type**
i)	SDEF	General Source
ii)	SIn	Source Information
iii)	SPn	Source Probability

iv) SBn Source Bias
v) DSn Dependent Source Distribution
vi) SCn Source Comment
vii) SSW Surface Source Write
viii) SSR Surface Source Read
ix) KCODE Criticality Source
x) KSRC Source Points for KCODE Calculation

i) SDEF General Source Card

This card is required for problems using the general source, but is optional for problems using the criticality source. The MODE card also serves as part of the source specification, in some cases by implying the type of particle to be started from the source. In our case, the proton is the source particle.

The source has to define the values of the following MCNP variables for each particle it produces:

ERG	the energy of the particle (MeV).
TME	the time when the particle started (in 'shakes') (1 shake=10^{-8} sec)
UUU, VVV, WWW	the direction of the flight of the particle
XXX, YYY, ZZZ	the position of the particle
IPT	the type of the particle
WGT	the statistical weight of the particle
ICL	the cell where the particle started
JSU	the surface where the particle started, or zero if the starting point is not on any surface

ii) SIn Source Information

Form: SI*n* option I_1 .... I_k

N = distribution number (*n* =1,...,999)

option = how the *Ii* are to be interpreted. Allowed values are omitted or H-bin boundaries for a histogram distribution, for scalar variables only. This is the default.
L- discrete source variable values
A-points where a probability density distribution is defined
S-distribution numbers

I_1 .... I_k source variable values or distribution numbers

Example SI1 h 0.0 0.5
This is distribution 1, sampling of source point proton particle along radial coordinate up to 0.5cm radius

iii) SPn Source Probability

Form: SP*n* option P_1 ....P_k

or: SP*n* *f* *a* *b*

n = distribution number (*n* = 1,..., 999)

option = how the *Pi* are to be interpreted. Allowed values are omitted same as D for an H or L distribution. Probability density for an A distribution on SI card.

D- bin probabilities for an H or L distribution on SI card. This is the default.
C- cumulative bin probabilities for an H or L distribution on SI card.
V- for cell distributions only. Probability is proportional to cell volume (times *Pi* if the *Pi* are present).
P_i ...P_k = source variable probabilities
f = designator (negative number) for a built-in function
a b = parameters for the built-in function

Example: SP1 -21 1
Probability of sampling of source point in radial dimension: Power law: $p(x)= c|x|^a$
The default depends on the variable. For DIR, *a* =1. For RAD, *a* =2, unless AXS is defined or SUR≠0, in which case *a* =1. For EXT, *a* =0.

[See Appendix 1 under Source Definition for a complete SDEF card used in our calculations.]

(e) Tally Specification

Tally cards are used to specify the information the user wants to obtain from the Monte Carlo run. These vary from current across a surface, flux at a point, heating in a region, etc. [11]. This information is requested by the user by using a combination of the following cards. To obtain tally results, only the Fn card is required; the other tally cards provide various optional features.[12]

Mnemonic	**Card Type**
i) Fn	Tally
ii) FMn	Tally Multiplier
iii) En	Tally Energy
iv) DEn/DFn	Dose Energy/Dose Function
v) TMESHn	Mesh Tally plot
vi) FCn	Tally Comment
vii) Tn	Tally Time
viii) Cn	Cosine
ix) FQn	Print Hierarchy
x) EMn	Energy Multiplier
xi) TMn	Time Multiplier
xii) CMn	Cosine Multiplier
xiii) CFn	Cell Flagging
xiv) SFn	Surface Flagging
xv) FSn	Tally Segment
xvi) SDn	Segment Divisor
xvii) FUn	TALLYX Input
xviii) TFn	Tally Fluctuation
xix) DDn	Detector Diagnostics
xx) DXT	DXTRAN
xxi) FTn	Special Treatments for Tallies

In our Monte Carlo calculations we used the following i); ii); iii); iv) and v) Tally Cards and thus we limit our descriptions to them:

The *n* is a user-chosen tally number (n = 1,...,999). When a choice of *n* is made for a particular tally type, any other input card used with that tally must be given the same value of *n* by the user.

i) Fn Tally

Mnemonic	**Tally Description**	**Fn units**	**Fn units**
F1:N or F1:P or F1:E	Current integrated over a	surface particles	MeV
F2:N or F2:P or F2:E	Flux averaged over a surface	particles/cm^2	MeV/cm^2
F4:N or F4:P or F4:E	Flux averaged over a cell	particles/cm^2	MeV/cm^2
F5a:N or F5a:P	Flux at a point or ring detector	particles/cm^2	MeV/cm^2
FIP5:N or FIP5:P	Array of point detectors for pinhole flux image	particles/cm^2	MeV/cm^2
FIR5:N or FIR5:P	Array of point detectors for planar radiograph flux image	particles/cm^2	MeV/cm^2
FIC5:N or FIC5:P	Array of point detectors for cylindrical radiograph flux image	particles/cm^2	MeV/cm^2
F6:N or F6:N,P or F6:P	Energy deposition averaged over a cell	MeV/g	jerks/g
F7:N	Fission energy deposition averaged over a cell	MeV/g	jerks/g
F8:P or F8:E or F8:P,E	Energy distribution of pulses created in a detector	pulses	MeV
*F8:E	Charge deposition	charge	N/A

To identify tallies, we use tally and particle type to specify. Tallies are given the numbers 1,2, 4, 5, 6, 7, 8, or increments of 10 thereof, and are given the particle designator :N, :P, or :E ; or :N,P only for tally type 6; P,E only for tally type 8.

The user may have as many of any basic tally as possible, each with different energy bins or flagging or anything else. For an example F4:N, F14:N, F104:N, and F234:N are all legitimate neutron cell flux tallies. However, both F1:N card and F1:P card in the same INP file is not allowed.
Tally types 1, 2, 4, and 5 are normally weight tallies, however, if the Fn card is flagged with an asterisk (for example, *F1:N), energy times weight will be tallied.

In tally types 6 and 7 asterisks maybe used to change the units from MeV/g to jerks/g
(1 jerk = 1 GJ = 10^9 J).

Tally type 8 can also be flagged with a plus (+) to convert it from an energy deposition tally (*F8) to a charge deposition tally.

Only the F2 surface flux tally requires the surface area to be specified.

Look at the forms of F*n* Tally that apply on Surfaces and Cells (tally types 1, 2, 4, 6, and 7)
Simple Form: F*n*: *pl* S_1 ....S_k
General Form: F*n*: *pl* S_1 (S_2....S_3) (S_4 ....S_5) S_6 S_7 ....
n = tally number.
pl = N or P or N,P or E
Si = problem number of surface or cell for tallying, or *T*.
Example: F14:n 81

tally type 4 of 1 for an averaged neutron flux over cell 81

ii) FM*n* Tally Multiplier Card

Form: FM*n (bin set 1) (bin set 2)* .....*T*

n = tally number

(bin set i) = ((multiplier set 1) (multiplier set 2) ....(attenuator set))

T = absent for no total over bins

= present for total over all bins

C = cumulative tally bins

attenuator set = *C* ...m_1 px_1 m_2 px_2 ....

multiplier set *i* = *C m* (reaction list 1) (reaction list 2) ....

special multiplier set *i* = *C -k*

C = multiplicative constant

-1 = flag indicating attenuator rather than multiplier set

m = material number identified on an Mm card

px = density times thickness of attenuating material; atom density if positive, mass density if negative

k = special multiplier option;

(reaction list *i*) = sums and products of ENDF or special reaction numbers, described below.

If the FM*n* card consists only of a single bin set, and that bin set consists only of a single multiplier or attenuator bin, surrounding parentheses can be omitted.

Example: F24:p 81
FM24 2.185E15

This Tally Multiplier Factor (FM24) applies to the F24 above. Where the factor 2.185E15 is the number of protons per second impinging on the target if the proton beam is of 350 μA (current).

iii) E*n* Tally Energy Card

Use: Required if the EM*n* card is used.

Form: E*n* E_1 ...E_k

n = tally number.

Ei = upper bound (in MeV) of the i^{th} energy bin for tally *n*.

Default: If the E*n* card is absent, there will be one bin over all energies unless this default has been changed by an E0 card.

The entries on the E*n* card must be entered in the order of increasing magnitude. If a particle has energy greater than the last entry, it will not be tallied, but you will be warned that this has happened. If the last entry is greater than the upper energy limit E_{max} specified on the PHYS card, the last bin will be lowered to E_{max}. If there are several bins above E_{max}, the extra bins are eliminated.

Example:

E0 1E-11 1e-7 1e-3 1e-1 1 2 3 4 5 6 7 8 9 10 12 14 16 18 20 25 30 35 40 45 50 55 60 65 70

This E0 imposes a one bin over all energies with lower bound energy 1-E11MeV and upper bound 70MeV

vi) DE*n*/DF*n* Dose Energy/Dose Function

This card allows the user to gain response function at a certain point (such as flux-to-dose conversion factors) as a function of energy to modify a regular tally. Both cards must have the same number of numerical entries and they must be monotonically increasing in energy. Particle energies outside the energy range defined on these cards use either the highest or lowest value.[12]

Form: DE*n* *A* E_1...E_k
DF*n* *B* F_1...F_k
n = tally number.
E_i = an energy (in MeV).
F_i = the corresponding value of the dose function.
A = LOG or LIN interpolation method for energy table.
B = LOG or LIN interpolation method for dose function table.

To allow user-supplied dose functions, the dose conversion capability provides several standard default dose functions. These are invoked by omitting the DE card and using keywords on the DF card: then the form becomes:

DF*n* IU=*j* FAC=*f* INT IC=*i*

j = Controls units.
If j = 1, US units (rem/h/source_particle1).
If j =2, international units (sieverts/h/source_particle) (DEFAULT)

f = Normalization factor for dose. (DEFAULT = 1.0)
If f = -1, then use ICRP60 (1990) normalization (i.e., normalize results to Q = 20)
If f = -2, then use LANSCE albatross response function.
If f >0, then is user-supplied normalization factor. (DEFAULT:f = 1)

INT Energy interpolation. (Note: Dose interpolation always linear.)
If INT=LOG, then LOGLIN interpolation.† (DEFAULT)
If INT=LIN, then LINLIN interpolation.†

i IC is standard dose function as given in Appendix 1. (DEFAULT:IC=10)

v) TMESH*n* Mesh Tally Card

The mesh tally is a method of graphically displaying particle flux, dose, or other quantities on a rectangular, cylindrical, or spherical grid overlaid on top of the standard problem geometry. Particles are tracked through the independent mesh as part of the regular transport problem. The contents of each mesh cell are written to the RUNTPE file and can be plotted with the MCNPX geometry plotter superimposed over a plot of the problem geometry. The mesh tally data are also written to the MCTAL file and can be plotted with the MCNPX tally plotter, MCPLOT. [11]

Further, the mesh tally data are written to the MDATA file at the end of each initial or continue run. The MDATA file can be converted into a number of standard formats suitable for reading by various graphical analysis packages. The conversion program, GRIDCONV, is supplied as part of the overall MCNPX package.

RMESH*n*:<*pl*> KEYWORD=*value(s)* ...
CMESH*n*:<*pl*> KEYWORD=*value(s)* ...

SMESH*n*:<*pl*> KEYWORD=*value(s)* ...

RMESH is a rectangular mesh, CMESH is a cylindrical mesh, and SMESH is a spherical mesh. (R/C/S)MESH will mean either of the three.

where *n* is a user-defined mesh number. The mesh number *n* must end in 1, 2, 3, or 4 corresponding to the mesh tally type, and must not be the number of any other tally in the problem.

Up to 10 keywords are permitted, depending on mesh type.

CORA*n corra(n,1), corra(n,2), ...*,
CORB*n corrb(n,1), corrb(n,2), ...*, and
CORC*n corrc(n,1), corrc(n,2), ...*,

The entries on the CORA, CORB, and CORC cards describe a mesh in three coordinate directions as defined by the mesh type (rectangular, cylindrical, or spherical)

To describe a rectangular mesh, the entries on the CORA card represent planes perpendicular to the x-axis, CORB entries are planes perpendicular to the y-axis, and CORC entries are planes perpendicular to the z-axis.

ENDMD

This is a terminating card.

Therefore, the form of this tally is:

TMESH
(R/C/S) MESH*n*:<*pl*> KEYWORD=*value(s)* ...
CORA*n corra(n,1), corra(n,2), ...*,
CORB*n corrb(n,1), corrb(n,2), ...*, and
CORC*n corrc(n,1), corrc(n,2), ...*,
ENDMD

See Appendix 1 under Mesh tally plots to see how entries meant to cover graphical display of the area of interest were entered. For an example we wanted to see how the dose-rate strength changes from the neutron source to the areas beyond shielding.

(f) Material Specification

The cards in this section specify the isotopic composition of the materials in the cells. This, in turn, determines which cross-section evaluations will be used.

	Mnemonic	**Card Type**
i)	M*n*	Material
ii)	MPN*n*	Photonuclear Nuclide Selector
iii)	DRXS	Discrete Reaction Cross Section
iv)	TOTNU	Total Fission
v)	NONU	Fission Turnoff
vi)	AWTAB	Atomic Weight
vii)	XS*n*	Cross-Section File
viii)	VOID	Material Void

ix) PIKMT Photon–Production Bias
x) MGOPT Multigroup Adjoint Transport Option

For our calculations we only used M*n* Material Card as it covers all the physics we need for transporting neutrons and photons in the ordinary concrete shield. Had it been an engineered concrete, we would have had to have more specifications in our INP file.

i) M*n* Material Card

Form: M*n* $ZAID_1$ $fraction_1$ $ZAID_2$ $fraction_2$ ...keyword=value ...

n corresponds to the material number on the cell cards

$ZAID_i$ = either a full ZZZAAA.nnX or partial ZZZAAA element or nuclide identifier for constituent *i,* where ZZZ is the atomic number, AAA is the atomic mass, *nn* is the library identifier, and X is the class of data

$fraction_i$ = atomic fraction (or weight fraction if entered as a negative number) of constituent *i* in the material.

keyword = value, where = sign is optional. Keywords are:

GAS = *m* flag for density–effect correction to electron stopping power.
m = 0 calculation appropriate for material in the condensed (solid or liquid) state used.
m = 1 calculation appropriate for material in the gaseous state used.

ESTEP = *n* causes the number of electron substeps per energy step to be increased to *n* for the material. If *n* is smaller than the built–in default found for this material, the entry is ignored.

NLIB = *id* changes the default neutron table identifier to the string *id*.

PLIB = *id* changes the default photoatomic table identifier to *id*.

PNLIB = *id* changes the default photonuclear table identifier to *id*.

ELIB = *id* changes the default electron table identifier to *id*.

COND = *id* sets conduction state of a material only for el03 evaluation.
< 0 nonconductor
= 0 (default) nonconductor if at least one nonconducting component; otherwise a conductor
> 0 conductor if at least one conducting component.

For our calculations we used Material Cards of vertical input format:

M*n* $ZAID_1$ $fraction_1$
$ZAID_2$ $fraction_2$
... .
... .
$ZAID_i$ $fraction_i$

In some cases we had ZZZAAA.nnX or partial ZZZAAA for ZAID entries and no keywords were used

Example: m1 6000 -1.24E-4
7014 -0.755267
8016 -0.231781
18000 -0.012827

Here material number ‘1’ is reflected in the cells and partial ZZZAAA nuclide identifier.

6000 is natural Carbon as ZZZ000 and -1.24E-4 is the weight fraction because of negative
7014 is Nitrogen with atomic Number 7 and 14 the Atomic Mass
18000 is natural Argon

Adding the weight fractions of these four isotopes gives a unit '1'

(g) Energy and Thermal Treatment Specification

The following cards control energy and other physics aspects of MCNP. All energies are in units of MeV.

Mnemonic	Card Type
i) PHYS	Energy Physics Cutoff
ii) TMP	Free-Gas Thermal Temperature
iii) THTME	Thermal Times
iv) MTm	*S*(α,β) Material

For our calculations we only used the PHYS card which was relevant. As TMP and THTME are linked cards for neutrons are transport other than in room temperature.[11] MTm card is effective below 2eV [12], which is of no interest with us here.

i) PHYS Energy Physics Cutoff

Protons

Form: PHYS:H EMAX EAN TABL J ISTRG J RECL

EMAX — Upper proton energy limit. (DEFAULT=EMAX on PHYS:N card or 100 MeV if no PHYS:N card)

EAN — Analogue energy limit. (DEFAULT=0 MeV)
If E is the energy of the proton and E > EAN, perform implicit capture.
If E is the energy of the proton and E < EAN, perform analog capture.

TABL — Table-based physics cutoff.
For TABL > 0, use physics models for energies (E) above *TABL* and data tables for those below TABL, if available (otherwise use models).
For TABL = -1, then mix and match. When tables are available, use them up to their upper limit for each nuclide, then use the physics models above. (DEFAULT)

J — Unused placeholder. (Be sure to put the J in the keyword string.)

ISTRG — Controls charged-particle straggling.
If ISTRG = 0, then use Vavilov model for charged-particle straggling. (DEFAULT)
If ISTRG = 1, use continuous slowing-down approximation for charged-particle straggling.
If ISTRG=-1, use old Vavilov model.

J — Unused placeholder. (Be sure to put the J in the keyword string.)

RECL — Light ion recoil control.
If RECL=0, then no light ion recoil. (DEFAULT)
For 0<RECL≤1, RECL is the number of light ions (protons, deuterons, tritons, 3He, and alphas) to be created at each proton elastic scatter event with light nuclei H, D, T, 3He, and 4He.

Default: PHYS:H 100 0 -1 J 0 J 0 [11]

Neutrons

Form: PHYS: N EMAX EMCNF IUNR DNB

EMAX = upper limit for neutron energy, MeV.

EMCNF = energy boundary above which neutrons are treated with implicit capture and below which they are treated with analog capture.

IUNR = 0/1 = on/off unresolved resonance range probability tables.

DNB = number of delayed neutrons produced from fission
–1/0/>0 = natural sampling/no delayed neutrons produced/DNB delayed neutrons per fission.
DNB > 0 not allowed in KCODE calculation.

Default: PHYS:N 100 0 0 -1 -1 0 0 [11]

Photons

Form: PHYS:P EMCPF IDES NOCOH ISPN NODOP

EMCPF = upper energy limit for detailed photon physics treatment, MeV.

IDES = 0 photons will produce electrons in MODE E problems or bremsstrahlung photons with the thick target bremsstrahlung model.

= 1 photons will not produce electrons as above.

NOCOH = 0 coherent scattering occurs.

= 1 coherent scattering will not occur.

ISPN = -1 analog photonuclear collision sampling.

= 0 no photonuclear collisions.

= 1 biased photonuclear collision sampling.

NODOP = 0 Doppler energy broadening occurs.

= 1 Doppler energy broadening will not occur.

Default: PHYS:P 100 0 0 0 1 0 [11]

See Appendix under the Physics Cards to see how Energy Physics Cutoff cards were entered in a vertical input format for our calculations.

(h) Problem Cutoff Cards

The following cards can be used in an initiate-run or a continue-run input file to specify parameters for some of the ways to terminate tracks in MCNP.

	Mnemonic	**Card Type**
i)	CUT	Cutoffs
ii)	ELPT	Cell-by-Cell Energy Cutoff
iii)	NOTRN	Direct-Only Neutral Particle Point Detector Contributions
iv)	NPS	History Cutoff
v)	CTME	Computer Time Cutoff

i) CUT Cutoffs

Form: CUT: *n T E WC1 WC2 SWTM*

n = *N* for neutrons, *P* for photons, *E* for electrons.

T = time cutoff in shakes, 1 shake=10^{-8} sec.
E = lower energy cutoff in MeV.
WC1 and *WC2* = weight cutoffs.
SWTM = minimum source weight.

Example CUT: H J 3 J J J.....$ In our calculation we added this cutoff card for protons at 3MeV. Below this energy the code just discards following them. J is a unused placeholder.

ii) ELPT Cell–by–Cell Energy Cutoff

This card enables the user to use energy to cutoff particles in cells and is dependent on the CUT card and whichever is higher between the two takes effect on the calculation.

Form: ELPT:*n* *x1* *x2* ... *xi* ... *xI*
n = *N* for neutrons, *P* for photons, *E* for electrons.
xi = lower energy cutoff of cell i
I = number of cells in the problem.

We used CUT card for our calculations.

iii) NOTRN Direct-Only Neutral Particle Point Detector Contributions

This card is useful for doing a faster calculation for which the direct tallying and no particle transport is required. In our calculations we need to transport neutrons and photons through concrete shield. So this card is not useful.

iv) NPS History Cutoff

Form: NPS N NPSMG
N = total number of histories to be run in the problem.
NPSMG = number of histories for which source contributions are to be made to the pixels of the (flux image radiograph) FIR image grid

For our calculations we need no FIR image grids. We could consider the single entry *N* on this card which is used to terminate the Monte Carlo calculation after *N* histories have been transported unless the calculation is terminated earlier for some other reason such as computer time cutoff.

v) CTME Computer Time Cutoff

This card is for terminating Monte Carlo run. There are several ways of terminating runs, whichever that gets met first controls the calculation.

Form: CTME *x*
x = maximum amount of computer time (in minutes) to be spent in the Monte Carlo calculations.

For a continue-run job the time on the CTME card is the time relative to the start of the continue-run; it is not cumulative.

The last two cards (i & j below) are useful for user-modified MCNP [12] meanwhile for our calculations we used an original version.

(i) User Data Arrays

(j) Peripheral Cards

Executing MCNPX code

Command line

The execution command is required to initiate the run and below is its form:

mcnpx *Options* *Files*

Files

Default File Name	Description
INP	Problem input specification
OUTP	Filename to which results are printed. Created by MCNPX during problem execution
RUNTPE	Binary start-restart data
XSDIR	Cross-section directory

These four above are the most useful and below is the rest of the list of file names in MCNPX environment

WWINP	Name of input file containing either cell- or mesh-based lower weight window bounds.
WWOUT	Name of weight-window generator output file containing either cell- or mesh-based lower weight-window bounds.
WWONE	Name of weight-window generator output file containing cell- or mesh-based time- and/or energy-integrated weight windows.
DUMN1 & DUMN2 , File creation card.	
COMOUT	File to which all plot requests is written.
PLOTM	Name of graphics metafile.
MCTAL	Tally results file (ASCII).

Options:

execution_option is a character or string of characters that informs MCNPX which of five execution module(s) to run[11].

Mnemonic	Module	Operation
i	IMCN	Process problem input file
p	PLOT	Plot geometry
x	XACT	Process cross sections
r	MCRUN	Particle transport
z	MCPLOT	Plot tally results or cross section data

When *Options* are omitted, the default is **ixr**. The execution of the modules is controlled by entering the proper mnemonic on the execution line. If more than one operation is desired, combine the single characters (in any order) to form a string. Examples of use are as follows: **i** to look for input errors, **ip** to debug a geometry by plotting, **ixz** to plot cross-section data, and **z** to plot tally results from the RUNTPE or MCTAL files. [12]

Example of the command line:

mcnpx ixr i=Test.INP o=Test.OUT.

This line (i) processes the input file ‘Test’; (x) processes cross-sections (r) transport particles ‘Test.INP’ specifies the input specifications and ‘Test.OUT’ directs to which file results must be written.

Interrupts

MCNPX allows five types of interactive interrupts while it is running:

<ctrl-c><cr>	MCNPX status (DEFAULT)
<ctrl-c>s	MCNPX status
<ctrl-c>m	Make interactive plots of tallies or the geometry
<ctrl-c>q	Terminate MCNPX gracefully after current history
<ctrl-c>k	Kill MCNPX immediately

Example, if one wants to learn the status of the run, one may press simultaneously <ctrl> & <c> keys on the keyboard then key in s afterwards.

Continue-Run

In section 2.6.1, the need for the user to Continue-run is described together with the structure of the input file for this option.

Mnemonic	Operation
C m	Continues a run starting with *mth* dump. If *m* is omitted, the last dump is used.
CN	Like C, but dumps are written immediately after the fixed part of the RUNTPE, rather than at the end. [11]

Appendix 2: Explanation of input data files

Explanation of input data: New Cyclotron

```
c Cell Cards:
c Cell Cards:
01  0            -76   +75       imp:h=1   imp:n=1         imp:p=1        $ Vacuum inside BeamLine
02  4  -8.0       -75             imp:h=1   imp:n=1         imp:p=1        $ SS-304 Target
03  1  -1.205E-3    -1   +76       imp:h=0   imp:n=1         imp:p=1        $ Air in Vault
c
11  2  -2.35       -2    +1       imp:h=0   imp:n=1.000E+00 imp:p=1.000E+00  $ CRT Shell 01
12  2  -2.35       -3    +2       imp:h=0   imp:n=1.000E+00 imp:p=1.630E+00  $ CRT Shell 02
13  2  -2.35       -4    +3       imp:h=0   imp:n=1.000E+00 imp:p=3.193E+00  $ CRT Shell 03
14  2  -2.35       -5    +4       imp:h=0   imp:n=1.487E+00 imp:p=6.169E+00  $ CRT Shell 04
15  2  -2.35       -6    +5       imp:h=0   imp:n=2.587E+00 imp:p=1.199E+01  $ CRT Shell 05
16  2  -2.35       -7    +6       imp:h=0   imp:n=4.580E+00 imp:p=2.361E+01  $ CRT Shell 06
17  2  -2.35       -8    +7       imp:h=0   imp:n=8.333E+00 imp:p=4.611E+01  $ CRT Shell 07
18  2  -2.35       -9    +8       imp:h=0   imp:n=1.576E+01 imp:p=8.923E+01  $ CRT Shell 08
19  2  -2.35      -10    +9       imp:h=0   imp:n=3.045E+01 imp:p=1.716E+02  $ CRT Shell 09
20  2  -2.35      -11   +10       imp:h=0   imp:n=5.919E+01 imp:p=3.260E+02  $ CRT Shell 10
21  2  -2.35      -12   +11       imp:h=0   imp:n=1.140E+02 imp:p=6.135E+02  $ CRT Shell 11
22  2  -2.35      -13   +12       imp:h=0   imp:n=2.168E+02 imp:p=1.144E+03  $ CRT Shell 12
23  2  -2.35      -14   +13       imp:h=0   imp:n=4.102E+02 imp:p=2.120E+03  $ CRT Shell 13
24  2  -2.35      -15   +14       imp:h=0   imp:n=7.774E+02 imp:p=3.907E+03  $ CRT Shell 14
25  2  -2.35      -16   +15       imp:h=0   imp:n=1.427E+03 imp:p=7.194E+03  $ CRT Shell 15
26  2  -2.35      -17   +16       imp:h=0   imp:n=2.562E+03 imp:p=1.319E+04  $ CRT Shell 16
27  2  -2.35      -18   +17       imp:h=0   imp:n=4.562E+03 imp:p=2.403E+04  $ CRT Shell 17
28  2  -2.35      -19   +18       imp:h=0   imp:n=7.939E+03 imp:p=4.351E+04  $ CRT Shell 18
29  2  -2.35      -20   +19       imp:h=0   imp:n=1.365E+04 imp:p=7.811E+04  $ CRT Shell 19
30  2  -2.35      -21   +20       imp:h=0   imp:n=2.322E+04 imp:p=1.389E+05  $ CRT Shell 20
31  2  -2.35      -22   +21       imp:h=0   imp:n=3.912E+04 imp:p=2.437E+05  $ CRT Shell 21
32  2  -2.35      -23   +22       imp:h=0   imp:n=6.502E+04 imp:p=4.225E+05  $ CRT Shell 22
33  2  -2.35      -24   +23       imp:h=0   imp:n=1.065E+05 imp:p=7.187E+05  $ CRT Shell 23
34  2  -2.35      -25   +24       imp:h=0   imp:n=1.739E+05 imp:p=1.188E+06  $ CRT Shell 24
35  2  -2.35      -26   +25       imp:h=0   imp:n=2.825E+05 imp:p=1.904E+06  $ CRT Shell 25
36  2  -2.35      -27   +26       imp:h=0   imp:n=4.577E+05 imp:p=2.945E+06  $ CRT Shell 26
37  2  -2.35      -28   +27       imp:h=0   imp:n=7.422E+05 imp:p=4.342E+06  $ CRT Shell 27
38  2  -2.35      -29   +28       imp:h=0   imp:n=1.213E+06 imp:p=6.137E+06  $ CRT Shell 28
39  2  -2.35      -30   +29       imp:h=0   imp:n=2.021E+06 imp:p=8.557E+06  $ CRT Shell 29
40  2  -2.35      -31   +30       imp:h=0   imp:n=4.012E+06 imp:p=1.293E+07  $ CRT Shell 30
c
81  3   1.0       -81             imp:h=0   imp:n=4.012E+06  imp:p=1.293E+07 $ Phantom in front of Target
c
91  1  -1.205E-3  -99  +31 +81     imp:h=0   imp:n=4.012E+06  imp:p=1.293E+07 $ Outside Air
c
99  0               +99          imp:h=0   imp:n=0         imp:p=0        $ UmWelt = External Void
c ========================================
```

Cell cards

```
c Surface Cards
01  RPP  -2000   +2000    -2000   +2000      0    +1000              $ Inner Surface: CRT Shell 01
02  RPP  -2010   +2010    -2010   +2010    -10    +1010              $ Inner Surface: CRT Shell 02
03  RPP  -2020   +2020    -2020   +2020    -20    +1020              $ Inner Surface: CRT Shell 03
04  RPP  -2030   +2030    -2030   +2030    -30    +1030              $ Inner Surface: CRT Shell 04
05  RPP  -2040   +2040    -2040   +2040    -40    +1040              $ Inner Surface: CRT Shell 05
06  RPP  -2050   +2050    -2050   +2050    -50    +1050              $ Inner Surface: CRT Shell 06
07  RPP  -2060   +2060    -2060   +2060    -60    +1060              $ Inner Surface: CRT Shell 07
08  RPP  -2070   +2070    -2070   +2070    -70    +1070              $ Inner Surface: CRT Shell 08
09  RPP  -2080   +2080    -2080   +2080    -80    +1080              $ Inner Surface: CRT Shell 09
10  RPP  -2090   +2090    -2090   +2090    -90    +1090              $ Inner Surface: CRT Shell 10
11  RPP  -2100   +2100    -2100   +2100   -100    +1100              $ Inner Surface: CRT Shell 11
12  RPP  -2110   +2110    -2110   +2110   -110    +1110              $ Inner Surface: CRT Shell 12
13  RPP  -2120   +2120    -2120   +2120   -120    +1120              $ Inner Surface: CRT Shell 13
14  RPP  -2130   +2130    -2130   +2130   -130    +1130              $ Inner Surface: CRT Shell 14
```

```
15  RPP  -2140   +2140    -2140   +2140    -140   +1140              $ Inner Surface: CRT Shell 15
16  RPP  -2150   +2150    -2150   +2150    -150   +1150              $ Inner Surface: CRT Shell 16
17  RPP  -2160   +2160    -2160   +2160    -160   +1160              $ Inner Surface: CRT Shell 17
18  RPP  -2170   +2170    -2170   +2170    -170   +1170              $ Inner Surface: CRT Shell 18
19  RPP  -2180   +2180    -2180   +2180    -180   +1180              $ Inner Surface: CRT Shell 19
20  RPP  -2190   +2190    -2190   +2190    -190   +1190              $ Inner Surface: CRT Shell 20
21  RPP  -2200   +2200    -2200   +2200    -200   +1200              $ Inner Surface: CRT Shell 21
22  RPP  -2210   +2210    -2210   +2210    -210   +1210              $ Inner Surface: CRT Shell 22
23  RPP  -2220   +2220    -2220   +2220    -220   +1220              $ Inner Surface: CRT Shell 23
24  RPP  -2230   +2230    -2230   +2230    -230   +1230              $ Inner Surface: CRT Shell 24
25  RPP  -2240   +2240    -2240   +2240    -240   +1240              $ Inner Surface: CRT Shell 25
26  RPP  -2250   +2250    -2250   +2250    -250   +1250              $ Inner Surface: CRT Shell 26
27  RPP  -2260   +2260    -2260   +2260    -260   +1260              $ Inner Surface: CRT Shell 27
28  RPP  -2270   +2270    -2270   +2270    -270   +1270              $ Inner Surface: CRT Shell 28
29  RPP  -2280   +2280    -2280   +2280    -280   +1280              $ Inner Surface: CRT Shell 29
30  RPP  -2290   +2290    -2290   +2290    -290   +1290              $ Inner Surface: CRT Shell 30
31  RPP  -2300   +2300    -2300   +2300    -300   +1300              $ Inner Surface: CRT Shell 31
c
75  RCC    1980  0  120       +0.85   0   0      +1                  $ SS-304 "Target"
76  RPP    +1974   +1981       -1.1     +1.1     +118.9     +121.1        $ Vacuum Around Target
c
81  RCC    2332  0  0        0  0  300     +12                      $ Phantom in front of Target
c
99  RPP  -9000   +9000    -9000   +9000 -1000    +9000                $ External Void = UmWelt Boundary
c ==========================================
```

Surface cards

```
MODE H N P
CUT:H J 3 J J J
c
c PHYSICS CARDS:
c **** Physics Table FOR MCNPX 2.6.0 *****
phys:h   75                $ Emax
         0                 $ 0 always
        -1                 $-1 always
         J                 $ J always
         0                 $ 0 always
         J                 $ J always
         0                 $ 0 always
phys:n   75                $ Emax
         0                 $ 0 always
         0                 $ 0 always
     -1001                 $-1001 (analog production of delayed neutrons from fission using models when libraries are missing)
        -1                 $-1 always
         0                 $ 0 always
         0                 $ 0 always
phys:p   75                $ Emax
         0                 $ 0 always
         0                 $ 0 always
        -1                 $-1 always
         1                 $ 1 always
         0                 $ 0 always
```

Physics cards

```
C
SDEF    PAR = H              $ particle type: proton
       ERG = 70             $ energy 70MeV
       pos = +1975  0  +120     $ its position in the xyz coordinate system
       axs = 1  0   0         $ traversing along x-axis (1 0 0)
       vec = 1  0   0         $ reference vector for EXT or RAD
       dir = +1             $ azimuthal angle between -1 & +1
       ext = 0              $ use default (distance from POS along AXS)
       rad = d1             $ radius according to distribution 1
```

```
si1 h  0.0  0.5              $ Sampling of source point along radial coordinate from R.min to R.max
sp1   -21   1                $ Probability of sampling of source point in radial dimension: power law: r**1 (disk/cyl)
c
c =====
```

Source definition cards

```
c Materials:
c AIR at STP:
m1     6000   -1.24E-4         $ Air, dry.  Density = 1.205E-03 g/cc
       7014   -0.755267        $ Air, dry.  Density = 1.205E-03 g/cc
       8016   -0.231781        $ Air, dry.  Density = 1.205E-03 g/cc
      18000   -0.012827        $ Air, dry.  Density = 1.205E-03 g/cc
c Ordinary CRT
m2     1001   -0.013           $ Type 04 Ordinary Concrete
       8016   -1.165           $ Type 04 Ordinary Concrete
      11023   -0.040           $ Type 04 Ordinary Concrete
      12000   -0.010           $ Type 04 Ordinary Concrete
      13027   -0.108           $ Type 04 Ordinary Concrete
      14000   -0.740           $ Type 04 Ordinary Concrete
      16000   -0.003           $ Type 04 Ordinary Concrete
      19000   -0.045           $ Type 04 Ordinary Concrete
      20000   -0.196           $ Type 04 Ordinary Concrete
      26054   -1.7400E-03      $ Type 04 Ordinary Concrete
      26056   -2.7510E-02      $ Type 04 Ordinary Concrete
      26057   -6.4200E-04      $ Type 04 Ordinary Concrete
      26058   -9.3000E-05      $ Type 04 Ordinary Concrete
c TEM:
m3     8016   -6.143E-01       $ TEM
       6000   -2.286E-01       $ TEM
       1001   -1.000E-01       $ TEM
       7014   -2.571E-02       $ TEM
      20000   -1.429E-02       $ TEM
      15031   -1.114E-02       $ TEM
      19000   -2.000E-03       $ TEM
      16000   -2.000E-03       $ TEM
      11023   -1.429E-03       $ TEM
      17000   -1.357E-03       $ TEM
      12000   -2.714E-04       $ TEM
      26000   -6.000E-05       $ TEM
c
m4      6000    -0.03           $ SS-304L
       14028    -0.5532         $ SS-304L
       14029    -0.0282         $ SS-304L
       14030    -0.0186         $ SS-304L
       15031    -0.02           $ SS-304L
       16000    -0.03           $ SS-304L
       24050    -0.827          $ SS-304L
       24052   -15.920          $ SS-304L
       24053    -1.805          $ SS-304L
       24054    -0.448          $ SS-304L
       25055    -1.70           $ SS-304L
       26054    -3.980          $ SS-304L
       26056   -62.925          $ SS-304L
       26057    -1.468          $ SS-304L
       26058    -0.213          $ SS-304L
       28058    -6.776          $ SS-304L
       28060    -2.642          $ SS-304L
       28061    -0.116          $ SS-304L
       28062    -0.371          $ SS-304L
       28064    -0.095          $ SS-304L
c =====
```

Material definition cards

```
c TALLY DEFINITIONS:
```

```
c Dose Rates inside the Phantoms:
F14:n   81
FM14  2.185E15                $ Beam current of 350 microAmps
c
c Dose Rates inside the Phantoms:
F24:p   81
FM24  2.185E15                $ Beam current of 350 microAmps
c
c flux at each surface subdivision
f11:n 1.1                     $ neutron flux at surface 1
f21:n 2.1
f31:n 3.1
f41:n 4.1
f51:n 5.1
f61:n 6.1
f71:n 7.1
f81:n 8.1
f91:n 9.1
f101:n 10.1
f111:n 11.1
f121:n 12.1
f131:n 13.1
f141:n 14.1
f151:n 15.1
f161:n 16.1
f171:n 17.1
f181:n 18.1
f191:n 19.1
f201:n 20.1
f211:n 21.1
f221:n 22.1
f231:n 23.1
f241:n 24.1
f251:n 25.1
f261:n 26.1
f271:n 27.1
f281:n 28.1
f291:n 29.1
f301:n 30.1
f311:n 31.1
c
f611:p 1.1                     $ proton flux at surface 1
f621:p 2.1
f631:p 3.1
f641:p 4.1
f651:p 5.1
f661:p 6.1
f671:p 7.1
f681:p 8.1
f691:p 9.1
f701:p 10.1
f711:p 11.1
f721:p 12.1
f731:p 13.1
f741:p 14.1
f751:p 15.1
f761:p 16.1
f771:p 17.1
f781:p 18.1
f791:p 19.1
f801:p 20.1
f811:p 21.1
f821:p 22.1
f831:p 23.1
f841:p 24.1
```

```
f851:p 25.1
f861:p 26.1
f871:p 27.1
f881:p 28.1
f891:p 29.1
f901:p 30.1
f911:p 31.1
c
fm11 2.185E15          $ flux tally multiplication factor for neutrons, beam current of 350 microAmps
fm21 2.185E15
fm31 2.185E15
fm41 2.185E15
fm51 2.185E15
fm61 2.185E15
fm71 2.185E15
fm81 2.185E15
fm91 2.185E15
fm101 2.185E15
fm111 2.185E15
fm121 2.185E15
fm131 2.185E15
fm141 2.185E15
fm151 2.185E15
fm161 2.185E15
fm171 2.185E15
fm181 2.185E15
fm191 2.185E15
fm201 2.185E15
fm211 2.185E15
fm221 2.185E15
fm231 2.185E15
fm241 2.185E15
fm251 2.185E15
fm261 2.185E15
fm271 2.185E15
fm281 2.185E15
fm291 2.185E15
fm301 2.185E15
fm311 2.185E15
c
fm611 2.185E15          $ flux tally multiplication factor for protons, beam current of 350 microAmps
fm621 2.185E15
fm631 2.185E15
fm641 2.185E15
fm651 2.185E15
fm661 2.185E15
fm671 2.185E15
fm681 2.185E15
fm691 2.185E15
fm701 2.185E15
fm711 2.185E15
fm721 2.185E15
fm731 2.185E15
fm741 2.185E15
fm751 2.185E15
fm761 2.185E15
fm771 2.185E15
fm781 2.185E15
fm791 2.185E15
fm801 2.185E15
fm811 2.185E15
fm821 2.185E15
fm831 2.185E15
fm841 2.185E15
fm851 2.185E15
```

```
fm861 2.185E15
fm871 2.185E15
fm881 2.185E15
fm891 2.185E15
fm901 2.185E15
fm911 2.185E15
c Energy deposition tally at the Phantom
F6:n,p 81                    $ Energy deposited by neutrons & photons on to cell 81
FM6 2.185E15                 $ Beam current of 350 microAmps
c
E0 1E-11 1e-7  1e-3  1e-1  1   2    3   4   5    6    7   8    9 &
  10   12   14   16     18     20    25   30    35     40 &
  45   50   55   60     65     70
```

Tally cards

```
c Dose Conversion Function:
DF14  IU=2  FAC=1  IC=31  $ Convert Flux to Equivalent dose in unit Sv/hr
DF24  IU=2  FAC=1  IC=31
DF11  IU=2  FAC=1  IC=31
DF21  IU=2  FAC=1  IC=31
DF31  IU=2  FAC=1  IC=31
DF41  IU=2  FAC=1  IC=31
DF51  IU=2  FAC=1  IC=31
DF61  IU=2  FAC=1  IC=31
DF71  IU=2  FAC=1  IC=31
DF81  IU=2  FAC=1  IC=31
DF91  IU=2  FAC=1  IC=31
DF101 IU=2  FAC=1  IC=31
DF111 IU=2  FAC=1  IC=31
DF121 IU=2  FAC=1  IC=31
DF131 IU=2  FAC=1  IC=31
DF141 IU=2  FAC=1  IC=31
DF151 IU=2  FAC=1  IC=31
DF161 IU=2  FAC=1  IC=31
DF171 IU=2  FAC=1  IC=31
DF181 IU=2  FAC=1  IC=31
DF191 IU=2  FAC=1  IC=31
DF201 IU=2  FAC=1  IC=31
DF211 IU=2  FAC=1  IC=31
DF221 IU=2  FAC=1  IC=31
DF231 IU=2  FAC=1  IC=31
DF241 IU=2  FAC=1  IC=31
DF251 IU=2  FAC=1  IC=31
DF261 IU=2  FAC=1  IC=31
DF271 IU=2  FAC=1  IC=31
DF281 IU=2  FAC=1  IC=31
DF291 IU=2  FAC=1  IC=31
DF301 IU=2  FAC=1  IC=31
DF311 IU=2  FAC=1  IC=31
c
DF611 IU=2  FAC=1  IC=31
DF621 IU=2  FAC=1  IC=31
DF631 IU=2  FAC=1  IC=31
DF641 IU=2  FAC=1  IC=31
DF651 IU=2  FAC=1  IC=31
DF661 IU=2  FAC=1  IC=31
DF671 IU=2  FAC=1  IC=31
DF681 IU=2  FAC=1  IC=31
DF691 IU=2  FAC=1  IC=31
DF701 IU=2  FAC=1  IC=31
DF711 IU=2  FAC=1  IC=31
DF721 IU=2  FAC=1  IC=31
DF731 IU=2  FAC=1  IC=31
DF741 IU=2  FAC=1  IC=31
DF751 IU=2  FAC=1  IC=31
```

```
DF761 IU=2  FAC=1  IC=31
DF771 IU=2  FAC=1  IC=31
DF781 IU=2  FAC=1  IC=31
DF791 IU=2  FAC=1  IC=31
DF801 IU=2  FAC=1  IC=31
DF811 IU=2  FAC=1  IC=31
DF821 IU=2  FAC=1  IC=31
DF831 IU=2  FAC=1  IC=31
DF841 IU=2  FAC=1  IC=31
DF851 IU=2  FAC=1  IC=31
DF861 IU=2  FAC=1  IC=31
DF871 IU=2  FAC=1  IC=31
DF881 IU=2  FAC=1  IC=31
DF891 IU=2  FAC=1  IC=31
DF901 IU=2  FAC=1  IC=31
DF911 IU=2  FAC=1  IC=31 $ Convert Flux to Equivalent dose in unit Sv/hr
```

Dose conversions

```
c Mesh Tally Plots:
c 1001 = Neutrons in Vault
c 3001 = photons  inside  vault
c 1011 = neutrons inside  wall where detectors are.
c 1021 = neutrons outside wall where detectors are.
c 2011 = photons  inside  wall where detectors are.
c 2021 = photons  outside wall where detectors are.
TMESH
 RMESH1001:n flux
  CORA1001  -500   249i   +500
  CORB1001  -500   249i   +500
  CORC1001  +119          +121
 RMESH3001:p flux
  CORA3001  -500   249i   +500
  CORB3001  -500   249i   +500
  CORC3001  +119          +121
  RMESH1011:n flux
  CORA1011  -2000  399i  +2000
  CORB1011  -1910        -1900
  CORC1011      0  29i    +300
 RMESH1021:n flux
  CORA1021  -2000  399i  +2000
  CORB1021  -2410        -2400
  CORC1021      0  29i    +300
 RMESH2011:p flux
  CORA2011  -2000  399i  +2000
  CORB2011  -1910        -1900
  CORC2011      0  29i    +300
 RMESH2021:p flux
  CORA2021  -2000  399i  +2000
  CORB2021  -2410        -2400
  CORC2021      0  29i    +300
ENDMD
```

Mesh tally plots

```
c =====
PRINT  10  40  50  60  72  100  110  120  128  170  200
c
```

Print card

```
CTME 480
```

Computer time card

Explanation of input data file: RIB demonstrator: closed vault

```
c Cell Cards:
01  4 -11.35          -100          imp:h=1 imp:n=1      imp:p=1    $ Pb Sphere
02  1 -1.205E-3   -1   +100 +55       imp:h=0 imp:n=1      imp:p=1    $ Air in Vault
c
11  2 -2.35  -2   +1  +60     imp:h=0   imp:n=1.000E+00  imp:p=1.000E+00 $ CRT Shell 01
12  2 -2.35  -3   +2  +61     imp:h=0   imp:n=1.000E+00  imp:p=1.000E+00 $ CRT Shell 02
13  2 -2.35  -4   +3  +62     imp:h=0   imp:n=1.000E+00  imp:p=1.154E+00 $ CRT Shell 03
14  2 -2.35  -5   +4  +63     imp:h=0   imp:n=1.372E+00  imp:p=1.680E+00 $ CRT Shell 04
15  2 -2.35  -6   +5  +64     imp:h=0   imp:n=2.175E+00  imp:p=2.776E+00 $ CRT Shell 05
16  2 -2.35  -7   +6  +65     imp:h=0   imp:n=3.426E+00  imp:p=4.683E+00 $ CRT Shell 06
17  2 -2.35  -8   +7  +66     imp:h=0   imp:n=5.412E+00  imp:p=7.976E+00 $ CRT Shell 07
18  2 -2.35  -9   +8  +67     imp:h=0   imp:n=8.776E+00  imp:p=1.336E+01 $ CRT Shell 08
19  2 -2.35 -10   +9  +68     imp:h=0   imp:n=1.440E+01  imp:p=2.210E+01 $ CRT Shell 09
20  2 -2.35 -11   +10  +69     imp:h=0   imp:n=2.376E+01  imp:p=3.657E+01 $ CRT Shell 10
21  2 -2.35 -12   +11  +70     imp:h=0   imp:n=3.898E+01  imp:p=5.890E+01 $ CRT Shell 11
22  2 -2.35 -13   +12  +71     imp:h=0   imp:n=6.326E+01  imp:p=9.332E+01 $ CRT Shell 12
23  2 -2.35 -14   +13  +72     imp:h=0   imp:n=1.043E+02  imp:p=1.455E+02 $ CRT Shell 13
24  2 -2.35 -15   +14  +73     imp:h=0   imp:n=1.732E+02  imp:p=2.270E+02 $ CRT Shell 14
25  2 -2.35 -16   +15  +74     imp:h=0   imp:n=2.817E+02  imp:p=3.423E+02 $ CRT Shell 15
26  2 -2.35 -17   +16  +75     imp:h=0   imp:n=4.531E+02  imp:p=5.338E+02 $ CRT Shell 16
27  2 -2.35 -18   +17  +76     imp:h=0   imp:n=7.319E+02  imp:p=8.483E+02 $ CRT Shell 17
28  2 -2.35 -19   +18  +77     imp:h=0   imp:n=1.177E+03  imp:p=1.334E+03 $ CRT Shell 18
29  2 -2.35 -20   +19  +78     imp:h=0   imp:n=1.871E+03  imp:p=2.142E+03 $ CRT Shell 19
30  2 -2.35 -21   +20  +79     imp:h=0   imp:n=2.959E+03  imp:p=3.498E+03 $ CRT Shell 20
31  2 -2.35 -22   +21  +80     imp:h=0   imp:n=4.638E+03  imp:p=5.600E+03 $ CRT Shell 21
32  2 -2.35 -23   +22  +81     imp:h=0   imp:n=7.175E+03  imp:p=8.972E+03 $ CRT Shell 22
33  2 -2.35 -24   +23  +82     imp:h=0   imp:n=1.097E+04  imp:p=1.424E+04 $ CRT Shell 23
34  2 -2.35 -25   +24  +83     imp:h=0   imp:n=1.666E+04  imp:p=2.266E+04 $ CRT Shell 24
35  2 -2.35 -26   +25  +84     imp:h=0   imp:n=2.504E+04  imp:p=3.577E+04 $ CRT Shell 25
36  2 -2.35 -27   +26  +85     imp:h=0   imp:n=3.736E+04  imp:p=5.501E+04 $ CRT Shell 26
37  2 -2.35 -28   +27  +86     imp:h=0   imp:n=5.560E+04  imp:p=8.337E+04 $ CRT Shell 27
38  2 -2.35 -29   +28  +87     imp:h=0   imp:n=8.325E+04  imp:p=1.278E+05 $ CRT Shell 28
39  2 -2.35 -30   +29  +88     imp:h=0   imp:n=1.285E+05  imp:p=2.085E+05 $ CRT Shell 29
40  2 -2.35 -31 +30 +41 +49 +89 imp:h=0   imp:n=2.288E+05  imp:p=3.831E+05 $ CRT Shell 30
c
41  2 -2.35   -99   -41 +31    imp:h=0   imp:n=2.288E+05  imp:p=3.831E+05 $ CRT wall passage towards beam dumper
42  2 -2.35   -99   -42       imp:h=0   imp:n=2.288E+05  imp:p=3.831E+05 $ CRT wall dumper
43  2 -2.35   -99   -43       imp:h=0   imp:n=2.288E+05  imp:p=3.831E+05 $ CRT wall dumper
44  2 -2.35   -99   -44       imp:h=0   imp:n=2.288E+05  imp:p=3.831E+05 $ CRT wall dumper
45  2 -2.35   -99   -45       imp:h=0   imp:n=2.288E+05  imp:p=3.831E+05 $ CRT wall dumper
46  2 -2.35   -99   -46       imp:h=0   imp:n=2.288E+05  imp:p=3.831E+05 $ CRT wall dumper
47  2 -2.35   -99   -47       imp:h=0   imp:n=2.288E+05  imp:p=3.831E+05 $ CRT wall labyrinth
48  2 -2.35   -99   -48       imp:h=0   imp:n=2.288E+05  imp:p=3.831E+05 $ CRT wall labyrinth
49  2 -2.35   -99   -49       imp:h=0   imp:n=2.288E+05  imp:p=3.831E+05 $ CRT wall labyrinth
50  2 -2.35   -99   -50       imp:h=0   imp:n=2.288E+05  imp:p=3.831E+05 $ CRT wall experimental room
51  2 -2.35   -99   -51       imp:h=0   imp:n=2.288E+05  imp:p=3.831E+05 $ CRT wall experimental room
52  2 -2.35   -99   -52       imp:h=0   imp:n=2.288E+05  imp:p=3.831E+05 $ CRT wall experimental room
53  2 -2.35   -99   -53       imp:h=0   imp:n=2.288E+05  imp:p=3.831E+05 $ CRT wall passage vault entrance
54  2 -2.35   -99   -54       imp:h=0   imp:n=2.288E+05  imp:p=3.831E+05 $ CRT wall passage vault entrance
55  2 -2.35   -99   -55       imp:h=0   imp:n=2.288E+05  imp:p=3.831E+05 $ CRT wall passage spectrometre
56  2 -2.35   -99   -56       imp:h=0   imp:n=2.288E+05  imp:p=3.831E+05 $ CRT wall passage spectrometre
57  2 -2.35   -99   -57       imp:h=0   imp:n=2.288E+05  imp:p=3.831E+05 $ CRT underground slab
58  2 -2.35   -99   -58       imp:h=0   imp:n=2.288E+05  imp:p=3.831E+05 $ CRT underground slab
59  2 -2.35   -99   -59       imp:h=0   imp:n=2.288E+05  imp:p=3.831E+05 $ CRT underground slab
591 2  -2.35  -99 -591 +593 +57  imp:h=0   imp:n=2.288E+05  imp:p=3.831E+05 $ CRT roof passage slab from vault entrance
592 2  -2.35   -99   -592      imp:h=0   imp:n=2.288E+05  imp:p=3.831E+05 $ CRT roof slab on top of the spectrometre
593 2  -2.35   -99   -593 +31   imp:h=0   imp:n=2.288E+05  imp:p=3.831E+05 $ CRT extended thickness of the vault in the passage corner
c
60  1 -1.205E-3   -60        imp:h=0   imp:n=1.000E+00  imp:p=1.000E+00  $ Air Disk 01
61  1 -1.205E-3   -61        imp:h=0   imp:n=1.000E+00  imp:p=1.000E+00  $ Air Disk 02
62  1 -1.205E-3   -62        imp:h=0   imp:n=1.000E+00  imp:p=1.154E+00  $ Air Disk 03
63  1 -1.205E-3   -63        imp:h=0   imp:n=1.372E+00  imp:p=1.680E+00  $ Air Disk 04
64  1 -1.205E-3   -64        imp:h=0   imp:n=2.175E+00  imp:p=2.776E+00  $ Air Disk 05
```

```
65  1  -1.205E-3   -65        imp:h=0   imp:n=3.426E+00  imp:p=4.683E+00  $ Air Disk 06
66  1  -1.205E-3   -66        imp:h=0   imp:n=5.412E+00  imp:p=7.976E+00  $ Air Disk 07
67  1  -1.205E-3   -67        imp:h=0   imp:n=8.776E+00  imp:p=1.336E+01  $ Air Disk 08
68  1  -1.205E-3   -68        imp:h=0   imp:n=1.440E+01  imp:p=2.210E+01  $ Air Disk 09
69  1  -1.205E-3   -69        imp:h=0   imp:n=2.376E+01  imp:p=3.657E+01  $ Air Disk 10
70  1  -1.205E-3   -70        imp:h=0   imp:n=3.898E+01  imp:p=5.890E+01  $ Air Disk 11
71  1  -1.205E-3   -71        imp:h=0   imp:n=6.326E+01  imp:p=9.332E+01  $ Air Disk 12
72  1  -1.205E-3   -72        imp:h=0   imp:n=1.043E+02  imp:p=1.455E+02  $ Air Disk 13
73  1  -1.205E-3   -73        imp:h=0   imp:n=1.732E+02  imp:p=2.270E+02  $ Air Disk 14
74  1  -1.205E-3   -74        imp:h=0   imp:n=2.817E+02  imp:p=3.423E+02  $ Air Disk 15
75  1  -1.205E-3   -75        imp:h=0   imp:n=4.531E+02  imp:p=5.338E+02  $ Air Disk 16
76  1  -1.205E-3   -76        imp:h=0   imp:n=7.319E+02  imp:p=8.483E+02  $ Air Disk 17
77  1  -1.205E-3   -77        imp:h=0   imp:n=1.177E+03  imp:p=1.334E+03  $ Air Disk 18
78  1  -1.205E-3   -78        imp:h=0   imp:n=1.871E+03  imp:p=2.142E+03  $ Air Disk 19
79  1  -1.205E-3   -79        imp:h=0   imp:n=2.959E+03  imp:p=3.498E+03  $ Air Disk 20
80  1  -1.205E-3   -80        imp:h=0   imp:n=4.638E+03  imp:p=5.600E+03  $ Air Disk 21
81  1  -1.205E-3   -81        imp:h=0   imp:n=7.175E+03  imp:p=8.972E+03  $ Air Disk 22
82  1  -1.205E-3   -82        imp:h=0   imp:n=1.097E+04  imp:p=1.424E+04  $ Air Disk 23
83  1  -1.205E-3   -83        imp:h=0   imp:n=1.666E+04  imp:p=2.266E+04  $ Air Disk 24
84  1  -1.205E-3   -84        imp:h=0   imp:n=2.504E+04  imp:p=3.577E+04  $ Air Disk 25
85  1  -1.205E-3   -85        imp:h=0   imp:n=3.736E+04  imp:p=5.501E+04  $ Air Disk 26
86  1  -1.205E-3   -86        imp:h=0   imp:n=5.560E+04  imp:p=8.337E+04  $ Air Disk 27
87  1  -1.205E-3   -87        imp:h=0   imp:n=8.325E+04  imp:p=1.278E+05  $ Air Disk 28
88  1  -1.205E-3   -88        imp:h=0   imp:n=1.285E+05  imp:p=2.085E+05  $ Air Disk 29
89  1  -1.205E-3   -89        imp:h=0   imp:n=2.288E+05  imp:p=3.831E+05  $ Air Disk 30
c
150  3   1.0       -150       imp:h=0 imp:n=2.288E+05  imp:p=3.831E+05  $ Phantom in the labyrinth
151  3   1.0       -151       imp:h=0 imp:n=2.288E+05  imp:p=3.831E+05  $ Phantom just outside yard
152  3   1.0       -152       imp:h=0 imp:n=2.288E+05  imp:p=3.831E+05  $ Phantom in the experimental room
c
91  1  -1.205E-3  -99 +31 +41 +42 +43 +44 +45 +46 +47 +48 +49 +50 +51 +52 +53
     +54 +55 56 +57 +58 +59 +89 +150 +151 +152  +591
     +592 +593              imp:h=0 imp:n=2.288E+05 imp:p=3.831E+05  $ Outside Air
c
99  0              +99       imp:h=0 imp:n=0  imp:p=0  $ UmWelt = External Void
```

Cell cards

```
c Surface Cards
01  RPP   -225   +225  -225   +225  -0.00     +600.00   $ Inner Surface: CRT Shell 01
02  RPP   -235   +235  -235   +235  -6.67     +606.67   $ Inner Surface: CRT Shell 02
03  RPP   -245   +245  -245   +245  -13.33    +613.33   $ Inner Surface: CRT Shell 03
04  RPP   -255   +255  -255   +255  -20.00    +620.00   $ Inner Surface: CRT Shell 04
05  RPP   -265   +265  -265   +265  -26.67    +626.66   $ Inner Surface: CRT Shell 05
06  RPP   -275   +275  -275   +275  -33.33    +633.33   $ Inner Surface: CRT Shell 06
07  RPP   -285   +285  -285   +285  -40.00    +639.99   $ Inner Surface: CRT Shell 07
08  RPP   -295   +295  -295   +295  -46.67    +646.66   $ Inner Surface: CRT Shell 08
09  RPP   -305   +305  -305   +305  -53.33    +653.32   $ Inner Surface: CRT Shell 09
10  RPP   -315   +315  -315   +315  -60.00    +659.99   $ Inner Surface: CRT Shell 10
11  RPP   -325   +325  -325   +325  -66.67    +666.65   $ Inner Surface: CRT Shell 11
12  RPP   -335   +335  -335   +335  -73.33    +673.32   $ Inner Surface: CRT Shell 12
13  RPP   -345   +345  -345   +345  -80.00    +679.98   $ Inner Surface: CRT Shell 13
14  RPP   -355   +355  -355   +355  -86.66    +686.65   $ Inner Surface: CRT Shell 14
15  RPP   -365   +365  -365   +365  -93.33    +693.31   $ Inner Surface: CRT Shell 15
16  RPP   -375   +375  -375   +375  -100.00   +699.98   $ Inner Surface: CRT Shell 16
17  RPP   -385   +385  -385   +385  -106.66   +706.64   $ Inner Surface: CRT Shell 17
18  RPP   -395   +395  -395   +395  -113.33   +713.31   $ Inner Surface: CRT Shell 18
19  RPP   -405   +405  -405   +405  -120.00   +719.97   $ Inner Surface: CRT Shell 19
20  RPP   -415   +415  -415   +415  -126.66   +726.64   $ Inner Surface: CRT Shell 20
21  RPP   -425   +425  -425   +425  -133.33   +733.30   $ Inner Surface: CRT Shell 21
22  RPP   -435   +435  -435   +435  -140.00   +739.97   $ Inner Surface: CRT Shell 22
23  RPP   -445   +445  -445   +445  -146.66   +746.63   $ Inner Surface: CRT Shell 23
24  RPP   -455   +455  -455   +455  -153.33   +753.30   $ Inner Surface: CRT Shell 24
25  RPP   -465   +465  -465   +465  -160.00   +759.96   $ Inner Surface: CRT Shell 25
26  RPP   -475   +475  -475   +475  -166.66   +766.63   $ Inner Surface: CRT Shell 26
27  RPP   -485   +485  -485   +485  -173.33   +773.29   $ Inner Surface: CRT Shell 27
```

```
28  RPP    -495    +495  -495    +495  -180.00   +779.96   $ Inner Surface: CRT Shell 28
29  RPP    -505    +505  -505    +505  -186.66   +786.62   $ Inner Surface: CRT Shell 29
30  RPP    -515    +515  -515    +515  -193.33   +793.29   $ Inner Surface: CRT Shell 30
31  RPP    -525    +525  -525    +525  -200.00   +799.95   $ Inner Surface: CRT Shell 31
c
41  RPP  -1125    -525    -225    -75     0.00     +600.00   $ CRT wall passage towards beam dumper
42  RPP  -1125    -975    -75     +75     0.00     +600.00   $ CRT wall dumper
43  RPP  -1125    -825    +75     +225    0.00     +600.00   $ CRT wall dumper
44  RPP  -975     -825    -75     +75     180      +230.00   $ CRT wall dumper
45  RPP  -875     -825    +20     +75     0.00     +180.00   $ CRT wall dumper
46  RPP  -875     -825    -75     -20     0.00     +180.00   $ CRT wall dumper
47  RPP  -1425    -1125   -75     -45     0.00     +600.00   $ CRT wall labyrinth
48  RPP  -1425    -1395   -45     +225    0.00     +600.00   $ CRT wall labyrinth
49  RPP  -1275    -1245   +75     +1075   0.00     +600.00   $ CRT wall labyrinth
50  RPP  -1245    +645    +1045   +1075   0.00     +600.00   $ CRT wall experimental room
51  RPP  +645     +675    +525    +1075   0.00     +600.00   $ CRT wall experimental room
52  RPP  +525     +675    +495    +525    0        +600.00   $ CRT wall experimental room
53  RPP  +225     +525    -975    -525    0        +600      $ CRT wall passage vault entrance
54  RPP  -1125    +225    -975    -675    0        +600      $ CRT wall passage vault entrance
55  RPP  -1275    -825    -525    -375    0        +600      $ CRT wall passage spectrometre
56  RPP  -1575    -1275   -525    -225    0        +600      $ CRT wall passage spectrometre
57  RPP  -1275    -525    -975    +1075   -200     0         $ CRT underground slab
58  RPP  -525     +675    +525    +1075   -200     0         $ CRT underground slab
59  RPP  -525     +525    -975    -525    -200     0.00      $ CRT underground slab
591 RPP  -675     +525    -975    -525    +600     +900      $ CRT roof passage slab from vault entrance
592 RPP  -1125    -675    -975    -225    +600     +675      $ CRT roof slab on top of the spectrometre
593 RPP  -675     -525    -525    -225    0        +600      $ CRT extended thickness of the vault in the passage corner
c
60 RCC    -225     0    +120     -10    0     0    +5    $ Air Disk 01
61 RCC    -235     0    +120     -10    0     0    +5    $ Air Disk 02
62 RCC    -245     0    +120     -10    0     0    +5    $ Air Disk 03
63 RCC    -255     0    +120     -10    0     0    +5    $ Air Disk 04
64 RCC    -265     0    +120     -10    0     0    +5    $ Air Disk 05
65 RCC    -275     0    +120     -10    0     0    +5    $ Air Disk 06
66 RCC    -285     0    +120     -10    0     0    +5    $ Air Disk 07
67 RCC    -295     0    +120     -10    0     0    +5    $ Air Disk 08
68 RCC    -305     0    +120     -10    0     0    +5    $ Air Disk 09
69 RCC    -315     0    +120     -10    0     0    +5    $ Air Disk 10
70 RCC    -325     0    +120     -10    0     0    +5    $ Air Disk 11
71 RCC    -335     0    +120     -10    0     0    +5    $ Air Disk 12
72 RCC    -345     0    +120     -10    0     0    +5    $ Air Disk 13
73 RCC    -355     0    +120     -10    0     0    +5    $ Air Disk 14
74 RCC    -365     0    +120     -10    0     0    +5    $ Air Disk 15
75 RCC    -375     0    +120     -10    0     0    +5    $ Air Disk 16
76 RCC    -385     0    +120     -10    0     0    +5    $ Air Disk 17
77 RCC    -395     0    +120     -10    0     0    +5    $ Air Disk 18
78 RCC    -405     0    +120     -10    0     0    +5    $ Air Disk 19
79 RCC    -415     0    +120     -10    0     0    +5    $ Air Disk 20
80 RCC    -425     0    +120     -10    0     0    +5    $ Air Disk 21
81 RCC    -435     0    +120     -10    0     0    +5    $ Air Disk 22
82 RCC    -445     0    +120     -10    0     0    +5    $ Air Disk 23
83 RCC    -455     0    +120     -10    0     0    +5    $ Air Disk 24
84 RCC    -465     0    +120     -10    0     0    +5    $ Air Disk 25
85 RCC    -475     0    +120     -10    0     0    +5    $ Air Disk 26
86 RCC    -485     0    +120     -10    0     0    +5    $ Air Disk 27
87 RCC    -495     0    +120     -10    0     0    +5    $ Air Disk 28
88 RCC    -505     0    +120     -10    0     0    +5    $ Air Disk 29
89 RCC    -515     0    +120     -10    0     0    +5    $ Air Disk 30
c
100  SPH    0     0    120    +0.85          $ Pb Sphere
c
150  RCC   -1155    0    0          0  0  300    +12          $ Phantom in the labyrinth
151  RCC   -1455    0    0          0  0  300    +12          $ Phantom just outside yard
152  RCC   -825    +300  0          0  0  300    +12          $ Phantom in the experimental room
c
```

```
99  RPP  -9000   +9000    -9000   +9000 -1000    +9000    $ External Void = UmWelt Boundary
c ==========================================
```

Surface cards

```
MODE H N P
CUT:H J 3 J J J
c
c PHYSICS CARDS:
c **** Physics Table FOR MCNPX 2.6.0 *****
phys:h    75
          0
         -1
          J
          0
          J
          0
phys:n    75
          0
          0
       -1001
         -1
          0
          0
phys:p    75
          0
          0
         -1
          1
          0
C
```

Physics cards

```
SDEF    PAR = H
        ERG = 70
        pos = 0  0  +120
c
```

Source definition cards

```
c Materials:
c AIR at STP:
m1     6000   -1.24E-4          $ Air, dry.  Density = 1.205E-03 g/cc
       7014   -0.755267         $ Air, dry.  Density = 1.205E-03 g/cc
       8016   -0.231781         $ Air, dry.  Density = 1.205E-03 g/cc
      18000   -0.012827         $ Air, dry.  Density = 1.205E-03 g/cc
c Ordinary CRT
m2     1001   -0.013            $ Type 04 Ordinary Concrete
       8016   -1.165            $ Type 04 Ordinary Concrete
      11023   -0.040            $ Type 04 Ordinary Concrete
      12000   -0.010            $ Type 04 Ordinary Concrete
      13027   -0.108            $ Type 04 Ordinary Concrete
      14000   -0.740            $ Type 04 Ordinary Concrete
      16000   -0.003            $ Type 04 Ordinary Concrete
      19000   -0.045            $ Type 04 Ordinary Concrete
      20000   -0.196            $ Type 04 Ordinary Concrete
      26054   -1.7400E-03       $ Type 04 Ordinary Concrete
      26056   -2.7510E-02       $ Type 04 Ordinary Concrete
      26057   -6.4200E-04       $ Type 04 Ordinary Concrete
      26058   -9.3000E-05       $ Type 04 Ordinary Concrete
c TEM:
m3     8016   -6.143E-01        $ TEM
       6000   -2.286E-01        $ TEM
       1001   -1.000E-01        $ TEM
       7014   -2.571E-02        $ TEM
      20000   -1.429E-02        $ TEM
```

```
     15031   -1.114E-02      $ TEM
     19000   -2.000E-03      $ TEM
     16000   -2.000E-03      $ TEM
     11023   -1.429E-03      $ TEM
     17000   -1.357E-03      $ TEM
     12000   -2.714E-04      $ TEM
     26000   -6.000E-05      $ TEM
c
m4  82206 +24.1          &        $ Lead
   82207 +22.1          &        $ Lead
   82208 +52.4                   $ Lead
c BoratedParrafin Wax
m5   1001      -1.4267E-01  &    $ Paraffin wax
    6012      -8.2603E-01  &    $ Paraffin wax
    5010      -5.7699E-03  &    $ Paraffin wax
    5011      -2.5535E-02       $ Paraffin wax
c =====
```

Material definition cards

```
c TALLY DEFINITIONS:
c
c Neutron Flux leaving the source:
F1:n  100
FM1  2.185E15   $ Beam current of 350 microAmps
c
c Dose Rates inside the Phantoms:
F14:n   150  151  152
FM14  2.185E15   $ Beam current of 350 microAmps
c
c Dose Rates inside the Phantoms:
F24:p   150  151  152
FM24  2.185E15   $ Beam current of 350 microAmps
c
c Neutron Flux through the hole
f15:n  -525   0  120   5.0
FM15 2.185E15   $ Beam current of 350 microAmps
c
c Energy deposition tally at the Phantom
F6:n,p 150  151  152
FM6 2.185E15   $ Beam current of 350 microAmps
c
E0 1E-11 1e-7  1e-3  1e-1  1    2    3    4    5    6    7    8    9 &
  10   12   14   16      18      20      25      30      35      40 &
  45   50   55   60      65      70
```

Tally cards

```
c Dose Conversion Function:
DF14  IU=2  FAC=1  IC=31  $ Convert Flux to Equivalent dose in unit Sv/hr
DF24  IU=2  FAC=1  IC=31  $ Convert Flux to Equivalent dose in unit Sv/hr
c
```

Dose conversions

```
c Mesh Tally Plots:
c 201 = Neutrons in Vault
c 301 = photons  inside  vault
c 111 = neutrons inside  wall where detectors are.
c 121 = neutrons outside wall where detectors are.
c 211 = photons  inside  wall where detectors are.
c 221 = photons  outside wall where detectors are.
TMESH
 RMESH201:n flux
  CORA201  -2500   249i   +2500
  CORB201  -2500   249i   +2500
  CORC201  +119          +121
```

```
 RMESH301:p flux
  CORA301  -2500   249i   +2500
  CORB301  -2500   249i   +2500
  CORC301  +119          +121
  RMESH111:n flux
  CORA111  -2000  399i  +2000
  CORB111  -1910        -1900
  CORC111      0  29i    +300
 RMESH121:n flux
  CORA121  -2000  399i  +2000
  CORB121  -2410        -2400
  CORC121      0  29i    +300
 RMESH211:p flux
  CORA211  -2000  399i  +2000
  CORB211  -1910        -1900
  CORC211      0  29i    +300
 RMESH221:p flux
  CORA221  -2000  399i  +2000
  CORB221  -2410        -2400
  CORC221      0  29i    +300
ENDMD
```

Mesh tally plots

```
c =====
PRINT  10  40  50  60  72  100  110  120  128  170  200
c
```

Print card

```
CTME 1440
```

Computer time card

Explanation of input data file: RIB demonstrator: open vault

```
c Cell Cards:
01  4 -11.35          -100          imp:h=1 imp:n=1      imp:p=1          $ Pb Sphere
02  1 -1.205E-3   -1   +100          imp:h=0 imp:n=1      imp:p=1          $ Air in Vault
c
11  2 -2.35    -2    +1  +3          imp:h=0   imp:n=1      imp:p=1        $ CRT Vault wall
12  1 -1.205E-3   -3  +4            imp:h=0   imp:n=1      imp:p=1        $ Air in the Vault entrance passage
13  1 -1.205E-3 -4 +2 +3 +202 +53 +201 +591 +593 +157 +8
     imp:h=0 imp:n=1 imp:p=1                                              $ Air vault passage
14  1 -1.205E-3  -5  +6 +54 +55 +592   imp:h=0   imp:n=4  imp:p=4            $ Air towards spectrometre entrance
15  1 -1.205E-3  -6  +7 +55 +53 +592 +593 +202 +156 imp:h=0 imp:n=4 imp:p=4    $ Air passage around spectrometre
16  1 -1.205E-3  -7  +6 +155      imp:h=0   imp:n=4      imp:p=4            $ Air passage around spectrometre
17  5 -0.94398     -8 -4 +54 +53 +1 +591     imp:h=0   imp:n=1      imp:p=1  $ boron-wax neutron absorber strip down the passage vault entrance
c
41  2 -2.35   -99   -41 +2  imp:h=0   imp:n=4  imp:p=4      $ CRT wall passage towards beam dumper
42  2 -2.35   -99   -42     imp:h=0   imp:n=4  imp:p=4      $ CRT wall dumper
43  2 -2.35   -99   -43     imp:h=0   imp:n=4  imp:p=4      $ CRT wall dumper
44  2 -2.35   -99   -44     imp:h=0   imp:n=4  imp:p=4      $ CRT wall dumper
45  2 -2.35   -99   -45     imp:h=0   imp:n=4  imp:p=4      $ CRT wall dumper
46  2 -2.35   -99   -46     imp:h=0   imp:n=4  imp:p=4      $ CRT wall dumper
47  2 -2.35   -99   -47     imp:h=0   imp:n=4  imp:p=4      $ CRT wall labyrinth
48  2 -2.35   -99   -48     imp:h=0   imp:n=4  imp:p=4      $ CRT wall labyrinth
49  2 -2.35   -99   -49     imp:h=0   imp:n=4  imp:p=4      $ CRT wall labyrinth
50  2 -2.35   -99   -50     imp:h=0   imp:n=4  imp:p=4      $ CRT wall experimental room
51  2 -2.35   -99   -51     imp:h=0   imp:n=4  imp:p=4      $ CRT wall experimental room
52  2 -2.35   -99   -52     imp:h=0   imp:n=4  imp:p=4      $ CRT wall experimental room
53  2 -2.35   -99   -53 +8  imp:h=0   imp:n=4  imp:p=4      $ CRT wall passage vault entrance
54  2 -2.35   -99   -54     imp:h=0   imp:n=4  imp:p=4      $ CRT wall passage vault entrance
55  2 -2.35   -99   -55     imp:h=0   imp:n=4  imp:p=4      $ CRT wall passage spectrometre
56  2 -2.35   -99   -56     imp:h=0   imp:n=4  imp:p=4      $ CRT wall passage spectrometre
57  2 -2.35   -99   -57     imp:h=0   imp:n=4  imp:p=4      $ CRT underground slab
58  2 -2.35   -99   -58     imp:h=0   imp:n=4  imp:p=4      $ CRT underground slab
59  2 -2.35   -99   -59     imp:h=0   imp:n=4  imp:p=4      $ CRT underground slab
591 2  -2.35   -99   -591    imp:h=0   imp:n=4  imp:p=4      $ CRT roof passage slab from vault entrance
592 2  -2.35   -99   -592    imp:h=0   imp:n=4  imp:p=4      $ CRT roof slab on top of the spectrometre
593 2  -2.35  -593 +5 +4 +202 imp:h=0   imp:n=4  imp:p=4      $ CRT extended thickness of the vault in the passage corner
c
150  3   1.0       -150       imp:h=0 imp:n=4  imp:p=4      $ Phantom in the labyrinth
151  3   1.0       -151       imp:h=0 imp:n=4  imp:p=4      $ Phantom just outside yard
152  3   1.0       -152       imp:h=0 imp:n=4  imp:p=4      $ Phantom in the experimental room
153  3   1.0       -153       imp:h=0 imp:n=4  imp:p=4      $ Phantom on top of the mass spectrometre
154  3   1.0       -154       imp:h=0 imp:n=4  imp:p=4      $ Phantom just outside the door1 in the passage entrance
155  3   1.0       -155       imp:h=0 imp:n=4  imp:p=4      $ Phantom just behind the door1
156  3   1.0       -156       imp:h=0 imp:n=4  imp:p=4      $ Phantom just outside the door2 towards vault entrance
157  3   1.0       -157       imp:h=0 imp:n=1  imp:p=1      $ Phantom just behind the door2
158  3   1.0       -158       imp:h=0 imp:n=1  imp:p=1      $ Phantom on top of the vault
c
201  5   -0.94398      -201       imp:h=0 imp:n=4  imp:p=4    $ boron wax door1
202  5   -0.94398      -202       imp:h=0 imp:n=4  imp:p=4    $ boron wax door2
c
91  1  -1.205E-3  -99 +2 +4 +5 +6 +7 +41 +42 +43 +44 +45 +46 +47 +48 +49 +50
      +52 +53 +54 +55 +56 +57 +58 +59 +150 +151 +152 +153 +201 +591 +592 +593
      +51 +154 +202 +8 +158 imp:h=0  imp:n=4 imp:p=4          $ Outside Air
c
99  0                +99          imp:h=0 imp:n=0  imp:p=0   $ UmWelt = External Void
c ==========================================
```

Cell cards

```
c Surface Cards
01  RPP  -225    +225     -225     +225   0.00      +600.00    $ Inner Surface: CRT wall, vault
02  RPP  -525    +525     -525     +525   -300      +900       $ Outer Surface: CRT wall, vault
03  RPP  -75     225      -525    -225    0.00      +600.00    $ Inner Surface: Air vault entrance
04  RPP  -665    225      -675    -525    0.00      +600.00    $ Inner Surface: Air vault passage
```

```
05  RPP  -1125  -825     -675    -525    0.00      +600.00    $ Inner Surface: Air towards spectrometre entrance
06  RPP  -825   -675     -675    -225    0.00      +600.00    $ Inner Surface: Air passage around spectrometre
07  RPP  -1115  -825     -375    -225    0.00      +600.00    $ Inner Surface: Air passage around spectrometre
08  RPP  -75    +225     -675    -665    0         +600       $ Inner Surface: boron-wax neutron absorber strip down the passage vault entrance
c
41  RPP  -1125   -525    -225     -75     0.00     +600.00    $ CRT wall passage towards beam dumper
42  RPP  -1125   -975     -75     +75     0.00     +600.00    $ CRT wall dumper
43  RPP  -1125   -825     +75     +225    0.00     +600.00    $ CRT wall dumper
44  RPP   -975   -825     -75     +75     180      +230.00    $ CRT wall dumper
45  RPP   -875   -825     +20     +75     0.00     +180.00    $ CRT wall dumper
46  RPP   -875   -825     -75     -20     0.00     +180.00    $ CRT wall dumper
47  RPP  -1425  -1125     -75     -45     0.00     +600.00    $ CRT wall labyrinth
48  RPP  -1425  -1395     -45     +225    0.00     +600.00    $ CRT wall labyrinth
49  RPP  -1275  -1245     +75     +1075   0.00     +600.00    $ CRT wall labyrinth
50  RPP  -1245   +645     +1045   +1075   0.00     +600.00    $ CRT wall experimental room
51  RPP   +645   +675     +525    +1075   0.00     +600.00    $ CRT wall experimental room
52  RPP   +525   +675     +495    +525    0        +600.00    $ CRT wall experimental room
53  RPP   +225   +525     -975    -525    0        +600       $ CRT wall passage vault entrance
54  RPP  -1125   +225     -975    -675    0        +600       $ CRT wall passage vault entrance
55  RPP  -1275   -825     -525    -375    0        +600       $ CRT wall passage spectrometre
56  RPP  -1575  -1275     -525    -225    0        +600       $ CRT wall passage spectrometre
57  RPP  -1275   -525     -975   +1075    -200     0          $ CRT underground slab
58  RPP   -525   +675     +525    +1075   -200     0          $ CRT underground slab
59  RPP   -525   +525     -975    -525    -200     0.00       $ CRT underground slab
591 RPP   -675   +525     -975    -525    +600     +900       $ CRT roof passage slab from vault entrance
592 RPP  -1575   -675     -975    -225    +600     +675       $ CRT roof slab on top of the spectrometre
593 RPP   -675   -525     -525    -225    0        +600       $ CRT extended thickness of the vault in the passage corner
c
100  SPH    0     0   120    +0.85                    $ Pb Sphere
c
201 RPP   -525   -515     -675    -525    0        +600       $ boron wax door1
202 RPP   -675   -665     -675    -525    0        +600       $ boron wax door2
c
150 RCC  -1155      0     0    0    0     300    +12          $ Phantom in the labyrinth
151 RCC  -1455      0     0    0    0     300    +12          $ Phantom just outside yard
152 RCC   -825    +300     0    0    0     300    +12          $ Phantom in the experimental room
153 RCC  -1425    -525  +675    0    0     300    +12          $ Phantom on top of the mass spectrometre
154 RCC  -1155    -305     0    0    0     300    +12          $ Phantom just outside the door1 in the passage entrance
155 RCC  -1050    -305     0    0    0     300    +12          $ Phantom just behind the door1
156 RCC   -750    -605     0    0    0     300    +12          $ Phantom just outside the door2 towards vault entrance
157 RCC   -600    -605     0    0    0     300    +12          $ Phantom just behind the door2
158 RCC      0      0    +900    0    0     300    +12          $ Phantom on top of the vault
c
99  RPP  -9000   +9000    -9000   +9000 -1000    +9000    $ External Void = UmWelt Boundary
c ==========================================
```

Surface cards

```
MODE H N P
CUT:H J 3 J J J
c
c PHYSICS CARDS:
c **** Physics Table FOR MCNPX 2.6.0 *****
phys:h    75                $ Emax
          0                 $ 0 always
         -1                 $-1 always
          J                 $ J always
          0                 $ 0 always
          J                 $ J always
          0                 $ 0 always
phys:n    75                $ Emax
          0                 $ 0 always
          0                 $ 0 always
      -1001                 $-1001 (analog production of delayed neutrons from fission using models when libraries are missing)
         -1                 $-1 always
          0                 $ 0 always
```

```
        0                $ 0 always
phys:p  75                 $ Emax
        0                $ 0 always
        0                $ 0 always
       -1                $-1 always
        1                $ 1 always
        0                $ 0 always
C
```

Physics cards

```
SDEF   PAR = H              $ particle type proton
       ERG = 70             $ particle energy 70MeV
       pos = 0  0  +120     $ position in the xyz coordinate
c
```

Source definition cards

```
c Materials:
c AIR at STP:
m1    6000   -1.24E-4         $ Air, dry.  Density = 1.205E-03 g/cc
      7014   -0.755267        $ Air, dry.  Density = 1.205E-03 g/cc
      8016   -0.231781        $ Air, dry.  Density = 1.205E-03 g/cc
     18000   -0.012827        $ Air, dry.  Density = 1.205E-03 g/cc
c Ordinary CRT
m2    1001   -0.013           $ Type 04 Ordinary Concrete
      8016   -1.165           $ Type 04 Ordinary Concrete
     11023   -0.040           $ Type 04 Ordinary Concrete
     12000   -0.010           $ Type 04 Ordinary Concrete
     13027   -0.108           $ Type 04 Ordinary Concrete
     14000   -0.740           $ Type 04 Ordinary Concrete
     16000   -0.003           $ Type 04 Ordinary Concrete
     19000   -0.045           $ Type 04 Ordinary Concrete
     20000   -0.196           $ Type 04 Ordinary Concrete
     26054   -1.7400E-03      $ Type 04 Ordinary Concrete
     26056   -2.7510E-02      $ Type 04 Ordinary Concrete
     26057   -6.4200E-04      $ Type 04 Ordinary Concrete
     26058   -9.3000E-05      $ Type 04 Ordinary Concrete
c TEM:
m3    8016   -6.143E-01       $ TEM
      6000   -2.286E-01       $ TEM
      1001   -1.000E-01       $ TEM
      7014   -2.571E-02       $ TEM
     20000   -1.429E-02       $ TEM
     15031   -1.114E-02       $ TEM
     19000   -2.000E-03       $ TEM
     16000   -2.000E-03       $ TEM
     11023   -1.429E-03       $ TEM
     17000   -1.357E-03       $ TEM
     12000   -2.714E-04       $ TEM
     26000   -6.000E-05       $ TEM
c
m4  82206 +24.1         &     $ Lead
   82207 +22.1          &     $ Lead
   82208 +52.4                $ Lead
c BoratedParrafin Wax
m5   1001     -1.4267E-01  &    $ Paraffin wax
     6012     -8.2603E-01  &    $ Paraffin wax
     5010     -5.7699E-03  &    $ Paraffin wax
     5011     -2.5535E-02       $ Paraffin wax
c =====
```

Material definition cards

```
c TALLY DEFINITIONS:
c Dose Rates inside the Phantoms:
F14:n   150  151  152   153  154  155 156 157 158
```

```
FM14  2.185E15   $ Beam current of 350 microAmps
c
c Dose Rates inside the Phantoms:
F24:p   150  151  152  153   154  155 156  157 158
FM24  2.185E15   $ Beam current of 350 microAmps
c Energy deposition tally at the Phantom
c
F6:n,p 150  151  152  153   154  155 156  157 158
FM6 2.185E15   $ Beam current of 350 microAmps
c
E0 1E-11 1e-7  1e-3  1e-1  1    2    3    4    5    6    7    8    9 &
  10   12   14   16     18     20     25    30     35     40 &
  45   50   55   60     65     70
```

Tally cards

```
c Dose Conversion Function:
DF14  IU=2  FAC=1  IC=31  $ Convert Flux to Equivalent dose in unit Sv/hr
DF24  IU=2  FAC=1  IC=31  $ Convert Flux to Equivalent dose in unit Sv/hr
c
```

Dose conversions

```
c Mesh Tally Plots:
c 201 = Neutrons in Vault
c 301 = photons  inside  vault
c 111 = neutrons inside  wall where detectors are.
c 121 = neutrons outside wall where detectors are.
c 211 = photons  inside  wall where detectors are.
c 221 = photons  outside wall where detectors are.
TMESH
 RMESH201:n flux
  CORA201  -2500   249i    +2500
  CORB201  -2500   249i    +2500
  CORC201  +119           +121
 RMESH301:p flux
  CORA301  -2500   249i    +2500
  CORB301  -2500   249i    +2500
  CORC301  +119           +121
 RMESH111:n flux
  CORA111  -2000   399i    +2000
  CORB111  -5             +5
  CORC111  -350    249i    +1300
 RMESH221:p flux
  CORA221  -2000   399i   +2000
  CORB221  -5             +5
  CORC221  -350    249i   +1300
 RMESH121:n flux
  CORA121  -5             +5
  CORB121  -1910   249i   -1900
  CORC121  -350    249i   +1300
 RMESH211:p flux
  CORA211  -5             +5
  CORB211  -1910   249i   -1900
  CORC211  -350    249i   +1300
ENDMD
```

mesh tally plots

```
c =====
PRINT  10  40  50  60  72  100  110  120  128  170  200
c
```

Print card

```
CTME 3600
```

Computer time card

Appendix 3: Explanation of output file: New Cyclotron vault: open vault

1neutron activity in each cell print table 126

cell	tracks entering	population	collisions	collisions * weight (per history)	number weighted energy	flux weighted energy	average track weight (relative)	average track mfp (cm)	
1	1	846689	845676	0	0.0000E+00	8.7731E-01	4.2762E+00	9.9738E-01	0.0000E+00
2	2	206	845891	182648	1.3949E-02	2.5058E+00	6.3825E+00	9.9801E-01	3.8542E+00
3	3	3538054	889899	1338034	6.8175E-02	4.1034E-04	9.7590E-01	7.5532E-01	5.6338E+03
4	11	5424386	937726	39547887	2.0726E+00	2.9121E-04	1.0883E+00	7.2785E-01	3.4311E+00
5	12	3811332	964990	29334801	1.4104E+00	1.3253E-04	6.9799E-01	6.6017E-01	3.0340E+00
6	13	2467184	982620	19399202	8.5754E-01	8.5168E-05	5.7449E-01	6.0350E-01	2.8606E+00
7	14	2204983	1265288	17436165	4.8038E-01	6.5528E-05	5.3180E-01	5.5706E-01	2.7674E+00
8	15	2174317	1383526	17206271	2.5599E-01	5.7467E-05	5.3665E-01	5.2197E-01	2.7203E+00
9	16	2088851	1364230	16487741	1.3217E-01	5.4615E-05	5.6968E-01	4.9710E-01	2.6986E+00
10	17	2005014	1339890	15759174	6.6877E-02	5.5263E-05	6.3201E-01	4.7830E-01	2.6967E+00
11	18	1962333	1339967	15353590	3.3528E-02	5.8811E-05	7.2089E-01	4.6562E-01	2.7124E+00
12	19	1942078	1341487	15124742	1.6823E-02	6.4234E-05	8.2257E-01	4.5854E-01	2.7384E+00
13	20	1934127	1339063	14970871	8.4867E-03	7.1218E-05	9.3810E-01	4.5485E-01	2.7736E+00
14	21	1916073	1324832	14786061	4.3369E-03	8.0073E-05	1.0780E+00	4.5434E-01	2.8163E+00
15	22	1893552	1306556	14551245	2.2468E-03	9.1008E-05	1.2421E+00	4.5591E-01	2.8662E+00
16	23	1890942	1303832	14445844	1.1848E-03	1.0279E-04	1.4100E+00	4.5923E-01	2.9184E+00
17	24	1918709	1317436	14623149	6.3768E-04	1.1572E-04	1.5791E+00	4.6400E-01	2.9733E+00
18	25	1915528	1301008	14545980	3.4886E-04	1.2922E-04	1.7488E+00	4.6980E-01	3.0287E+00
19	26	1907323	1285185	14403438	1.9458E-04	1.4328E-04	1.9149E+00	4.7612E-01	3.0826E+00
20	27	1924030	1287118	14478588	1.1106E-04	1.5602E-04	2.0616E+00	4.8247E-01	3.1275E+00
21	28	1922578	1274741	14424329	6.4308E-05	1.6810E-04	2.1933E+00	4.8889E-01	3.1677E+00
22	29	1926789	1271523	14441241	3.7796E-05	1.7921E-04	2.3211E+00	4.9424E-01	3.2047E+00
23	30	1939620	1271590	14481004	2.2492E-05	1.8859E-04	2.4208E+00	4.9946E-01	3.2343E+00
24	31	1961017	1278272	14615220	1.3573E-05	1.9722E-04	2.5128E+00	5.0384E-01	3.2611E+00
25	32	1966142	1271392	14622859	8.2277E-06	2.0438E-04	2.5866E+00	5.0792E-01	3.2818E+00
26	33	1956738	1259668	14556463	5.0393E-06	2.1141E-04	2.6577E+00	5.1218E-01	3.3027E+00
27	34	1959904	1256734	14562138	3.1018E-06	2.1587E-04	2.7035E+00	5.1506E-01	3.3171E+00
28	35	1966069	1257983	14608929	1.9234E-06	2.1967E-04	2.7420E+00	5.1727E-01	3.3274E+00
29	36	1972904	1260720	14648059	1.1951E-06	2.2269E-04	2.7760E+00	5.1944E-01	3.3337E+00
30	37	1971486	1265904	14604287	7.3886E-07	2.2823E-04	2.8241E+00	5.2254E-01	3.3493E+00
31	38	1950494	1269664	14426349	4.4835E-07	2.3719E-04	2.9127E+00	5.2530E-01	3.3761E+00
32	39	1855081	1272325	13641231	2.5645E-07	2.6270E-04	3.1737E+00	5.3093E-01	3.4491E+00
33	40	1642794	1265506	11742572	1.1309E-07	3.6563E-04	4.2299E+00	5.4614E-01	3.7281E+00
34	81	67948	63513	4329853	3.8668E-08	7.0184E-04	9.9685E+00	5.7647E-01	5.0142E-01
35	91	646417	529502	1240036	1.1918E-08	1.2209E-03	8.9509E+00	5.9620E-01	7.5409E+03
total		69471692	41035257	494920001	5.4261E+00				

1photon activity in each cell print table 126

cell	tracks entering	population	collisions	collisions * weight (per history)	number weighted energy	flux weighted energy	average track weight (relative)	average track mfp (cm)	
1	1	1730828	1730177	0	0.0000E+00	1.6730E+00	1.6730E+00	1.0035E+00	0.0000E+00
2	2	177	1985166	1013137	7.7782E-02	1.6773E+00	1.6773E+00	1.0034E+00	2.3013E+00
3	3	3187628	2172520	379694	3.0325E-02	1.0250E+00	1.0250E+00	1.0433E+00	1.1379E+04
4	11	3774097	3446425	17404435	1.4177E+00	1.0599E+00	1.0599E+00	1.0644E+00	5.6217E+00
5	12	2730473	3340082	12257282	7.0432E-01	1.1458E+00	1.1458E+00	1.2424E+00	5.7831E+00
6	13	2536574	3028154	10889941	4.0679E-01	1.2290E+00	1.2290E+00	1.6045E+00	5.9908E+00
7	14	2331687	2787293	9899256	2.4340E-01	1.2635E+00	1.2635E+00	2.0412E+00	6.0758E+00
8	15	2230192	2684905	9418372	1.4388E-01	1.2742E+00	1.2742E+00	2.4507E+00	6.0993E+00
9	16	2223708	2667017	9310289	8.3240E-02	1.2698E+00	1.2698E+00	2.8096E+00	6.0858E+00
10	17	2226470	2656982	9229726	4.6945E-02	1.2642E+00	1.2642E+00	3.1063E+00	6.0674E+00
11	18	2229605	2656145	9196070	2.6077E-02	1.2634E+00	1.2634E+00	3.3402E+00	6.0607E+00
12	19	2242420	2663853	9190770	1.4284E-02	1.2599E+00	1.2599E+00	3.5082E+00	6.0485E+00
13	20	2243101	2662067	9145229	7.7385E-03	1.2604E+00	1.2604E+00	3.6216E+00	6.0475E+00
14	21	2244583	2663848	9155886	4.2183E-03	1.2578E+00	1.2578E+00	3.7027E+00	6.0372E+00
15	22	2239892	2657561	9116367	2.2901E-03	1.2598E+00	1.2598E+00	3.7598E+00	6.0396E+00

16	23	2234558	2654462	9082783	1.2456E-03	1.2634E+00	1.2634E+00	3.8002E+00	6.0443E+00
17	24	2234269	2661783	9088891	6.8188E-04	1.2695E+00	1.2695E+00	3.8293E+00	6.0567E+00
18	25	2245822	2675367	9140026	3.7580E-04	1.2716E+00	1.2716E+00	3.8640E+00	6.0583E+00
19	26	2253023	2687273	9168288	2.0857E-04	1.2785E+00	1.2785E+00	3.9211E+00	6.0728E+00
20	27	2254903	2694750	9182661	1.1679E-04	1.2848E+00	1.2848E+00	3.9947E+00	6.0859E+00
21	28	2257476	2701567	9207637	6.6228E-05	1.2906E+00	1.2906E+00	4.0922E+00	6.0990E+00
22	29	2249552	2695121	9179313	3.7789E-05	1.2948E+00	1.2948E+00	4.2080E+00	6.1088E+00
23	30	2232997	2679320	9139846	2.1886E-05	1.2991E+00	1.2991E+00	4.3513E+00	6.1175E+00
24	31	2191645	2639219	8994967	1.2712E-05	1.3027E+00	1.3027E+00	4.5075E+00	6.1274E+00
25	32	2141329	2583212	8815192	7.4551E-06	1.3055E+00	1.3055E+00	4.6796E+00	6.1341E+00
26	33	2067868	2501959	8557715	4.4247E-06	1.3099E+00	1.3099E+00	4.8656E+00	6.1440E+00
27	34	1960447	2380850	8172769	2.6428E-06	1.3092E+00	1.3092E+00	5.0285E+00	6.1429E+00
28	35	1824221	2228701	7673631	1.5886E-06	1.3114E+00	1.3114E+00	5.1558E+00	6.1478E+00
29	36	1662344	2050680	7095300	9.5793E-07	1.3154E+00	1.3154E+00	5.1985E+00	6.1571E+00
30	37	1475955	1845833	6411456	5.7891E-07	1.3177E+00	1.3177E+00	5.1192E+00	6.1647E+00
31	38	1279278	1633216	5690857	3.4786E-07	1.3177E+00	1.3177E+00	4.8884E+00	6.1642E+00
32	39	1088571	1435142	4968016	2.0318E-07	1.3196E+00	1.3196E+00	4.5459E+00	6.1689E+00
33	40	849491	1232164	4009872	1.0067E-07	1.3762E+00	1.3762E+00	4.1911E+00	6.3309E+00
34	81	42537	78827	628674	1.5143E-08	1.0933E+00	1.0933E+00	4.0427E+00	1.1762E+00
35	91	477192	475233	327725	8.0570E-09	1.6218E+00	1.6218E+00	4.1330E+00	1.4150E+04
	total	69194913	82336874	270142073	3.2118E+00				

1proton activity in each cell print table 126

cell	tracks entering	population	substeps * weight (per history)	substeps weighted energy	number weighted energy	flux weighted (relative)	average track weight	average track mfp (cm)
1	1	13072651	13072458	13072651	1.0004E+00	6.9978E+01	6.9992E+01	1.0000E+00	0.0000E+00
2	2	13067569	14108207	2780553964	2.1278E+02	4.0335E+01	4.5236E+01	1.0000E+00	1.0095E-02
	total	26140220	27180665	2793626615	2.1378E+02				

1summary of photons produced in neutron collisions

cell		number of photons	weight per source neut	energy per source neut	avg photon energy	mev/gm per source neut	weight/neut collision	energy/neut collision
1	1	0	0.00000E+00	0.00000E+00	0.00000E+00	0.00000E+00	0.00000E+00	0.00000E+00
2	2	79981	6.61399E-03	1.08441E-02	1.63957E+00	5.07616E-04	4.74170E-01	7.77435E-01
3	3	6745	5.18088E-04	2.24444E-03	4.33216E+00	1.16413E-10	7.59935E-03	3.29216E-02
4	11	684774	5.32881E-02	1.53428E-01	2.87922E+00	1.35003E-10	2.57106E-02	7.40264E-02
5	12	485359	3.78693E-02	1.11182E-01	2.93595E+00	9.63861E-11	2.68503E-02	7.88312E-02
6	13	320941	2.50078E-02	7.39630E-02	2.95760E+00	6.31808E-11	2.91623E-02	8.62503E-02
7	14	287452	1.50286E-02	4.45611E-02	2.96509E+00	3.75120E-11	3.12847E-02	9.27619E-02
8	15	280044	8.39796E-03	2.49980E-02	2.97668E+00	2.07403E-11	3.28061E-02	9.76534E-02
9	16	263252	4.44880E-03	1.32506E-02	2.97847E+00	1.08365E-11	3.36596E-02	1.00254E-01
10	17	247494	2.29472E-03	6.84108E-03	2.98122E+00	5.51537E-12	3.43124E-02	1.02293E-01
11	18	239921	1.17473E-03	3.51506E-03	2.99222E+00	2.79399E-12	3.50373E-02	1.04839E-01
12	19	232653	5.89012E-04	1.76116E-03	2.99002E+00	1.38033E-12	3.50114E-02	1.04685E-01
13	20	229695	2.98982E-04	8.97843E-04	3.00300E+00	6.93939E-13	3.52295E-02	1.05794E-01
14	21	227143	1.53459E-04	4.59588E-04	2.99485E+00	3.50327E-13	3.53842E-02	1.05970E-01
15	22	223885	7.95311E-05	2.39270E-04	3.00850E+00	1.79896E-13	3.53968E-02	1.06491E-01
16	23	223914	4.20348E-05	1.26386E-04	3.00670E+00	9.37359E-14	3.54785E-02	1.06673E-01
17	24	227213	2.25047E-05	6.78329E-05	3.01416E+00	4.96325E-14	3.52914E-02	1.06374E-01
18	25	228254	1.23219E-05	3.71521E-05	3.01513E+00	2.68207E-14	3.53207E-02	1.06496E-01
19	26	228956	6.88338E-06	2.08203E-05	3.02472E+00	1.48312E-14	3.53757E-02	1.07002E-01
20	27	232945	3.93431E-06	1.19288E-05	3.03199E+00	8.38554E-15	3.54254E-02	1.07409E-01
21	28	233847	2.27041E-06	6.87637E-06	3.02869E+00	4.77069E-15	3.53051E-02	1.06928E-01
22	29	236751	1.33682E-06	4.05405E-06	3.03260E+00	2.77613E-15	3.53693E-02	1.07261E-01
23	30	239145	7.94138E-07	2.40974E-06	3.03441E+00	1.62887E-15	3.53071E-02	1.07136E-01
24	31	243384	4.79640E-07	1.45462E-06	3.03272E+00	9.70671E-16	3.53374E-02	1.07169E-01
25	32	244090	2.89559E-07	8.80047E-07	3.03926E+00	5.79796E-16	3.51933E-02	1.06962E-01
26	33	245289	1.77657E-07	5.40374E-07	3.04168E+00	3.51519E-16	3.52543E-02	1.07232E-01
27	34	246321	1.09267E-07	3.32346E-07	3.04160E+00	2.13484E-16	3.52263E-02	1.07145E-01
28	35	247884	6.76787E-08	2.06018E-07	3.04406E+00	1.30689E-16	3.51867E-02	1.07110E-01

29	36	250037	4.21486E-08	1.28325E-07	3.04457E+00	8.03969E-17	3.52665E-02	1.07371E-01
30	37	250476	2.60450E-08	7.91372E-08	3.03848E+00	4.89713E-17	3.52504E-02	1.07108E-01
31	38	248657	1.58188E-08	4.81554E-08	3.04418E+00	2.94356E-17	3.52822E-02	1.07406E-01
32	39	240250	9.17105E-09	2.79881E-08	3.05179E+00	1.69007E-17	3.57610E-02	1.09135E-01
33	40	223215	4.29038E-09	1.32450E-08	3.08715E+00	7.90170E-18	3.79392E-02	1.17124E-01
34	81	22850	4.36058E-10	1.25942E-09	2.88820E+00	8.89974E-16	1.12769E-02	3.25699E-02
35	91	11316	2.16136E-10	8.68939E-10	4.02033E+00	8.68939E-10	1.81354E-02	7.29104E-02
36	99	0	0.00000E+00	0.00000E+00	0.00000E+00	0.00000E+00	0.00000E+00	0.00000E+00
total		8134133	1.55856E-01	4.48467E-01	2.87744E+00			

1energy distribution of photons produced in neutron collisions

Input data 126

	tally 14					tally 24				
nps	mean	error	vov	slope	fom	mean	error	vov	slope	fom
8192000	4.8340E-01	0.1151	0.1076	6.1	3.0E-01	1.5257E+00	0.0963	0.0832	4.4	4.3E-01
16384000	4.7097E-01	0.0819	0.0578	3.9	3.0E-01	1.4736E+00	0.0677	0.0461	3.3	4.4E-01
24576000	4.5336E-01	0.0648	0.0405	3.9	3.2E-01	1.4376E+00	0.0534	0.0317	3.6	4.7E-01
32768000	4.5746E-01	0.0573	0.0308	3.9	3.1E-01	1.4544E+00	0.0473	0.0237	3.5	4.5E-01
40960000	4.6492E-01	0.0500	0.0232	4.3	3.2E-01	1.4803E+00	0.0415	0.0175	4.2	4.7E-01
49152000	4.7197E-01	0.0452	0.0183	4.7	3.3E-01	1.4990E+00	0.0378	0.0142	4.5	4.7E-01
57344000	4.6984E-01	0.0412	0.0150	5.1	3.4E-01	1.4879E+00	0.0345	0.0117	4.7	4.8E-01
65536000	4.7414E-01	0.0388	0.0133	4.2	3.3E-01	1.4987E+00	0.0326	0.0101	4.2	4.7E-01
73728000	4.7114E-01	0.0363	0.0115	3.4	3.4E-01	1.4906E+00	0.0304	0.0087	3.3	4.8E-01
81920000	4.7488E-01	0.0342	0.0100	3.4	3.4E-01	1.4997E+00	0.0288	0.0077	3.9	4.8E-01
90112000	4.7776E-01	0.0333	0.0111	3.4	3.3E-01	1.5077E+00	0.0280	0.0087	3.7	4.6E-01
98304000	4.7759E-01	0.0321	0.0104	3.3	3.2E-01	1.5044E+00	0.0269	0.0080	3.9	4.6E-01
106496000	4.7320E-01	0.0307	0.0096	3.5	3.3E-01	1.4928E+00	0.0257	0.0074	4.0	4.6E-01
114688000	4.7862E-01	0.0294	0.0084	4.8	3.3E-01	1.5063E+00	0.0247	0.0065	5.7	4.7E-01
122880000	4.7326E-01	0.0284	0.0078	4.8	3.3E-01	1.4941E+00	0.0238	0.0060	6.0	4.7E-01
131072000	4.7547E-01	0.0272	0.0072	4.1	3.4E-01	1.5010E+00	0.0228	0.0055	6.7	4.8E-01
139264000	4.7321E-01	0.0261	0.0068	4.6	3.4E-01	1.4961E+00	0.0219	0.0051	5.6	4.9E-01
140743675	4.7535E-01	0.0260	0.0066	5.2	3.4E-01	1.5014E+00	0.0219	0.0050	5.9	4.8E-01

Fluctuation chart

Appendix 4: MCNPX Surface Cards

Mnemonic	Type	Description	Equation	Card Entries
P	plane	general	$Ax + By + Cz - D = 0$	$A\ B\ C\ D$
PX		normal to x-axis	$x - D = 0$	D
PY		normal to y-axis	$y - D = 0$	D
PZ		normal to z-axis	$z - D = 0$	D
SO	sphere	centered at origin	$x^2 + y^2 + z^2 - R^2 = 0$	R
S		general	$(x-\bar{x})^2+(y-\bar{y})^2+(z-\bar{z})^2-R^2=0$	$\bar{x}\ \bar{y}\ \bar{z}\ R$
SX		centered on x-axis	$(x - \bar{x})^2 + y^2 + z^2 - R^2 = 0$	$\bar{x}\ R$
SY		centered on y-axis	$x^2 + (y - \bar{y})^2 + z^2 - R^2 = 0$	$\bar{y}\ R$
SZ		centered on z-axis	$x^2 + y^2 + (z - \bar{z})^2 - R^2 = 0$	$\bar{z}\ R$
C/X	cylinder	parallel to x-axis	$(y - \bar{y})^2 + (z - \bar{z})^2 - R^2 = 0$	$\bar{y}\ \bar{z}\ R$
C/Y		parallel to y-axis	$(x - \bar{x})^2 + (z - \bar{z})^2 - R^2 = 0$	$\bar{x}\ \bar{z}\ R$
C/Z		parallel to z-axis	$(x - \bar{x})^2 + (y - \bar{y})^2 - R^2 = 0$	$\bar{x}\ \bar{y}\ R$
CX		on x-axis	$y^2 + z^2 - R^2 = 0$	R
CY		on y-axis	$x^2 + z^2 - R^2 = 0$	R
CZ		on z-axis	$x^2 + y^2 - R^2 = 0$	R
K/X	cone	parallel to x-axis	$\sqrt{(y-\bar{y})^2 + (z-\bar{z})^2} - t(x-\bar{x}) = 0$	$\bar{x}\ \bar{y}\ \bar{z}\ t^2\ \pm 1$
K/Y		parallel to y-axis	$\sqrt{(x-\bar{x})^2 + (z-\bar{z})^2} - t(y-\bar{y}) = 0$	$\bar{x}\bar{y}\ \bar{z}\ t^2\ \pm 1$
K/Z		parallel to z-axis	$\sqrt{(x-\bar{x})^2 + (y-\bar{y})^2} - t(z-\bar{z}) = 0$	$\bar{x}\bar{y}\ \bar{z}\ t^2\ \pm 1$
KX		on x-axis	$\sqrt{y^2 + z^2} - t(x - \bar{x}) = 0$	$\bar{x}\ t^2\ \pm 1$
KY		on y-axis	$\sqrt{x^2 + z^2} - t(y - \bar{y}) = 0$	$\bar{y}\ t^2\ \pm 1$
KZ		on z-axis	$\sqrt{x^2 + y^2} - t(z - \bar{z}) = 0$	$\bar{z}\ t^2\ \pm 1$
			± 1 used only for 1-sheet cone	
SQ	ellipsoid hyperboloid paraboloid	axis parallel to x-, y-, or z-axis	$A(x - \bar{x})^2 + B(y - \bar{y})^2 + C(z - \bar{z})^2 + 2D(x - \bar{x}) + 2E(y - \bar{y}) + 2F(z - \bar{z}) + G = 0$	$A\ B\ C\ D\ E\ F\ G\ \bar{x}\ \bar{y}\ \bar{z}$
GQ	cylinder, cone ellipsoid paraboloid hyperboloid	axis not parallel to x-, y-, or z-axis	$Ax^2 + By^2 + Cz^2 + Dxy + Eyz + Fzx + Gz + Hy + Jz + K = 0$	$A\ B\ C\ D\ E\ F\ G\ H\ J\ K$
TX	elliptical or circular torus. Axis is parallel to x-, y-, or z-axis	$(x-\bar{x})^2/B^2 + (\sqrt{(y-\bar{y})^2 + (z-\bar{z})^2} - A)^2/C^2 - 1 = 0$		$\bar{x}\ \bar{y}\ \bar{z} A\ B\ C$
TY		$(y-\bar{y})^2/B^2 + (\sqrt{(x-\bar{x})^2 + (z-\bar{z})^2} - A)^2/C^2 - 1 = 0$		$\bar{x}\ \bar{y}\ \bar{z} A\ B\ C$
TZ		$(z-\bar{z})^2/B^2 + (\sqrt{(x-\bar{x})^2 + (y-\bar{y})^2} - A)^2/C^2 - 1 = 0$		$\bar{x}\ \bar{y}\ \bar{z} A\ B\ C$
XYZP	surfaces defined by points –			

Appendix 5: Standard Dose Functions

Value of IC	Description
Neutron Dose Function	
10	ICRP-21 1971
20	NCRP-38 1971, ANSI/ANS-6.1.1-1977
31	ANSI/ANS-6.1.1-1991 (AP anterior-posterior)
32	ANSI/ANS-6.1.1-1991 (PA posterior-anterior)
33	ANSI/ANS-6.1.1-1991 (LAT side exposure)
34	ANSI/ANS-6.1.1-1991(ROT normal to length & rotationally symmetric)
40	ICRP-74 1996 ambient dose equivalent
Photon Dose Function	
10	ICRP-21 1971
20	Claiborne & Trubey, ANSI/ANS 6.1.1-1977
31	ANSI/ANS-6.1.1-1991 (AP anterior-posterior)
32	ANSI/ANS-6.1.1-1991 (PA posterior-anterior)
33	ANSI/ANS-6.1.1-1991 (LAT side exposure)
34	ANSI/ANS-6.1.1-1991(ROT normal to length & rotationally symmetric)
35	(ISO isotropic)

Appendix 6: Random Number Generators

A random number generator (RNG) is necessary as random sampling means a Random Variable must pick random numbers uniformly distributed on the unit interval i.e. [0,1]

There are two general approaches for generating random numbers:

- Experimental (tables, on-line) – a sequence of random numbers is generated by performing an experiment. These sequences are then saved in computer memory as tables.
- Algorithmic (deterministic) – here a sequence of random numbers is determined by the algorithm linked to the probability function sometimes known as the 'pseudo-random' number generator (PRNG).

Factors which influence the decision on which RNG to use includes [14]:

- Randomness.
- Reproducibility.
- Length of the sequence of random numbers.
- Computer memory.
- Generating time.
- Computer time.

For particle transport, linear congruential random number generators are mostly used [9]:

The congruential RNG proposed by uses a form:

$$S_{k+1} = [S_k \cdot g + c] \bmod p \quad \text{..... (6)}$$

S_k, g, c and p are all given integers.

where $S_k = S_0$ = the seed,

g = a generator or multiplier,

c = the increment, and

p = a modulus.

Modulus is number by which two given numbers can be divided and produce the same remainder [16].

We can produce a sequence of numbers by choosing S_0 =1; g =3; c =1 and p =10

$$S_0 = 1$$
$$S_1 = (1\times 3+1) \bmod 10 = 4$$
$$S_2 = (4\times 3+1) \bmod 10 = 3$$
$$S_3 = (3\times 3+1) \bmod 10 = 0$$
$$S_4 = (0\times 3+1) \bmod 10 = 1$$
$$S_5 = (1\times 3+1) \bmod 10 = 4$$

This sequence starts to repeat a cycle at S_4 again. Now these are not really random numbers but sequences. This requires $S_0 ; g ; c$ and p to be chosen intelligently. For example, we want the cycle to be sufficiently big that the sequence seems random. We want p to be big e.g. 2^{13}. Thus the congruential RNG proposed by Lehmer [14] uses a form:

$$S_{k+1} = S_k \square g + c \bmod 2^m \quad \text{..... (7)}$$

This form will allow the sequence to repeat after a long period. The benefit of this pseudo-RNG is that it makes it easy to test and re-run the simulation.